

1 of 2

PNL-8829
UC-520

**LARGE-BREAK LOCA, IN-REACTOR
FUEL BUNDLE MATERIALS TEST MT-6A**

C. L. Wilson
G. M. Hesson
J. P. Pilger
L. L. King
F. E. Panisko

October 1989 - Completion Date
September 1993 - Publication Date

Prepared for
U.S. Nuclear Regulatory Commission
Under Contract DE-AC06-76RLO 1830

Pacific Northwest Laboratory
Richland, Washington 99352

MASTER

DISTRIBUTION OF THIS DOCUMENT IS UNLIMITED *yp*

ABSTRACT

This is a report on one of a series of experiments to simulate a loss-of-coolant accident (LOCA) using full-length fuel rods for pressurized water reactors (PWR). The experiments were conducted by Pacific Northwest Laboratory (PNL) under the LOCA simulation Program sponsored by the U. S. Nuclear Regulatory Commission (NRC). The major objective of this program was to simulate a LOCA in a PWR and recovery from the simulated accident, first by causing the maximum possible expansion of the cladding on the fuel rods from a short-term adiabatic temperature transient to 1200 K (1700 F) leading to the rupture of the cladding; and second, by reflooding the fuel rods to determine the rate at which the fuel bundle is cooled.

The subject of this report is Materials Test 6A (MT-6A) which was the last of the experiments in the LOCA Simulation Program. It was conducted in the Canadian National Research Universal (NRU) reactor at Chalk River, Ontario, Canada. All major objectives of the test were met, although a computer control system malfunctioned. All 21 fuel rods were initially pressurized to 6.03 MPa (875 psia) in order to cause the Zircaloy-4 cladding to expand and rupture at high temperatures in the alpha phase, from 1035 to 1200 K (1400 to 1700 F). Pressure sensors attached to the fuel rods using capillary tubing indicated that all 21 cladding tubes failed. All cladding tubes ruptured while the peak temperatures were between 1050 and 1140 K (1430 and 1600 F). During the reflood phase, the temperature measurements of the cladding indicated the rate at which the fuel bundle cooled. Although precise measurements of the cladding strain were not made due to lack of funds, visual inspection of a portion of one side of the fuel bundle revealed large amounts of cladding strain.

A subsequent test MT-6B indicated that small notches in the stainless steel shroud that surrounded the MT test bundles, is probably responsible for major changes in the MT-6A and previous MT tests, cladding strain. The notches (less stainless steel) produced a higher local neutron flux which caused higher local fuel temperatures which caused higher local cladding temperatures that produced much greater local cladding strain.

SUMMARY

The Loss-of-Coolant Accident (LOCA) Simulation Program was conducted by the Pacific Northwest laboratory (PNL) for the U. S. Nuclear Regulatory Commission (NRC) and completed in 1984. The major objective of this program was to simulate a LOCA in a PWR and recovery from the simulated accident, first by causing the maximum possible expansion of the cladding on the fuel rods from a short-term adiabatic temperature transient to 1200 K (1700 F) leading to the rupture of the cladding; and second, by reflooding the fuel rods to determine the rate at which the fuel bundle is cooled. The tests conducted under the program were designed to simulate the heat up, reflood and quench phases of a large break LOCA. The tests were conducted in the Canadian National Research Universal (NRU) reactor using nuclear fission heating to simulate the low level decay heat that is typical of LOCA accidents. In this report is presented a quick-look analysis of the data and results of materials Test 6A (MT-6A), the last of the tests to be conducted under the PNL/NRC LOCA Simulation Program.

For this test, the design of the 3.7 m (12 ft) long test bundle for the fuel rods was improved over the design of the test bundle used in previous MT tests. It was redesigned to minimize temperature gradients on the circumference of the cladding during the short term adiabatic heat up phase of the test. The purpose was to maximize the radial expansion of the bundle Zircaloy cladding on the fuel rods and the coplanar expansion in the bundle during the heat up phase of the test. The reduced temperature gradients were to be achieved, first by modifying the stainless steel shroud encompassing the bundle used in previous MT tests to include thermal insulation, and second, by replacing the 20 heater rods that surrounded the 12 test rods used in previous tests with 9 pressurized test rods for a total of 21 test rods.

All major objectives of the experiment were met, although a computer controlled system malfunctioned. All 21 fuel rods were initially pressurized to 6.03 MPa (875 psia) in order to cause the Zircaloy-4 cladding to expand and rupture at high temperatures in the alpha phase, from 1035 to 1200 K (1400 to 1700 F). Pressure sensors attached to the fuel rods using capillary tubing indicated that all 21 cladding tubes failed. All rods ruptured while the peak temperatures were between 1050 and 1140 K (1430 and 1600 F). During the reflood phase, the temperature measurements of the cladding indicated the rate at which the fuel bundle cooled. Although precise measurements of the cladding strain were not made due to lack of funds, visual inspection of a portion of one side of the fuel bundle revealed large amounts of cladding strain.

The data collected from thermocouples and pressure gages during heat up and from thermocouples during the quenching phase demonstrated the rate of cooling of the test bundle under LOCA conditions. To be able to predict the rate of cooling under other conditions, though, an in depth qualification of the data collected and a post test examination of the fuel rods would be needed, but funds are not available for either. Without post test strain and blockage measurements, no quantification of radial, axial, and coplanar values of bundle coolant blockage can be stated to relate with the measured quenching rates of the cladding during the final phase of the simulated LOCA.

The MT-6A (21 rod test) fuel bundle is being stored at this time (summer 1989) at CRL and plans are being made for its long term storage.

Though the malfunction of the computer did not affect the final outcome of the test, it did cause the following changes:

The pressure control valve closed at the start of the transient which resulted in a system pressure of 1.72 MPa (250 psia) instead of 0.28 MPa (40 psia).

The reflood system failed to control the desired flat top temperature transient.

PREFACE

A series of tests was conducted under the Loss of Coolant Accident (LOCA) Simulation Program, sponsored by the U. S. Nuclear Regulatory Commission (NRC), Office of Research, Division of Systems Research, between 1980 and 1984. This is a report on one of those tests. Included in the series were 1) three experiments comprised of 45 mini experiments on the thermal hydraulics of fuel bundles and 2) five materials tests on the amount of expansion of Zircaloy cladding both under simulated LOCA conditions. They were designed and performed by Pacific Northwest Laboratory (PNL).^(a) All were conducted in the Canadian National Research Universal (NRU) reactor with the support of the staff at the Chalk River Laboratory which is operated by Atomic Energy Canada, LTD. One of the five material tests was supported by the United Kingdom Atomic Energy Authority.

OBJECTIVES

The major objective of this program was to simulate a LOCA in a PWR and recovery from the simulated accident, first by causing the maximum possible expansion of the cladding on the fuel rods from a short-term adiabatic temperature transient to 1200 K (1700 F) leading to the rupture of the cladding; and second, by reflooding the fuel rods to determine the rate at which the fuel bundle is cooled.⁽¹⁾ An evaluation of the results of these tests was provided to NRC for their use in assessing the rate at which an accidentally over heated nuclear core in a commercial light water reactor could be cooled or quenched. In the fifth and last test in the series, it was demonstrated that the insulating shroud could provide thermal insulation for the pressure tube and the NRU test facility. To be evaluated was the effect of high temperatures and the resulting internal pressures on the fuel rods, i.e., the maximum extent of the radial and axial strain on the cladding of the fuel rods and other damage that might result. The experience and understanding to be gained from the tests was to enable successive simulations of more severe accidents to be performed.

BACKGROUND

The following is a brief review of the LOCA simulation Program. Included in the program were three experiments conducted at high temperatures, the thermal hydraulic experiments, and five experiments conducted at both high temperatures and high pressures, the material expansion tests, on the expansion of Zircaloy cladding on fuel rods. The experiments and tests are presented in the following sections according to kind rather than in the order in which they were conducted. However, the order in which each was conducted is stated. The basic objectives and results of each are also included.

(a) Operated for the U.S. Department of Energy (DOE) by Battelle Memorial Institute under Contract DE-AC06-76RLO 1830.

Thermal-Hydraulic Experiments

The initial thermal-hydraulic experiment (TH-1), using 32 fuel rods with instruments attached, was performed in October 1980 and provided a database for predicting the quenching characteristics of Zircaloy-clad fuel rods under various reflood conditions.⁽²⁾ It was the first in the program. Twenty-eight separate high temperature and pressure tests were included in TH-1. The specific objective of these experiments was to characterize the rates of initial heat up, reflood and quenching for as-fabricated fuel rods that were not deformed and not pressurized. The exact parameters for the experiments on the expansion of fuel cladding to be performed later were determined from the results of these experiments at high temperatures. Experimental results covered reflood rates of 1.88 to 28 cm/s and delay times to initiate reflood of 3 s to 66 s. The results indicate that current analysis methods can predict peak temperatures within 10% and the quench times measured for the bundle were significantly less than predicted. For reflood rates of 2.5 cm/s where long quench times were predicted (>2000 s), measured quench times of 200 s were found.

The thermal-hydraulic experiment (TH-2) was the fourth experiment and was conducted in October 1981. Used in it was a new thermal-hydraulic test bundle with fuel rods sealed at atmospheric pressure that was reconstituted in the MT-1/MT-2 guard rod and shroud assembly. In order to minimize the expense of the program, the test hardware was designed to be reused. Therefore, shroud, heater rods and T-H test rods were used in more than one test. Deformed rods, though, were never reused. Because used hardware was radioactive, handling operations were performed remotely. The remote operations with the test hardware located under about 2-m of water were performed efficiently with the help of a specially designed, computer-controlled disassembly, examination and reassembly machine (DERM). This experiment included 14 separate tests at high temperatures and pressures to determine the rates of reflooding necessary to obtain a "flat-top" or extended transient from 1035 to 1105 K (1400 to 1525°F). The delay time and automatic control system used to control the variable rate of reflood in this experiment demonstrated the capability of holding temperatures above 1035 K (1400°F) for periods of up to 280 s. The test conditions approached steady-state boiloff.

The fifth experiment was thermal-hydraulic experiment 3 (TH-3). Used in it was the same test bundle used in TH-2; several new thermocouples (TCs) and a spray desuperheater were added. Several modifications were also made to the logic of the loop control to improve control of the rate of reflooding and extend the length of the flat-top transient. TH-3 was performed just before MT-3 to verify the loop control system (LCS) and the data acquisition and control system (DACS) instrumentation and operation. TH-3 and MT-3 were both performed in November 1981. TH-3 also verified the power levels during test assembly and the improvements to the DACS performance. The results of the

TH-3 experiment that included three separate high temperature tests made it possible to extend the time above 1035 K (1400°F) from 280 s in TH-2.14 to 340 s in TH-3.03. In addition, the transient temperature history was modified to provide more two-phase cooling at the start of the transient. The addition of the spray desuperheater to the TH-3 assembly controlled the temperature of the exiting steam.

Material Expansion Tests

The first materials experiment (MT-1), i.e., the test on the expansion of Zircaloy fuel cladding, was the second in the program and was performed in April 1981, using a cruciform of 11 rods^a pressurized to 3.21 MPa (465 psia) and 1 water tube surrounded by 20 guard^a rods sealed at atmospheric pressure.⁽³⁾ The objective of this test was to assess the rate at which the expanded cladding can be cooled, based on evaluations of the rates of heat up and quenching and the measurements of post-test cladding strain. The delay time and the rate of reflood were selected to duplicate one of the experiments at high temperatures, specifically TH-1.10, in which the fuel cladding reached a peak temperature of 1145 K (1600°F). These conditions were achieved: 6 of the 11 rods ruptured and all 11 pressurized test rods expanded significantly.⁽⁴⁾ The average peak rupture strain was 43%; the average time to rupture was 43 s; and the average temperature at rupture was 1145 K (1600°F).

In the second materials experiment (MT-2), the third experiment in the program, performed in July 1981, the MT-1 guard rods and shroud assembly were reconstituted underwater and reused with a new cruciform test bundle. One of the objectives of the test was to perform a low-temperature, 1090 K (1500°F), test using variable rates of reflooding. The 12 test rods were pressurized to 3.21 MPa (465 psia). A malfunction of the reflood system, however, resulted in higher temperatures than desired and 8 of the 11 rods ruptured.⁽⁵⁾ The average peak rupture strain was 43%, the average time to rupture was 65 s, and the average temperature at rupture was 1160 K (1625°F).

The primary objective of the third materials experiment (MT-3), the sixth in the program, was to determine the expansion and restrictions on the flow channel for a flat-top temperature transient using pressurized fuel rods. Peak temperatures of the cladding were maintained above 1035 K (1400°F) for 180 s. The MT-3 experiment repeated the test conditions demonstrated by the TH-3.03 test using a completely new test train with 12 fuel rods pressurized to 3.9 MPa (565 psia) and 20 guard rods. All 12 test rods ruptured during the active two-phase cooling regime. The average peak rupture strain was 46%, the average time of rupture was 133 s, and the average temperature at rupture was 1070 K (1460°F). The MT-3 experiment had a lower average temperature at rupture and a longer time until rupture than any of the other materials experiments because of the significant amount of reflood water that was introduced early in the transient (the delay time for reflooding was 7 s).

^a The guard rods are unpressurized fuel rods that surround the periphery (guard) of the test fuel rods to minimize radial heat loss from the test fuel rods.

The active strain region was spread over ~2-m (80-in.) length, and no loss of cooling because of coplanar blockage or liftoff^a was observed.

The fourth materials experiment (MT-4) was the seventh in the program and was conducted in May 1982.⁽⁶⁾ Its primary objective was to evaluate the expansion and rupture of cladding during heat up in the temperature range from 1035 to 1200 K (1400 to 1700°F). The 12 test rods in the 32-rod bundle were initially pressurized to 4.62 MPa (670 psia) at 295 K (70°F) to assure rupture in the correct temperature range. The MT-4 experiment was most similar to the MT-2 experiment; three differences existed: 1) MT-4 rods were pressurized to 4.62 MPa (670 psia), whereas MT-2 rods were pressurized to 3.21 MPa (465 psia); 2) After the temperature turnaround following the heatup transient, the peak temperatures of the cladding were stabilized to measure the characteristics of the heat transfer of the expanded and ruptured fuel rods, whereas during MT-2 the peak temperatures of the cladding were not stabilized, and 3) self-powered neutron detectors (SPNDs) mounted on the shroud were moved to grid elevations to minimize distortion of axial fission power, whereas MT-2 had the SPNDs mounted away from the Inconel grids. During the test all 12 test rods ruptured with an average peak rod strain of 72.1%. The active strain region was spread over 0.189 m (7.42 in.), the average time of rupture was 55 s; and the average temperature at rupture was 1094 K (1511°F).

The MT-4 experiment used a new cruciform bundle of 12 pressurized test fuel rods and the guard fuel rods and shroud previously used in MT-3. Test operations most closely followed the operating conditions of the TH-1.16, during which cooling by reflooding was used to terminate the transient temperature of the heat up at ~1200 K (1700°F). Stabilized operations at the post-transient stage closely followed the operating conditions used in the MT-3 experiment.

The results from MT-4 provided data on the expansion of the cladding on full-length PWR nuclear-heated rods in the temperature range where crystalline Zircaloy is still in the alpha, hexagonal close-pack phase for variable conditions of reflooding. These conditions extended the existing data base on the response of the cladding to high temperatures and pressures for LOCA conditions not previously investigated by test programs that were conducted out of a reactor. The MT-4 test series yielded valuable information on 1) the control of quench fronts and two-phase cooling used for subsequent experiments at high temperatures and pressures on materials and 2) the quench characteristics of rods that were expanded as compared to rods that were not expanded for the flow conditions covered in these experiments.

Data from MT-4 have been used in conjunction with previous test results to assess various calculational models for reactor safety analyses and in conjunction with conclusions derived elsewhere from electrically heated tests⁽⁷⁾ and smaller scale tests⁽⁸⁾ conducted in a reactor. The experimental results of the program address 17 specific items outlined in the Code of Federal Regulations, 10 CFR 50.46 and 10 CFR 50, Appendix K. These results

^a Liftoff is a thermal decoupling of the cladding from the fuel that results in cooling of the cladding during deformation.

have been used to provide additional data for model calibration and to help define the primary mechanisms for heat transfer for new analytical models. The major contributions of these tests to light-water reactor (LWR) technology has been to quantify the uncertainty of the criteria for licensing and offer the potential for raising the operating limits on some commercial LWRs. (9)

The MT-5 test was proposed to the NRC but never approved. As proposed, MT-5 would have been similar to MT-4 except that irradiated fuel rods would have been used in this study of cladding expansion.

CONTRIBUTORS

The following Pacific Northwest Laboratory staff members contributed significantly to this particular test in the LOCA Simulation Program:

- B. J. Webb performed the thermal-hydraulic analyses.
- U. P. Jenquin provided neutronic and shielding analyses.
- G. E. Russcher coordinated the safety analysis.
- M. C. Wismer and W. N. Rausch made improvements to and operated the data acquisition and control system.
- L. J. Parchen was responsible for quality assurance and test assembly shipping.
- R. R. Lewis provided liaison between PNL and CRNL.
- N. J. Wildung provided computer plots.
- S. K. Edler edited this document and provided publication assistance.

The authors and project staff would like to thank Chalk River Nuclear Laboratories (CRNL) for their assistance in performing this experiment. A special acknowledgment is due to CRNL staff members D. T. Nishimura, P. E. Kelly, W. L. McCrea, and D. Thompson, who made major contributions in keeping this test on schedule. The project staff would also like to thank CRNL staff members I. C. Martin and D. J. Axford for ensuring the safety of the test. The support and direction of R. Van Houten, the NRC program manager, were also appreciated.

CONTENTS

ABSTRACT	iii
SUMMARY	v
PREFACE	vii
CONTRIBUTORS	xiii
INTRODUCTION	1
EXPERIMENT DESCRIPTION	3
TEST TRAIN ASSEMBLY	3
EXPERIMENT OPERATION	6
EXPERIMENT CONDITIONS AND RESULTS	23
FUEL ROD PRESSURES AND TEMPERATURES	23
AXIAL POWER DISTRIBUTION	26
EFFECT OF STEAM COOLING VERSUS WATER COOLING ON TEST ASSEMBLY POWER	31
REFERENCES	33
APPENDIX A -TRANSIENT FUEL PRESSURES AND TEMPERATURE DURING THE MT-6A TRANSIENT	A.1
APPENDIX B -TRANSIENT FUEL CLADDING TEMPERATURE DURING THE MT-6A TRANSIENT	B.1
APPENDIX C -TRANSIENT FUEL CLADDING AND SHROUD INSIDE AND OUTSIDE TEMPERATURES DURING THE MT-6A TRANSIENT	C.1
APPENDIX D -TRANSIENT SHROUD LINER TEMPERATURES DURING THE MT-6A TRANSIENT	D.1
APPENDIX E -TRANSIENT OUTSIDE SHROUD TEMPERATURES DURING THE MT-6A TRANSIENT	E.1
APPENDIX F -TRANSIENT COOLANT TEMPERATURES DURING THE MT-6A TRANSIENT	F.1
APPENDIX G -HANGER BAR TEMPERATURES DURING THE MT-6A TRANSIENT	G.1

FIGURES

1.	Closure, Pressure, Tube, and Hanger Tube Assembly for MT-6A and MT-6B, Upper Longitudinal Section	4
2.	MT-6A Pressure Tube with Insulating Shroud and Test Fuel Assembly, Lower Longitudinal Section	5
3.	MT-6A Test Train Shroud Assembly	7
4.	MT-6A Test Assembly Cross Section	9
5.	MT-6A Instrumentation Array from Level 0 to Level 67.5	11
6.	MT-6A Instrumentation Array from Level 69 to Level 109.5	13
7.	MT-6A Instrumentation Array from Level 110.2 Through 151.5	15
8.	MT-6A Instrumentation Array from Level 156 to Level 326.3	17
9.	NRU Reactor Core Configuration	20
10.	Reflood Rates During the MT-6A Transient	21
11.	Pressures and Temperatures for Rod 4A During the MT-6A Transient	24
12.	Pressures and Temperatures for Rod 5D During the MT-6A Transient	25
13.	Comparison of MT-4 Heatup Rate-Based, SPND, Flux Wire, NRU Reactor Preconditioning, and Calculated Axial Power Profiles	27
14.	Axial Neutron Flux Distribution During the MT-6A Transient	28
15.	Axial Strain Profile for MT-4	29
16.	Partial Axial Strain Profile for MT-4	30

TABLES

1. Fuel Rod Design Variables	9
2. Instrumentation at Each Level in the MT-6A Test Assembly	19
3. Fuel Rod Rupture Times and Pressures	23

DATA REPORT:
MATERIALS TEST MT-6A

INTRODUCTION

This is the final report on the results of Materials Test 6A (MT-6A) conducted by the Pacific Northwest Laboratory (PNL) under the Loss-of-Coolant Accident (LOCA) Simulation Program, sponsored by the U.S. Nuclear Regulatory Commission (NRC). The test was conducted in 1984 at the Canadian National Research Universal (NRU) Reactor at the Chalk River Nuclear Laboratory (CRNL), operated by Atomic Energy of Canada, Ltd (AECL). It was the last of the tests under the LOCA Simulation Program.

The major objective of this program was to simulate a LOCA in a pressurized water reactor and recovery from the simulated accident, first, by causing the maximum expansion of the cladding possible from a short-term adiabatic transient to temperatures as high as 1200K (1700°F) leading to the rupture of the cladding; and, second, by then reflooding to determine the rate at which the bundle can be cooled.

For this test, the design of the 3.7-m (12-ft) long test bundle for the fuel rods was improved over the design of the test bundle used in previous MT tests. It was redesigned to minimize temperature gradients on the circumference of the cladding during the short-term adiabatic heat-up phase of the test. The purpose was to maximize the radial and axial expansion of the Zircaloy cladding on the fuel rods and the coplanar expansion of the bundle during the heat-up phase of the test. The reduced temperature gradients were to be achieved first by modifying the metallic shroud encompassing the bundle used in previous test to include thermal insulation. Then the 20 heater rods that surrounded the 12 test rods in previous tests were replaced with 9 pressurized test rods, resulting in a test bundle containing a total of 21 test fuel rods.

Supporting objectives of the test were as follows:

- Provide the fuel cladding sufficient time in the alpha-Zircaloy temperature region--1050 to 1140K (1430 to 1600°F)--to maximize expansion and to cause the fuel rods to rupture before they were cooled by reflooding.
- Provide expansion values of the cladding with a test assembly surrounded by an insulated shroud to compare with expansion values from prior tests that were performed without insulating shrouds but with heater rods.

- Expand and rupture all pressurized rods of a 21-rod bundle to compare the results with the results of the expansion and rupture characteristics and rod-to-rod mechanical interactions in a bundle in which only some of the rods were pressurized, and therefore, in which only some of the rods expanded.
- Evaluate expansion characteristics of a bundle in which all rods expand and rod-to-rod interaction can occur.
- Provide data to compare the rate of cooling of a bundle in which all fuel rods that have expanded and ruptured with the rate of cooling of the configuration in which only the 12 center rods in a 32-rod bundle expanded and ruptured.
- Compare the rate at which expanded fuel rods can be cooled in a bundle with reduced bypass potential with that of MT-4 (large bypass via the flow areas around the heater rods).
- Determine the fission power as a function of elevation along the full-length bundle in the NRU.

The following are objectives that will be useful for future tests:

- Characterize test assembly power for both a steam environment and a water environment.
- Determine the change of the fission power in the fuel bundle in the NRU reactor when the steam coolant is replaced with water coolant.

The basic objective of the test was met and the results are reported here. This report begins with a description of the experiment; included are a description of the test train assembly and of the operations. Following it is a section on experimental conditions and results. Appendixes A through G contain graphs of data acquired during the test. All the data collected during the test were recorded for time intervals of 1/5s and "written" on magnetic tape in machine language unique to the hardware and software of the computer system used. The data were then converted to VAX binary at PNL and processed to produce the plots given in this report. PNL cannot, however, ensure the future "readability" of these magnetic tapes as no provisions have been made to preserve them.

The results and analysis of previous MT tests helped support the recent NRC regulation to accept best estimate calculations for the safety analyses of LWR LOCAs. (9)

EXPERIMENT DESCRIPTION

The components of the test assembly that were used for the MT-6A experiment are described, and the instrumentation that was provided is detailed. The experiment operation is also described, and experimental conditions and results are discussed.

TEST TRAIN ASSEMBLY

The test train (including the head closure, hanger tube, and fuel assembly) was ~9 m (30 ft) long. The closure region provided the primary pressure boundary and included penetrations for numerous instrumentation leads. The hanger tube was used to suspend the fuel assembly and shroud from the head closure, and instrument leads were attached to the hanger to protect them during transport and testing. The shroud supported the fuel rods through spacer grids, served as a protective liner and insulator, contained any ballooned fuel rods, and provided proper coolant flow distribution during various stages of the experiment. A schematic of the closure and upper sections of the pressure tube and hanger tube assembly is shown in Figure 1. The stainless steel shroud consisted of two ~4-m (14-ft) long halves that were welded together. A schematic of the insulated shroud is shown in Figure 2; an assembly drawing of the shroud is shown in Figure 3. The shroud contains ZrO₂ insulation between the outer stainless steel exterior and the Zircaloy inner liner.

The fuel assembly consisted of a 5 x 5 segment of a 17 x 17 PWR fuel assembly with the four corner rods removed (Figure 4) and provided a basic fuel bundle array of 21 rods (see Table 1). All rods were pressurized just before the transient test. A helium fill pressure of 6.03 MPa (875 psia) at 295K (70°F) was used. The prepressurization provided the necessary internal cladding stresses to cause test rod rupture in the desired temperature range.

Test train instrumentation included: 8 SPNDs, 150 TCs, 21 fuel rod pressure sensors, 2 liquid level detectors, and 2 flux wires. The instrumentation was located at 46 elevations or levels along the test assembly; these levels are defined in Figure 5 and detailed in Figures 5 through 8. Instrumentation for the various levels is shown in Table 2.

Turbine flowmeters (located outside the test assembly) and TCs provided the main source of thermal-hydraulic data. Local coolant temperatures were measured with TCs that protruded into the coolant channel and with TCs attached to the shroud. TCs were also spot welded to the inside of the cladding surface. These cladding TCs monitored the cladding temperature without interference from fuel pellet chips or unintentional TC relocation.

Flux wires along the inner liner provided a measure of the fuel power distribution during the transient portion of the test. The wires were

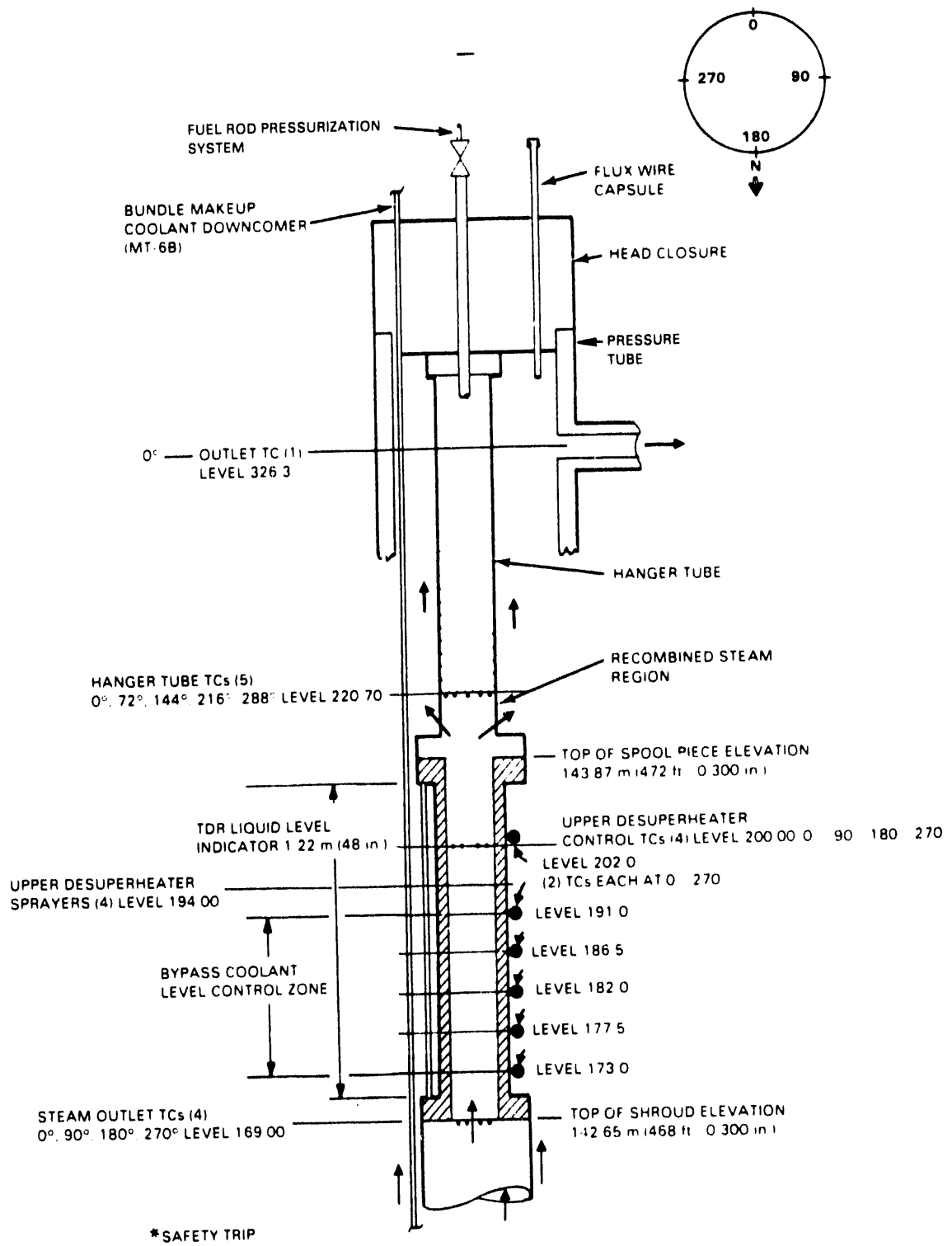


FIGURE 1. Closure, Pressure Tube, and Hanger Tube Assembly for MT-6A and MT-6B, Upper Longitudinal Section. (Levels are inches above the fuel bundle bottom tie plate.)

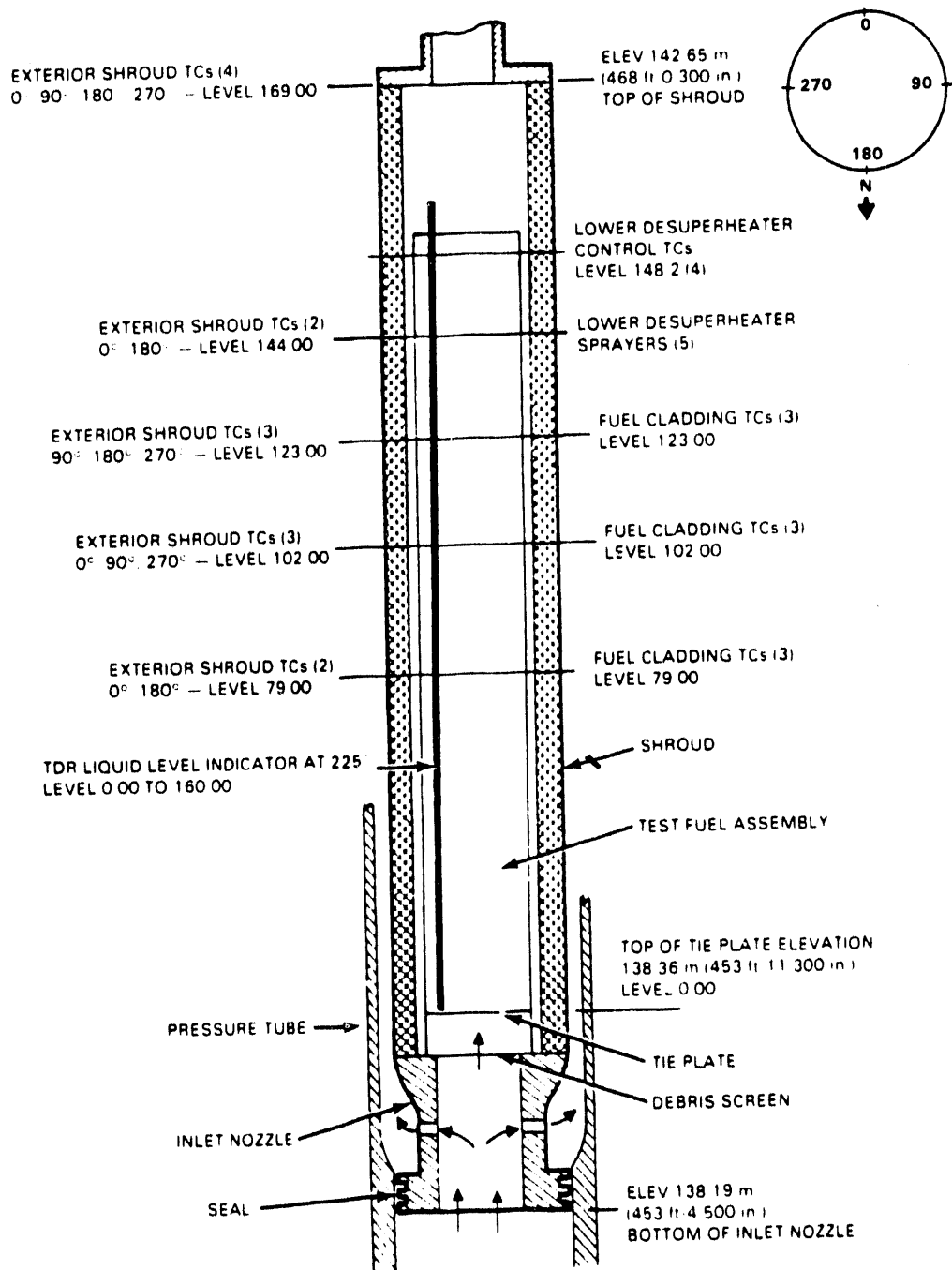


FIGURE 2. MT-6A Pressure Tube with Insulating Shroud and Test Fuel Assembly, Lower Longitudinal Section. (Levels are inches above the fuel bundle bottom tie plate.)

inserted just prior to the transient. In previous tests, flux wires were inside the fuel assembly during preconditioning and the transient.

The two liquid level detectors did not operate very well during MT-6A; therefore, liquid level data are not included in this report. The detectors are based on time domain reflectometry (TDR) and are described in more detail in (Marshall et al. (1983).

EXPERIMENT OPERATION

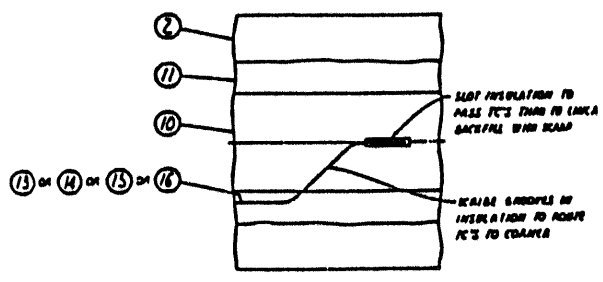
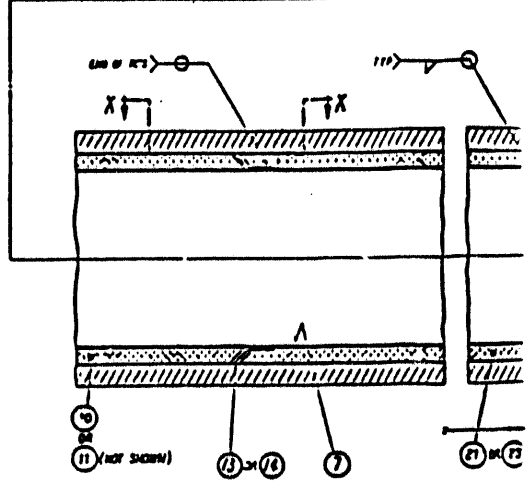
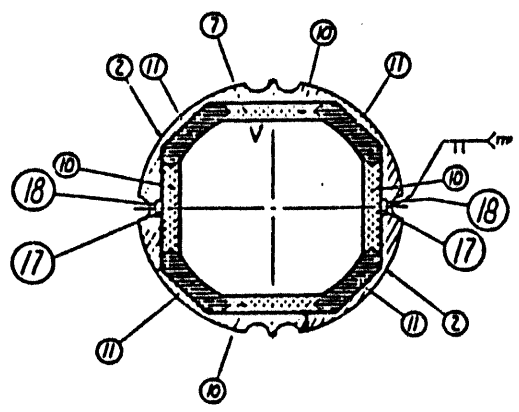
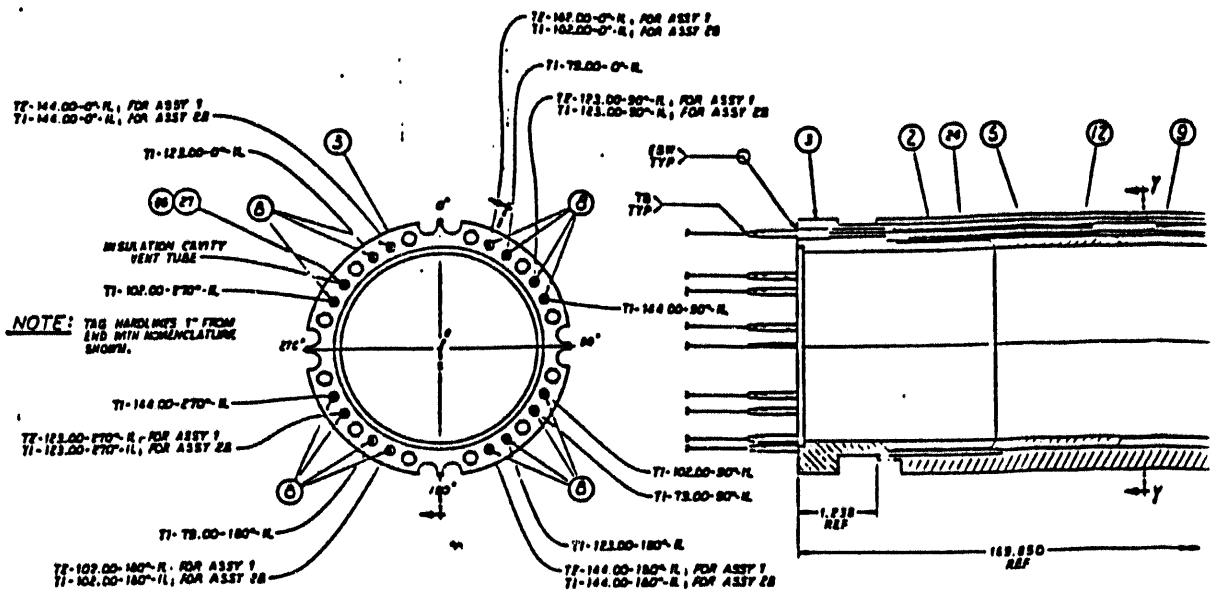
The MT-6A experiment consisted of a preconditioning phase, preliminary calibration tests, water and steam calorimetry tests, and a test in which all test rods ruptured (MT-6A). The experiment was performed in the L-24 site in the NRU reactor (Figure 9). The assembly was oriented in the reactor with side E (the side that has fuel rods designated E) facing north.

The preconditioning phase was initiated on May 23, 1984. Two rises to full NRU power operation and two conditional reactor trips assured fuel pellet cracking and good fuel/cladding mechanical contact.

Calibration tests were performed to insure proper operation and control using the LCS and the DACS. These tests calibrated reflood flow rates, delay times, and test assembly back pressures. The fuel temperature was maintained low enough so that there would be no rod deformation.

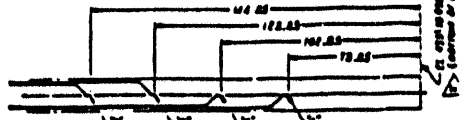
The main MT-6A test, in which all 21 pressurized test rods ruptured during the heatup phase, was performed on May 25, 1984. The conditions and results of this test are discussed in this section.

The MT-6A transient test used the LCS preprogrammed reflood rate control. After a preset reflood delay (controlled by the DACS), the LCS was programmed to control the reflood rate at 0.20 m/s (8 in./s) for 3 s, 0.18 m/s (7 in./s) for 3s, 0.051 m/s (2 in./s) for 3 s. At that time, the DACS was supposed to take over reflood control to maintain fuel temperatures approximately constant. An anomaly in the reflood control prevented the DACS from taking control once the reflood rate reached 0.051 m/s (2 in./s). The continued reflood at this rate caused the fuel to cool and quench, ending the test. The reflood rates are shown in Figure 10.



SECTION X-X
TYPICAL INSULATION ASSEMBLY

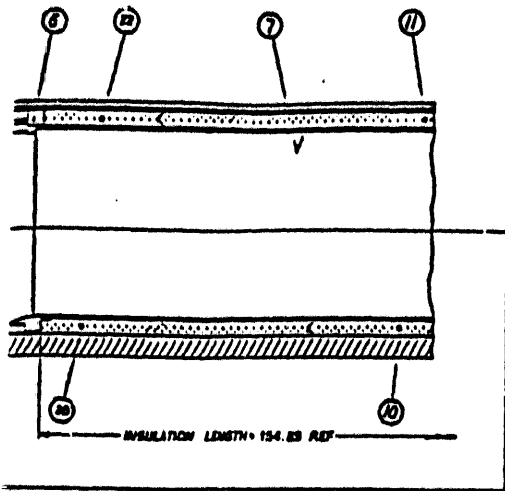
- 1 MT-6B ASSEMBLY
SEE INSTRUMENT LOCATIONS DETAIL (BELOW) & SECTIONS "X-X" THRU "Y-Y" (SHEET 2).
- 2B MT-6A ASSEMBLY
SEE ASSY 1 & 2 DETAIL WITHOUT TYPICAL IC'S AS CALLED OUT ON SHEET 1 & 2.



INSTRUMENT	IC'S	12°	180°	180°	180°
11	TI-144.00-0°-R	TI-144.00-0°-R	TI-144.00-0°-R	TI-144.00-0°-R	TI-144.00-0°-R
12	TI-123.00-0°-R	TI-123.00-0°-R	TI-123.00-0°-R	TI-123.00-0°-R	TI-123.00-0°-R
13	TI-102.00-0°-R	TI-102.00-0°-R	TI-102.00-0°-R	TI-102.00-0°-R	TI-102.00-0°-R
14	TI-144.00-90°-R	TI-144.00-90°-R	TI-144.00-90°-R	TI-144.00-90°-R	TI-144.00-90°-R
15	TI-123.00-90°-R	TI-123.00-90°-R	TI-123.00-90°-R	TI-123.00-90°-R	TI-123.00-90°-R
16	TI-102.00-90°-R	TI-102.00-90°-R	TI-102.00-90°-R	TI-102.00-90°-R	TI-102.00-90°-R
17	TI-144.00-180°-R	TI-144.00-180°-R	TI-144.00-180°-R	TI-144.00-180°-R	TI-144.00-180°-R
18	TI-123.00-180°-R	TI-123.00-180°-R	TI-123.00-180°-R	TI-123.00-180°-R	TI-123.00-180°-R

INSTRUMENT LOCATIONS

FIGURE 3. MT-6A Tes



QTY	DESCRIPTION	REF
1	MT-6B ASSEMBLY	
2	1ST SHELL	1011 3
1	TOP FLANGE	6
1	ASTRON FLANGE	6
2	END-TO-END TRANSITION	6
2	END ADAPTER	7
1	LINER	4
16	INSTA-PROT ADAPTER	10
4	END-UP GIRD	9
100	SIDE INSULATION	12
124	CORNER INSULATION	12
4	FILLER BLOCK	SHEET 11
16	WINDUP BRACKET	SEE NOTE 6
2	END BRACKET	SEE NOTE 6
2		PH 6
2		PH 6
2	SIDE BRACKET	SEE NOTE 6
12	12	11
16	16	11
4	4	19
4	4	20
4	4	21
4	4	22
4	4	23
1	1	24
1	1	25
1	1	26
1	1	27
2	2	28

GENERAL NOTES
(SMALL DIMENSIONS UNLESS NOTED)

- ALL DIMENSIONS ARE IN INCHES.
- DEFLECTIONS AND TOLERANCES ARE IN ACCORDANCE WITH ANSI Y14.3.
- ALL DIMENSIONS UNLESS AS NOTED IN ACCORDANCE WITH ANSI Y14.3.
- REMOVE ALL SHARP AND RADIUS ALL SHARP EDGES.
- FOLLOWERS: 1.1, 1.2, 1.3, 1.4, 1.5, 1.6, 1.7, 1.8, 1.9, 2.0, 2.1, 2.2, 2.3, 2.4, 2.5, 2.6, 2.7, 2.8, 2.9, 3.0, 3.1, 3.2, 3.3, 3.4, 3.5, 3.6, 3.7, 3.8, 3.9, 4.0, 4.1, 4.2, 4.3, 4.4, 4.5, 4.6, 4.7, 4.8, 4.9, 5.0, 5.1, 5.2, 5.3, 5.4, 5.5, 5.6, 5.7, 5.8, 5.9, 6.0, 6.1, 6.2, 6.3, 6.4, 6.5, 6.6, 6.7, 6.8, 6.9, 7.0, 7.1, 7.2, 7.3, 7.4, 7.5, 7.6, 7.7, 7.8, 7.9, 8.0, 8.1, 8.2, 8.3, 8.4, 8.5, 8.6, 8.7, 8.8, 8.9, 9.0, 9.1, 9.2, 9.3, 9.4, 9.5, 9.6, 9.7, 9.8, 9.9, 10.0, 10.1, 10.2, 10.3, 10.4, 10.5, 10.6, 10.7, 10.8, 10.9, 11.0, 11.1, 11.2, 11.3, 11.4, 11.5, 11.6, 11.7, 11.8, 11.9, 12.0, 12.1, 12.2, 12.3, 12.4, 12.5, 12.6, 12.7, 12.8, 12.9, 13.0, 13.1, 13.2, 13.3, 13.4, 13.5, 13.6, 13.7, 13.8, 13.9, 14.0, 14.1, 14.2, 14.3, 14.4, 14.5, 14.6, 14.7, 14.8, 14.9, 15.0, 15.1, 15.2, 15.3, 15.4, 15.5, 15.6, 15.7, 15.8, 15.9, 16.0, 16.1, 16.2, 16.3, 16.4, 16.5, 16.6, 16.7, 16.8, 16.9, 17.0, 17.1, 17.2, 17.3, 17.4, 17.5, 17.6, 17.7, 17.8, 17.9, 18.0, 18.1, 18.2, 18.3, 18.4, 18.5, 18.6, 18.7, 18.8, 18.9, 19.0, 19.1, 19.2, 19.3, 19.4, 19.5, 19.6, 19.7, 19.8, 19.9, 20.0, 20.1, 20.2, 20.3, 20.4, 20.5, 20.6, 20.7, 20.8, 20.9, 21.0, 21.1, 21.2, 21.3, 21.4, 21.5, 21.6, 21.7, 21.8, 21.9, 22.0, 22.1, 22.2, 22.3, 22.4, 22.5, 22.6, 22.7, 22.8, 22.9, 23.0, 23.1, 23.2, 23.3, 23.4, 23.5, 23.6, 23.7, 23.8, 23.9, 24.0, 24.1, 24.2, 24.3, 24.4, 24.5, 24.6, 24.7, 24.8, 24.9, 25.0, 25.1, 25.2, 25.3, 25.4, 25.5, 25.6, 25.7, 25.8, 25.9, 26.0, 26.1, 26.2, 26.3, 26.4, 26.5, 26.6, 26.7, 26.8, 26.9, 27.0, 27.1, 27.2, 27.3, 27.4, 27.5, 27.6, 27.7, 27.8, 27.9, 28.0, 28.1, 28.2, 28.3, 28.4, 28.5, 28.6, 28.7, 28.8, 28.9, 29.0, 29.1, 29.2, 29.3, 29.4, 29.5, 29.6, 29.7, 29.8, 29.9, 30.0, 30.1, 30.2, 30.3, 30.4, 30.5, 30.6, 30.7, 30.8, 30.9, 31.0, 31.1, 31.2, 31.3, 31.4, 31.5, 31.6, 31.7, 31.8, 31.9, 32.0, 32.1, 32.2, 32.3, 32.4, 32.5, 32.6, 32.7, 32.8, 32.9, 33.0, 33.1, 33.2, 33.3, 33.4, 33.5, 33.6, 33.7, 33.8, 33.9, 34.0, 34.1, 34.2, 34.3, 34.4, 34.5, 34.6, 34.7, 34.8, 34.9, 35.0, 35.1, 35.2, 35.3, 35.4, 35.5, 35.6, 35.7, 35.8, 35.9, 36.0, 36.1, 36.2, 36.3, 36.4, 36.5, 36.6, 36.7, 36.8, 36.9, 37.0, 37.1, 37.2, 37.3, 37.4, 37.5, 37.6, 37.7, 37.8, 37.9, 38.0, 38.1, 38.2, 38.3, 38.4, 38.5, 38.6, 38.7, 38.8, 38.9, 39.0, 39.1, 39.2, 39.3, 39.4, 39.5, 39.6, 39.7, 39.8, 39.9, 40.0, 40.1, 40.2, 40.3, 40.4, 40.5, 40.6, 40.7, 40.8, 40.9, 41.0, 41.1, 41.2, 41.3, 41.4, 41.5, 41.6, 41.7, 41.8, 41.9, 42.0, 42.1, 42.2, 42.3, 42.4, 42.5, 42.6, 42.7, 42.8, 42.9, 43.0, 43.1, 43.2, 43.3, 43.4, 43.5, 43.6, 43.7, 43.8, 43.9, 44.0, 44.1, 44.2, 44.3, 44.4, 44.5, 44.6, 44.7, 44.8, 44.9, 45.0, 45.1, 45.2, 45.3, 45.4, 45.5, 45.6, 45.7, 45.8, 45.9, 46.0, 46.1, 46.2, 46.3, 46.4, 46.5, 46.6, 46.7, 46.8, 46.9, 47.0, 47.1, 47.2, 47.3, 47.4, 47.5, 47.6, 47.7, 47.8, 47.9, 48.0, 48.1, 48.2, 48.3, 48.4, 48.5, 48.6, 48.7, 48.8, 48.9, 49.0, 49.1, 49.2, 49.3, 49.4, 49.5, 49.6, 49.7, 49.8, 49.9, 50.0, 50.1, 50.2, 50.3, 50.4, 50.5, 50.6, 50.7, 50.8, 50.9, 51.0, 51.1, 51.2, 51.3, 51.4, 51.5, 51.6, 51.7, 51.8, 51.9, 52.0, 52.1, 52.2, 52.3, 52.4, 52.5, 52.6, 52.7, 52.8, 52.9, 53.0, 53.1, 53.2, 53.3, 53.4, 53.5, 53.6, 53.7, 53.8, 53.9, 54.0, 54.1, 54.2, 54.3, 54.4, 54.5, 54.6, 54.7, 54.8, 54.9, 55.0, 55.1, 55.2, 55.3, 55.4, 55.5, 55.6, 55.7, 55.8, 55.9, 56.0, 56.1, 56.2, 56.3, 56.4, 56.5, 56.6, 56.7, 56.8, 56.9, 57.0, 57.1, 57.2, 57.3, 57.4, 57.5, 57.6, 57.7, 57.8, 57.9, 58.0, 58.1, 58.2, 58.3, 58.4, 58.5, 58.6, 58.7, 58.8, 58.9, 59.0, 59.1, 59.2, 59.3, 59.4, 59.5, 59.6, 59.7, 59.8, 59.9, 60.0, 60.1, 60.2, 60.3, 60.4, 60.5, 60.6, 60.7, 60.8, 60.9, 61.0, 61.1, 61.2, 61.3, 61.4, 61.5, 61.6, 61.7, 61.8, 61.9, 62.0, 62.1, 62.2, 62.3, 62.4, 62.5, 62.6, 62.7, 62.8, 62.9, 63.0, 63.1, 63.2, 63.3, 63.4, 63.5, 63.6, 63.7, 63.8, 63.9, 64.0, 64.1, 64.2, 64.3, 64.4, 64.5, 64.6, 64.7, 64.8, 64.9, 65.0, 65.1, 65.2, 65.3, 65.4, 65.5, 65.6, 65.7, 65.8, 65.9, 66.0, 66.1, 66.2, 66.3, 66.4, 66.5, 66.6, 66.7, 66.8, 66.9, 67.0, 67.1, 67.2, 67.3, 67.4, 67.5, 67.6, 67.7, 67.8, 67.9, 68.0, 68.1, 68.2, 68.3, 68.4, 68.5, 68.6, 68.7, 68.8, 68.9, 69.0, 69.1, 69.2, 69.3, 69.4, 69.5, 69.6, 69.7, 69.8, 69.9, 70.0, 70.1, 70.2, 70.3, 70.4, 70.5, 70.6, 70.7, 70.8, 70.9, 71.0, 71.1, 71.2, 71.3, 71.4, 71.5, 71.6, 71.7, 71.8, 71.9, 72.0, 72.1, 72.2, 72.3, 72.4, 72.5, 72.6, 72.7, 72.8, 72.9, 73.0, 73.1, 73.2, 73.3, 73.4, 73.5, 73.6, 73.7, 73.8, 73.9, 74.0, 74.1, 74.2, 74.3, 74.4, 74.5, 74.6, 74.7, 74.8, 74.9, 75.0, 75.1, 75.2, 75.3, 75.4, 75.5, 75.6, 75.7, 75.8, 75.9, 76.0, 76.1, 76.2, 76.3, 76.4, 76.5, 76.6, 76.7, 76.8, 76.9, 77.0, 77.1, 77.2, 77.3, 77.4, 77.5, 77.6, 77.7, 77.8, 77.9, 78.0, 78.1, 78.2, 78.3, 78.4, 78.5, 78.6, 78.7, 78.8, 78.9, 79.0, 79.1, 79.2, 79.3, 79.4, 79.5, 79.6, 79.7, 79.8, 79.9, 80.0, 80.1, 80.2, 80.3, 80.4, 80.5, 80.6, 80.7, 80.8, 80.9, 81.0, 81.1, 81.2, 81.3, 81.4, 81.5, 81.6, 81.7, 81.8, 81.9, 82.0, 82.1, 82.2, 82.3, 82.4, 82.5, 82.6, 82.7, 82.8, 82.9, 83.0, 83.1, 83.2, 83.3, 83.4, 83.5, 83.6, 83.7, 83.8, 83.9, 84.0, 84.1, 84.2, 84.3, 84.4, 84.5, 84.6, 84.7, 84.8, 84.9, 85.0, 85.1, 85.2, 85.3, 85.4, 85.5, 85.6, 85.7, 85.8, 85.9, 86.0, 86.1, 86.2, 86.3, 86.4, 86.5, 86.6, 86.7, 86.8, 86.9, 87.0, 87.1, 87.2, 87.3, 87.4, 87.5, 87.6, 87.7, 87.8, 87.9, 88.0, 88.1, 88.2, 88.3, 88.4, 88.5, 88.6, 88.7, 88.8, 88.9, 89.0, 89.1, 89.2, 89.3, 89.4, 89.5, 89.6, 89.7, 89.8, 89.9, 90.0, 90.1, 90.2, 90.3, 90.4, 90.5, 90.6, 90.7, 90.8, 90.9, 91.0, 91.1, 91.2, 91.3, 91.4, 91.5, 91.6, 91.7, 91.8, 91.9, 92.0, 92.1, 92.2, 92.3, 92.4, 92.5, 92.6, 92.7, 92.8, 92.9, 93.0, 93.1, 93.2, 93.3, 93.4, 93.5, 93.6, 93.7, 93.8, 93.9, 94.0, 94.1, 94.2, 94.3, 94.4, 94.5, 94.6, 94.7, 94.8, 94.9, 95.0, 95.1, 95.2, 95.3, 95.4, 95.5, 95.6, 95.7, 95.8, 95.9, 96.0, 96.1, 96.2, 96.3, 96.4, 96.5, 96.6, 96.7, 96.8, 96.9, 97.0, 97.1, 97.2, 97.3, 97.4, 97.5, 97.6, 97.7, 97.8, 97.9, 98.0, 98.1, 98.2, 98.3, 98.4, 98.5, 98.6, 98.7, 98.8, 98.9, 99.0, 99.1, 99.2, 99.3, 99.4, 99.5, 99.6, 99.7, 99.8, 99.9, 100.0, 100.1, 100.2, 100.3, 100.4, 100.5, 100.6, 100.7, 100.8, 100.9, 101.0, 101.1, 101.2, 101.3, 101.4, 101.5, 101.6, 101.7, 101.8, 101.9, 102.0, 102.1, 102.2, 102.3, 102.4, 102.5, 102.6, 102.7, 102.8, 102.9, 103.0, 103.1, 103.2, 103.3, 103.4, 103.5, 103.6, 103.7, 103.8, 103.9, 104.0, 104.1, 104.2, 104.3, 104.4, 104.5, 104.6, 104.7, 104.8, 104.9, 105.0, 105.1, 105.2, 105.3, 105.4, 105.5, 105.6, 105.7, 105.8, 105.9, 106.0, 106.1, 106.2, 106.3, 106.4, 106.5, 106.6, 106.7, 106.8, 106.9, 107.0, 107.1, 107.2, 107.3, 107.4, 107.5, 107.6, 107.7, 107.8, 107.9, 108.0, 108.1, 108.2, 108.3, 108.4, 108.5, 108.6, 108.7, 108.8, 108.9, 109.0, 109.1, 109.2, 109.3, 109.4, 109.5, 109.6, 109.7, 109.8, 109.9, 110.0, 110.1, 110.2, 110.3, 110.4, 110.5, 110.6, 110.7, 110.8, 110.9, 111.0, 111.1, 111.2, 111.3, 111.4, 111.5, 111.6, 111.7, 111.8, 111.9, 112.0, 112.1, 112.2, 112.3, 112.4, 112.5, 112.6, 112.7, 112.8, 112.9, 113.0, 113.1, 113.2, 113.3, 113.4, 113.5, 113.6, 113.7, 113.8, 113.9, 114.0, 114.1, 114.2, 114.3, 114.4, 114.5, 114.6, 114.7, 114.8, 114.9, 115.0, 115.1, 115.2, 115.3, 115.4, 115.5, 115.6, 115.7, 115.8, 115.9, 116.0, 116.1, 116.2, 116.3, 116.4, 116.5, 116.6, 116.7, 116.8, 116.9, 117.0, 117.1, 117.2, 117.3, 117.4, 117.5, 117.6, 117.7, 117.8, 117.9, 118.0, 118.1, 118.2, 118.3, 118.4, 118.5, 118.6, 118.7, 118.8, 118.9, 119.0, 119.1, 119.2, 119.3, 119.4, 119.5, 119.6, 119.7, 119.8, 119.9, 120.0, 120.1, 120.2, 120.3, 120.4, 120.5, 120.6, 120.7, 120.8, 120.9, 121.0, 121.1, 121.2, 121.3, 121.4, 121.5, 121.6, 121.7, 121.8, 121.9, 122.0, 122.1, 122.2, 122.3, 122.4, 122.5, 122.6, 122.7, 122.8, 122.9, 123.0, 123.1, 123.2, 123.3, 123.4, 123.5, 123.6, 123.7, 123.8, 123.9, 124.0, 124.1, 124.2, 124.3, 124.4, 124.5, 124.6, 124.7, 124.8, 124.9, 125.0, 125.1, 125.2, 125.3, 125.4, 125.5, 125.6, 125.7, 125.8, 125.9, 126.0, 126.1, 126.2, 126.3, 126.4, 126.5, 126.6, 126.7, 126.8, 126.9, 127.0, 127.1, 127.2, 127.3, 127.4, 127.5, 127.6, 127.7, 127.8, 127.9, 128.0, 128.1, 128.2, 128.3, 128.4, 128.5, 128.6, 128.7, 128.8, 128.9, 129.0, 129.1, 129.2, 129.3, 129.4, 129.5, 129.6, 129.7, 129.8, 129.9, 130.0, 130.1, 130.2, 130.3, 130.4, 130.5, 130.6, 130.7, 130.8, 130.9, 131.0, 131.1, 131.2, 131.3, 131.4, 131.5, 131.6, 131.7, 131.8, 131.9, 132.0, 132.1, 132.2, 132.3, 132.4, 132.5, 132.6, 132.7, 132.8, 132.9, 133.0, 133.1, 133.2, 133.3, 133.4, 133.5, 133.6, 133.7, 133.8, 133.9, 134.0, 134.1, 134.2, 134.3, 134.4, 134.5, 134.6, 134.7, 134.8, 134.9, 135.0, 135.1, 135.2, 135.3, 135.4, 135.5, 135.6, 135.7, 135.8, 135.9, 136.0, 136.1, 136.2, 136.3, 136.4, 136.5, 136.6, 136.7, 136.8, 136.9, 137.0, 137.1, 137.2, 137.3, 137.4, 137.5, 137.6, 137.7, 137.8, 137.9, 138.0, 138.1, 138.2, 138.3, 138.4, 138.5, 138.6, 138.7, 138.8, 138.9, 139.0, 139.1, 139.2, 139.3, 139.4, 139.5, 139.6, 139.7, 139.8, 139.9, 140.0, 140.1, 140.2, 140.3, 140.4, 140.5, 140.6, 140.7, 140.8, 140.9, 141.0, 141.1, 141.2, 141.3, 141.4, 141.5, 141.6, 141.7, 141.8, 141.9, 142.0, 142.1, 142.2, 142.3, 142.4, 142.5, 142.6, 142.7, 142.8, 142.9, 143.0, 143.1, 143.2, 143.3, 143.4, 143.5, 143.6, 143.7, 143.8, 143.9, 144.0, 144.1, 144.2, 144.3, 144.4, 144.5, 144.6, 144.7, 144.8, 144.9, 145.0, 145.1, 145.2, 145.3, 145.4, 145.5, 145.6, 145.7, 145.8, 145.9, 146.0, 146.1, 146.2, 146.3, 146.4, 146.5, 146.6, 146.7, 146.8, 146.9, 147.0, 147.1, 147.2, 147.3, 147.4, 147.5, 147.6, 147.7, 147.8, 147.9, 148.0, 148.1, 148.2, 148.3, 148.4, 148.5, 148.6, 148.7, 148.8, 148.9, 149.0, 149.1, 149.2, 149.3, 149.4, 149.5, 149.6, 149.7, 149.8, 149.9, 150.0, 150.1, 150.2, 150.3, 150.4, 150.5, 150.6, 150.7, 150.8, 150.9, 151.0, 151.1, 151.2, 151.3, 151.4, 151.5, 151.6, 151.7, 151.8, 151.9, 152.0, 152.1, 152.2, 152.3, 152.4, 152.5, 152.6, 152.7, 152.8, 152.9, 153.0, 153.1, 153.2, 153.3, 153.4, 153.5, 153.6, 153.7, 153.8, 153.9, 154.0, 154.1, 154.2, 154.3, 154.4, 154.5, 154.6, 154.7, 154.8, 154.9, 155.0, 155.1, 155.2, 155.3, 155.4, 155.5, 155.6, 155.7, 155.8, 155.9, 156.0, 156.1, 156.2, 156.3, 156.4, 156.5, 156.6, 156.7, 156.8, 156.9, 157.0, 157.1, 157.2, 157.3, 157.4, 157.5, 157.6, 157.7, 157.8, 157.9, 158.0, 158.1, 158.2, 158.3, 158.4, 158.5, 158.6, 158.7, 158.8, 158.9, 159.0, 159.1, 159.2, 159.3, 159.4, 159.5, 159.6, 159.7, 159.8, 159.9, 160.0, 160.1, 160.2, 160.3, 160.4, 160.5, 160.6, 160.7, 160.8, 160.9, 161.0, 161.1, 161.2, 161.3, 161.4, 161.5, 161.6, 161.7, 161.8, 161.9, 162.0, 162.1, 162.2, 162.3, 162.4, 162.5, 162.6, 162.7, 162.8, 162.9, 163.0, 163.1, 163.2, 163.3, 163.4, 163.5, 163.6, 163.7, 163.8, 163.9, 164.0, 164.1, 164.2, 164.3, 164.4, 164.5, 164.6, 164.7, 164.8, 164.9, 165.0, 165.1, 165.2, 165.3, 165.4, 165.5, 165.6, 165.7, 165.8, 165.9, 166.0, 166.1, 166.2, 166.3, 166.4, 166.5, 166.6, 166.7, 166.8, 166.9, 167.0, 167.1, 167.2, 167.3, 167.4, 167.5, 167.6, 167.7, 167.8, 167.9, 168.0, 168.1, 168.2, 168.3, 168.4, 168.5, 168.6, 168.7, 168.8, 168.9, 169.0, 169.1, 169.2, 169.3, 169.4, 169.5, 169.6, 169.7, 169.8, 169.9, 170.0, 170.1, 170.2, 170.3, 170.4, 170.5, 170.6, 170.7, 170.8, 170.9, 171.0, 171.1, 171.2, 171.3, 171.4, 171.5, 171.6, 171.7, 171.8, 171.9, 172.0, 172.1, 172.2, 172.3, 172.4, 172.5, 172.6, 172.7, 172.8, 172.9, 173.0, 173.1, 173.2, 173.3, 173.4, 173.5, 173.6, 173.7, 173.8, 173.9, 174.0, 174.1, 174.2, 174.3, 174.4, 174.5, 174.6, 174.7, 174.8, 174.9, 175.0, 175.1, 175.2, 175.3, 175.4, 175

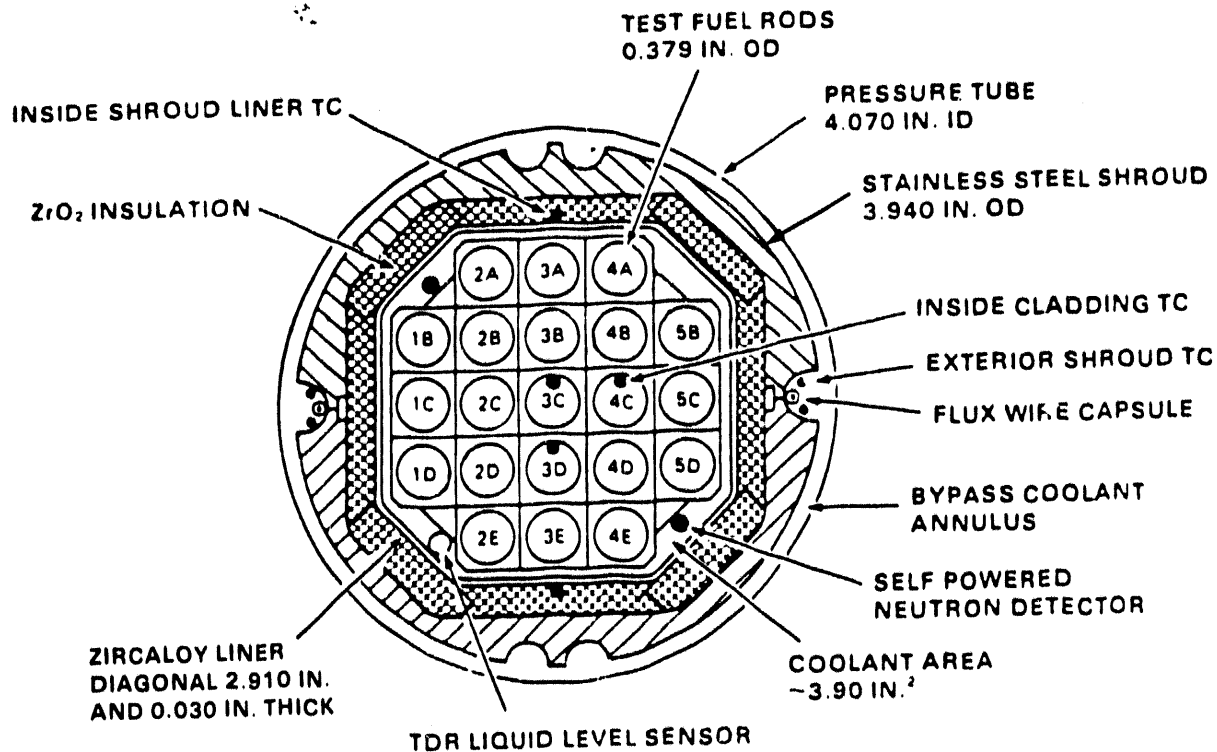


FIGURE 4. MT-6A Test Assembly Cross Section

TABLE 1. Fuel Rod Design Variables

Cladding material	Zircaloy-4
Cladding outside diameter (OD)	0.963 cm (0.379 in.)
Cladding inside diameter (ID)	0.841 cm (0.331 in.)
Pitch (rod to rod)	1.275 cm (0.502 in.)
Fuel pellet OD	0.826 cm (0.325 in.)
Fuel pellet length	0.953 cm (0.375 in.)
Active fuel length	3.66 m (12 ft)
Total shroud length	4.33 m (14.18 ft)
Helium pressurization	6.03 MPa (875 psia) at 295K (70°F)
Fuel enrichment	2.93% ²³⁵ U

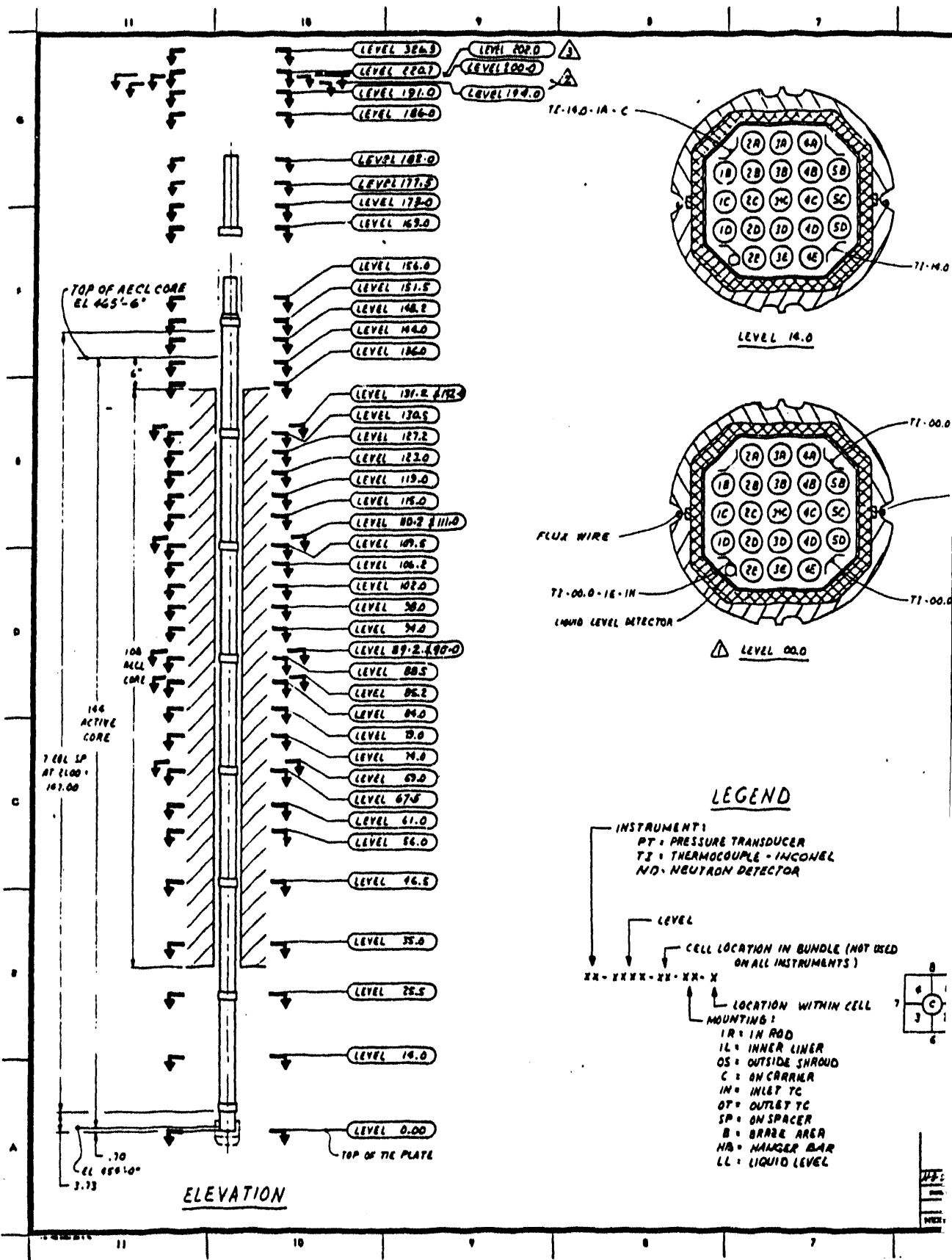
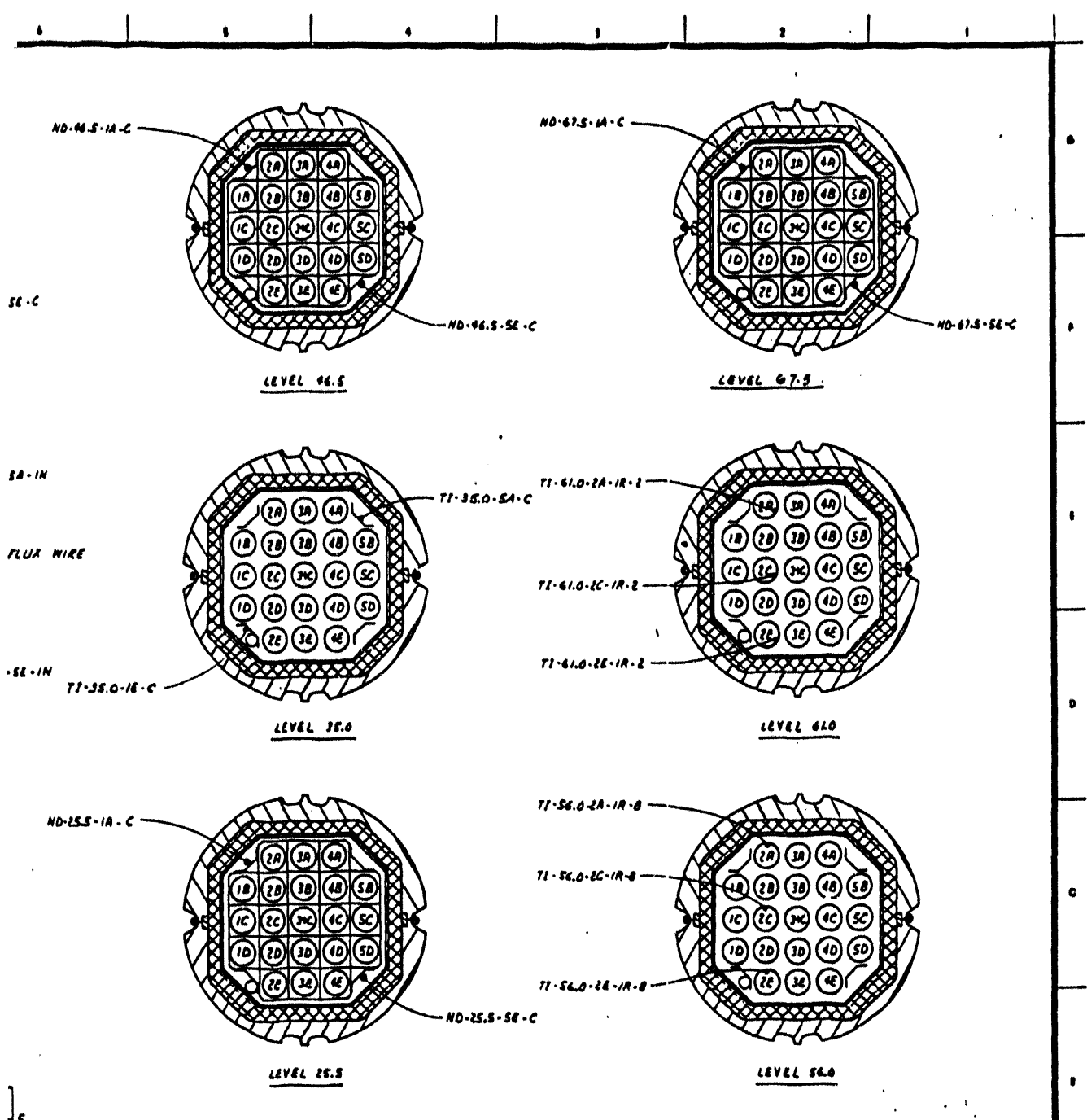


FIGURE 5. MT-6A Instrumentation



DRAWING INDEX		REVISIONS		APPROVED		DATE	
1							
2							
3							
4							
5							
6							
7							
8							
9							
10							
11							
12							
13							
14							
15							
16							
17							
18							
19							
20							
21							
22							
23							
24							
25							
26							
27							
28							
29							
30							
31							
32							
33							
34							
35							
36							
37							
38							
39							
40							
41							
42							
43							
44							
45							
46							
47							
48							
49							
50							
51							
52							
53							
54							
55							
56							
57							
58							
59							
60							
61							
62							
63							
64							
65							
66							
67							
68							
69							
70							
71							
72							
73							
74							
75							
76							
77							
78							
79							
80							
81							
82							
83							
84							
85							
86							
87							
88							
89							
90							
91							
92							
93							
94							
95							
96							
97							
98							
99							
100							

Array from Level 0 to Level 67.5

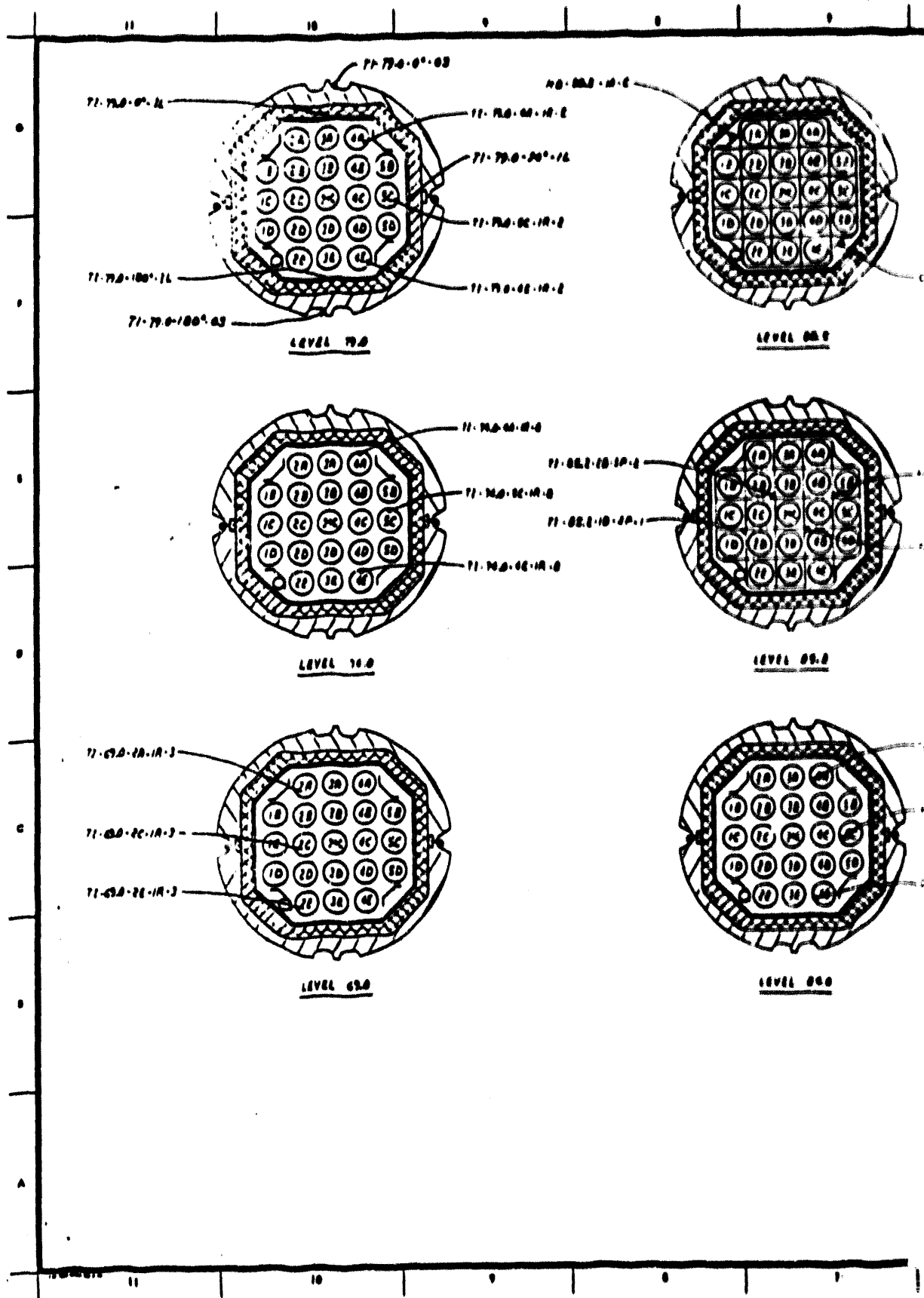


FIGURE 6. MT-6A Instrumentation A

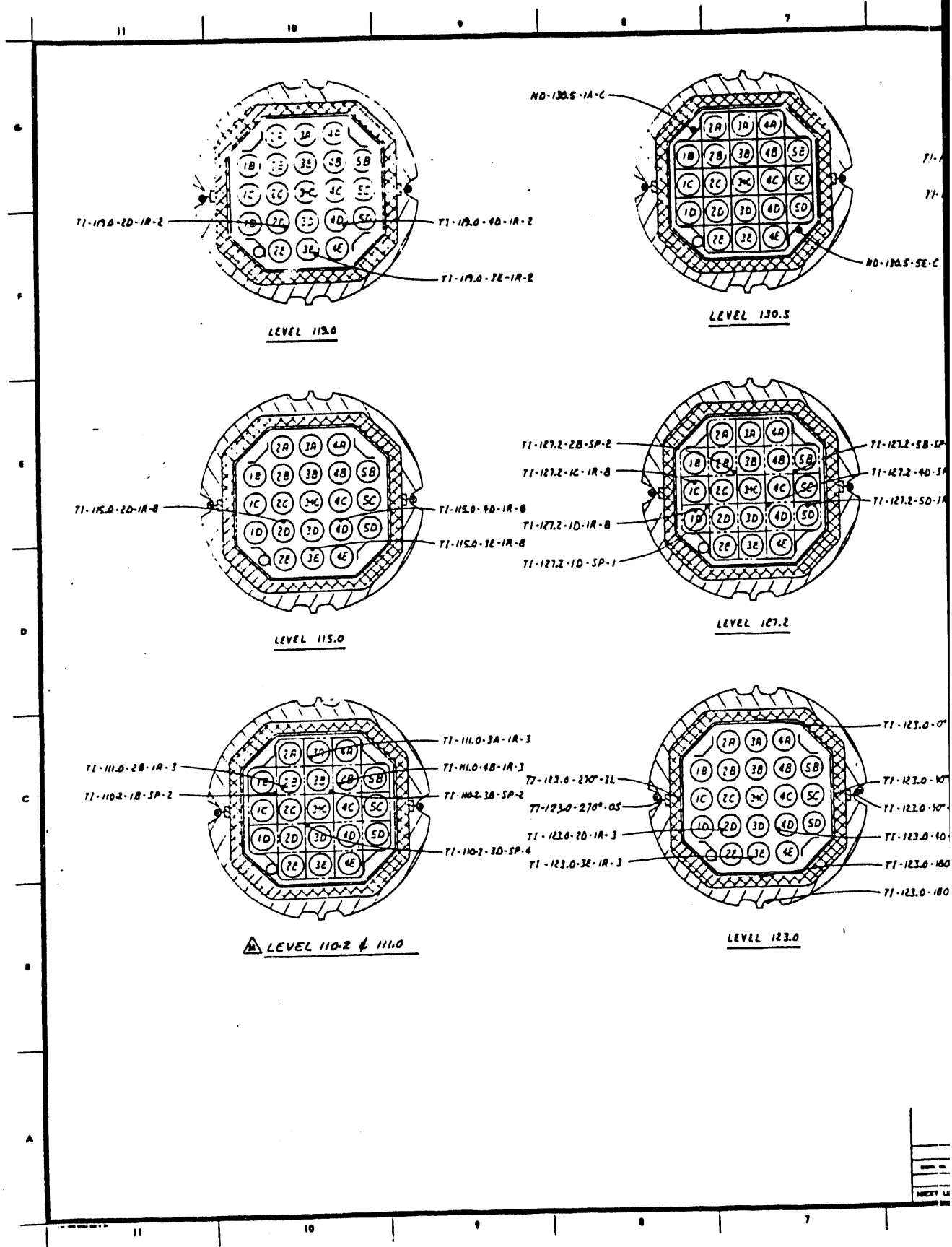
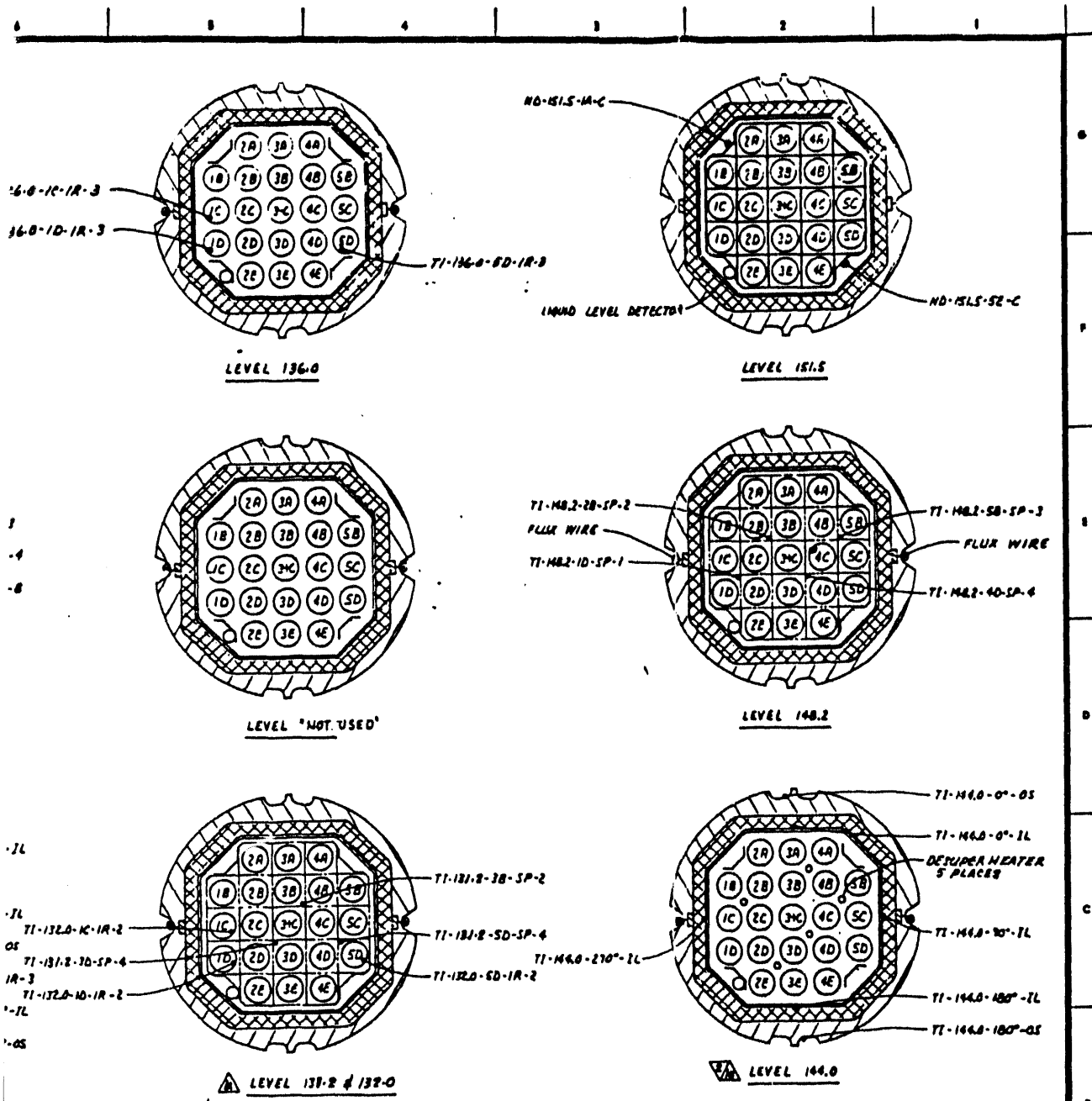


FIGURE 7. MT-6A Instrumentation Arrangement



▲ LEVEL 137.2 & 137.0

▲ LEVEL 144.0

REVISIONS NO. DATE BY DESCRIPTION 1 11/15/54 J. H. W. HEATER AT 144.0 2 1/16/55 J. H. W. HEATER AT 144.0 3 1/16/55 J. H. W. HEATER AT 144.0 4 1/16/55 J. H. W. HEATER AT 144.0 5 1/16/55 J. H. W. HEATER AT 144.0 6 1/16/55 J. H. W. HEATER AT 144.0 7 1/16/55 J. H. W. HEATER AT 144.0 8 1/16/55 J. H. W. HEATER AT 144.0 9 1/16/55 J. H. W. HEATER AT 144.0 10 1/16/55 J. H. W. HEATER AT 144.0		JOP# 1045 U. S. ATOMIC ENERGY COMMISSION RICHLAND OPERATIONS OFFICE PACIFIC NORTHWEST LABORATORY (OPERATED BY BATTELLE MEMORIAL INSTITUTE) MT-6A TEST TRAIN INSTRUMENTATION ARRAY NRU-CB & DPT 77R 2300 H-3-54152 3 4	
DRAWING STATUS NONE		H-3-54152 3 4	

ay from Level 110.2 Through 151.5

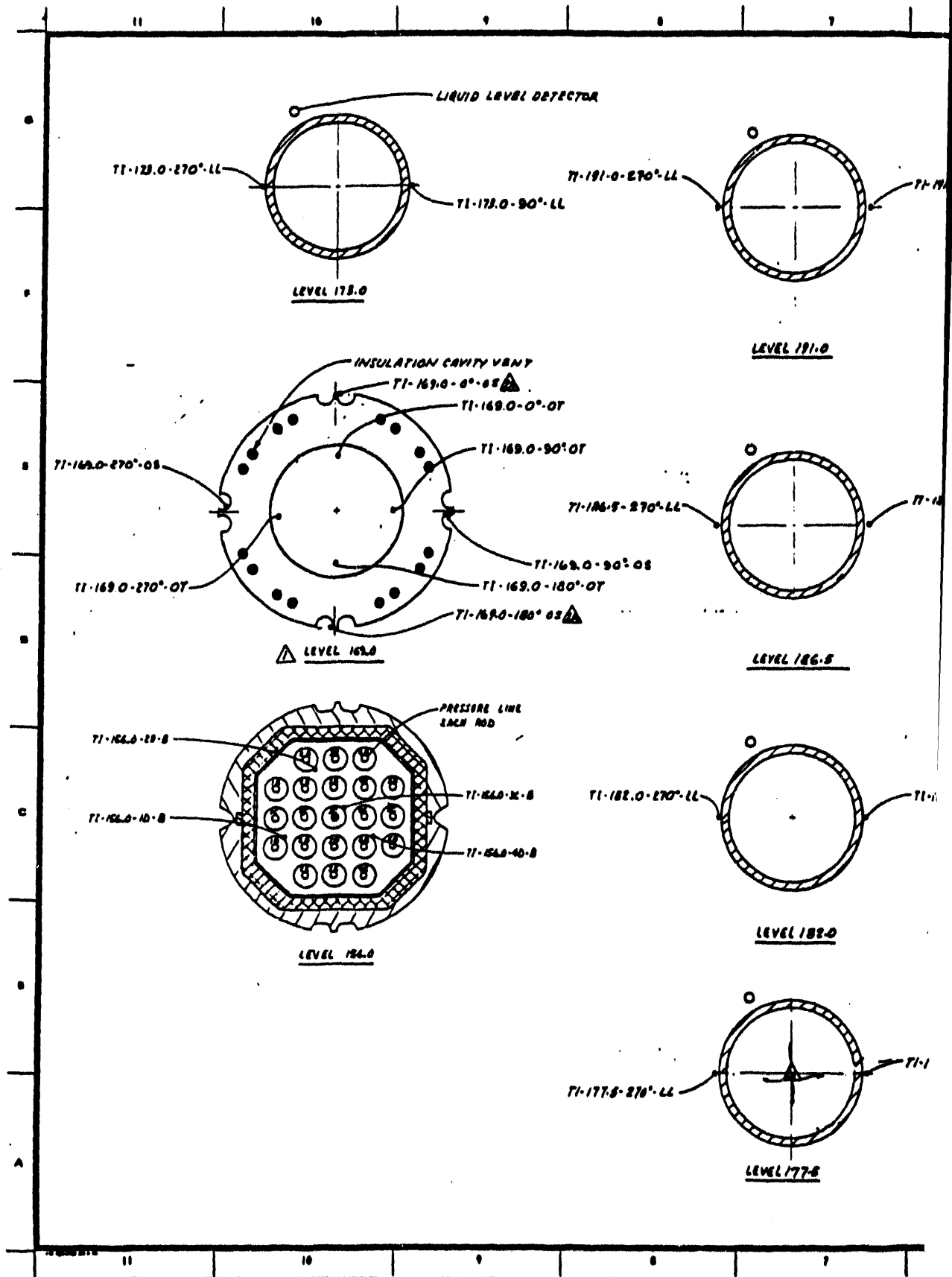
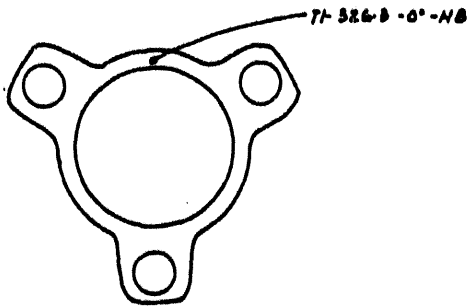
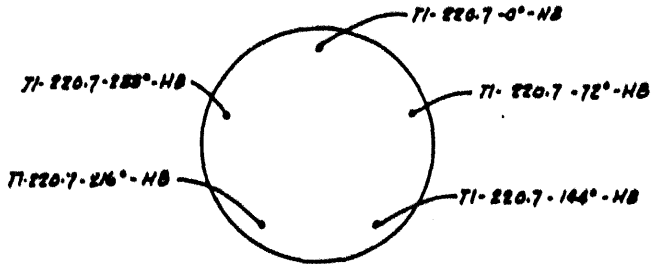


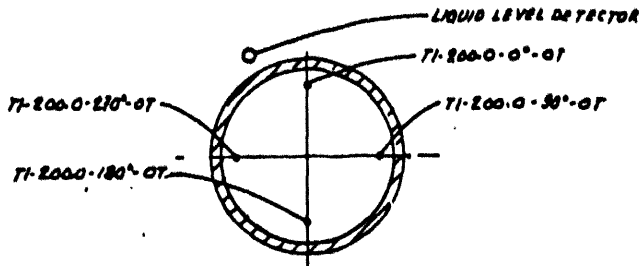
FIGURE 8. MT-6A Instrumentation Arrangement



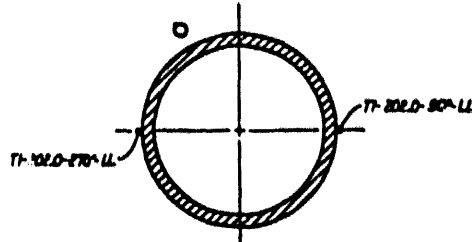
LEVEL 326.3



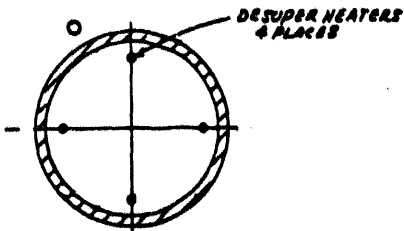
LEVEL 220.7



LEVEL 200.0



LEVEL 202.0



LEVEL 194.2

77-90°-LL

78-90°-LL

79-90°-LL

75-90°-LL

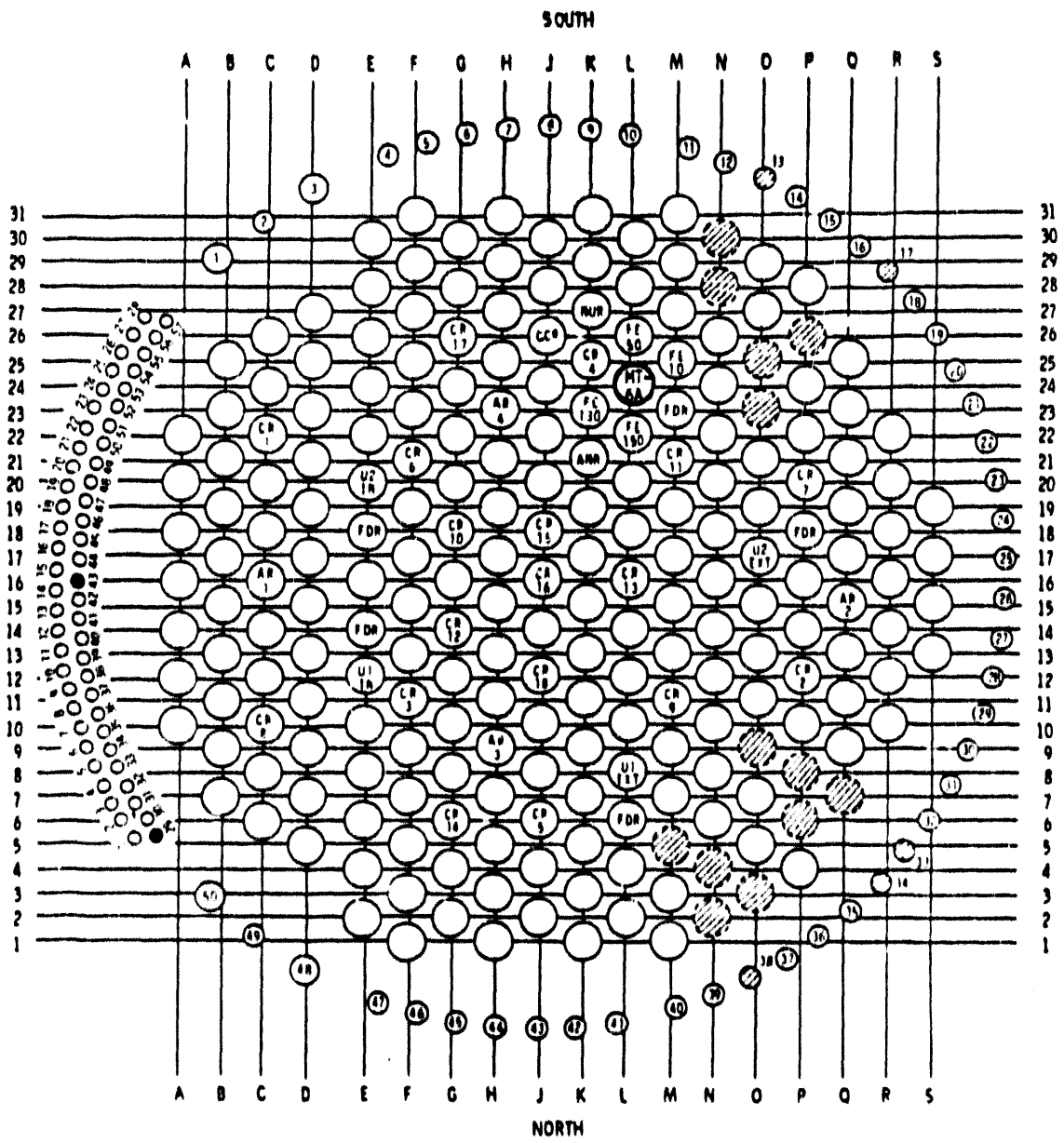
U. S. ATOMIC ENERGY COMMISSION BIGHAM OPERATIONS OFFICE PACIFIC NORTHWEST LABORATORY OPERATED BY BATTLES MEMORIAL INSTITUTE		JOP# 1005	
MT-6A TEST TRAIN INSTRUMENTATION ARRAY		H-3-54152	
NRU-CBEMP		97A 1100	
NONE		4 4	

ray from Level 156 to Level 326.3

TABLE 2. Instrumentation at Each Level in the MT-6A Test Assembly

<u>Level</u>	<u>Cladding Inside Diameter TCs</u>	<u>Shroud TCs</u>	<u>Carrier TCs</u>	<u>Inner Liner TCs</u>	<u>Spacer TCs</u>	<u>SPNDs</u>
0.0			3			
14.0			2			
25.5			2			
35.0			2			
46.5						2
56.03						
61.0	3					
67.5			2			
69.0	3					
74.0	3					
79.0	3	2		3		
84.0	3					
85.2					4	
88.5			2			
89.2 & 90.0	3				3	
94.0	3					
98.0	3					
102.0	3	3		4		
106.2	3				3	
109.5						2
110.2 & 111.0	3					
115.0	3					
119.0	3					
123.0	3	3		4		
127.2	3				4	
130.5						2
131.2 & 132.0	3		3			
136.0	3					
144.0		2		4		
148.2					4	
151.5						2
156.0						
169.0	—	4	—	—	—	—
Total	54	14	16	15	21	8

NOTE: Four braze TCs were at Level 156, 4 outlet TCs were at Level 169, 2 liquid level TCs were at Level 173, 2 liquid level TCs were at Level 177.5, 2 liquid level TCs were at Level 182, 2 liquid level TCs were at Level 186, 2 liquid level TCs were at Level 191, 4 outlet TCs were at Level 200, 5 hanger bar TCs were at Level 220.7, 1 hanger bar TC was at Level 326.3, 2 liquid level TCs were at Level 202, one liquid level detector ran from the top of the shroud to the top of the spool piece. Another liquid level detector ran from Level 0 to Level 160 inside the shroud.



- CR CONTROL ROD
- AR ADJUSTER ROD
- FDR FLUX DETECTOR ROD
- U-1 IN DOWN FLOW CHANNEL - DUMMY FUEL
- U-2 IN DOWN FLOW CHANNEL - DUMMY FUEL
- U-1 EXT UP FLOW CHANNEL - DUMMY FUEL
- U-2 EXT UP FLOW CHANNEL - DUMMY FUEL
- STANDARD LATTICE POSITION
- ◐ BLOCKED CHANNEL - NOT FUELED
- CCR COBALT CARRIER ROD
- NUR NATURAL URANIUM ROD
- ANR ALUMINUM NITRIDE ROD

FIGURE 9. NRU Reactor Core Configuration

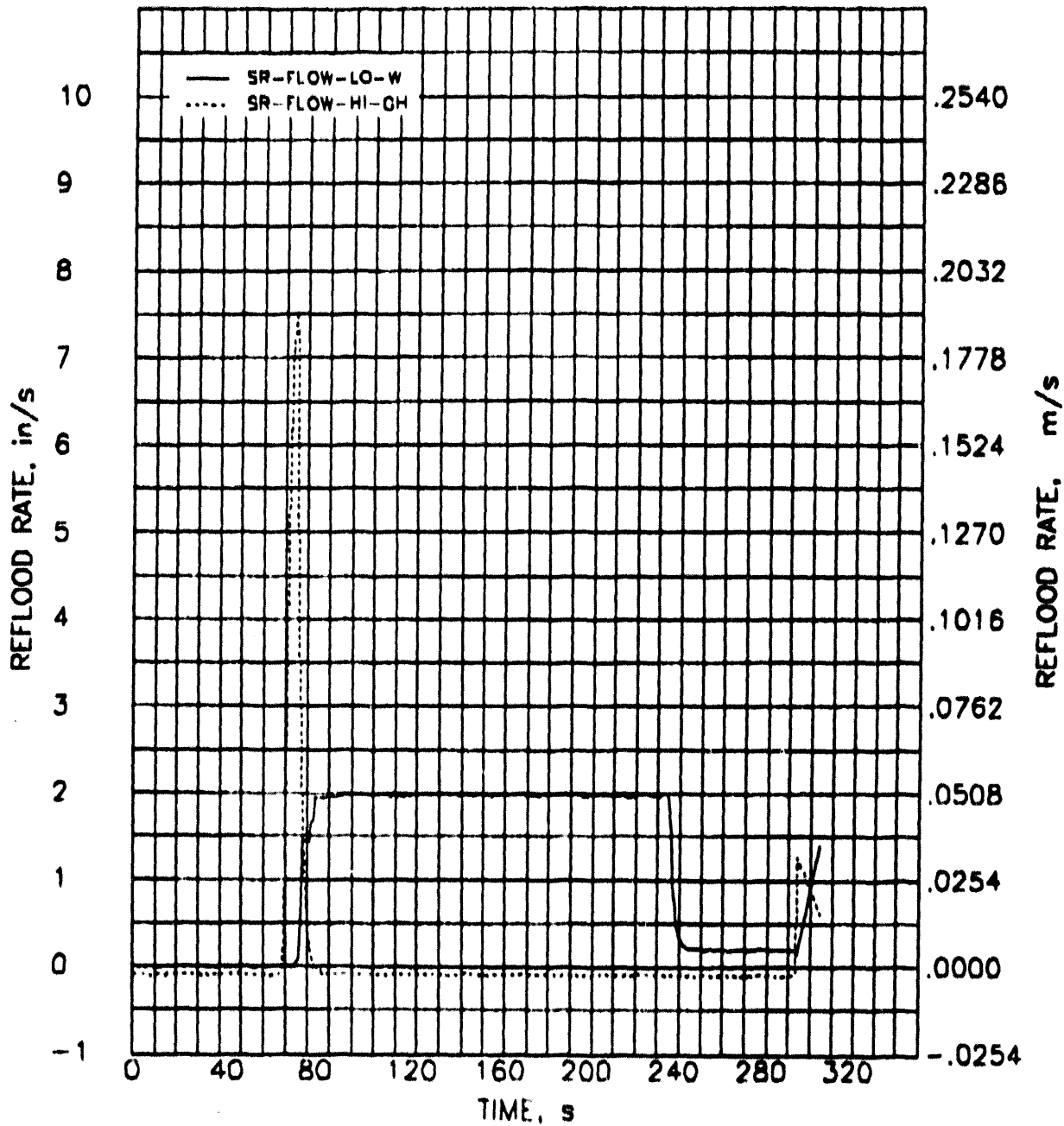


FIGURE 10. Reflood Rates During the MT-6A Transient

EXPERIMENT CONDITIONS AND RESULTS

The following factors are discussed in this section: fuel rod pressures and temperatures, axial power distribution, and the effects of steam cooling versus water cooling on test assembly power.

FUEL ROD PRESSURES AND TEMPERATURES

Gas pressure changes were measured as a function of time in the plenums of the 21 fuel rods using an out-of-reactor pressure transducer on each rod. Prior to the transient test, all 21 rods were initially filled with helium to a pressure of 6.03 MPa (875 psia) at 295K (70°F).

The pressure transducers indicated rod failure, as summarized in Table 3. The test rods were fitted with strain gauge-type pressure transducers. The pressure transducers were located outside the reactor above the test assembly and were connected to the fuel rod plenums by capillary tubes. Pressure transducer data for two rods are (4A and 5D) shown in Figures 11 and 12.

Prior to the transient, pressures were about 9.31 MPa (1350 psi). When the steam cooling to the test assembly was shut off and the power remained

TABLE 3. Fuel Rod Rupture Times and Pressures

<u>Pressure Sensor</u>	<u>Rupture Time, s</u>	<u>Rupture Pressure, MPa (psi)</u>
PT-M1-3C	63	6.21 (900)
PT-M2-4C	62	6.55 (950)
PT-M2-3D	60	6.72 (975)
PT-M1-1B	59	7.93 (1150)
PT-M1-1C	61	7.24 (1050)
PT-M1-1D	64	6.90 (1000)
PT-M1-2A	62	7.65 (1110)
PT-M1-2B	62	6.07 (880)
PT-M1-2C	61	6.55 (950)
PT-M2-2D	60	6.96 (1010)
PT-M2-2E	63	6.96 (1010)
PT-M1-3A	63	7.24 (1050)
PT-M1-3B	62	6.07 (880)
PT-M2-3E	60	7.24 (1050)
PT-M1-4A	64	7.24 (1050)
PT-M1-4B	62	6.72 (975)
PT-M2-4D	61	6.27 (910)
PT-M2-4E	62	6.90 (1000)
PT-M1-5B	61	7.58 (1100)
PT-M2-5C	60	7.52 (1090)
PT-M2-5D	58	7.93 (1150)

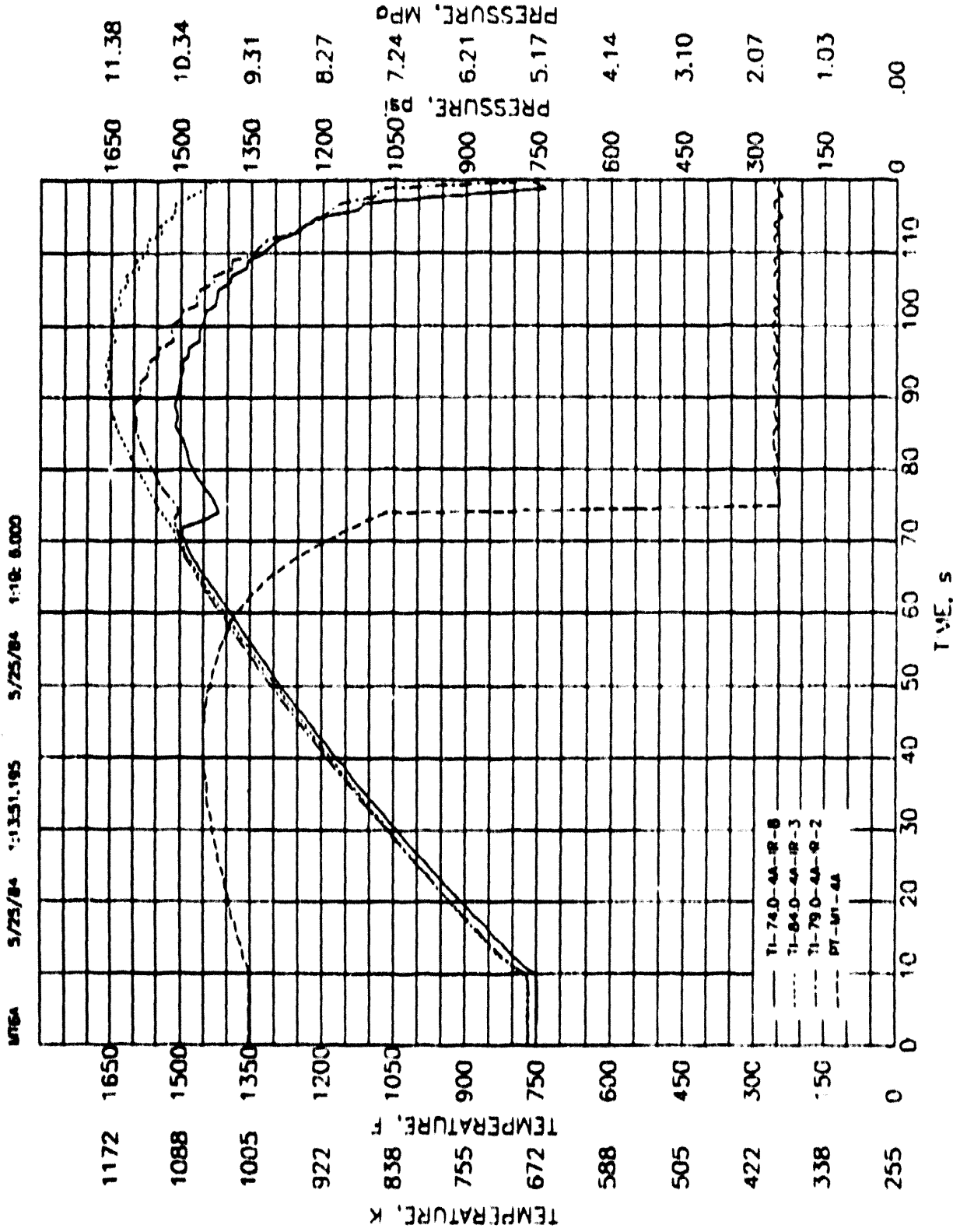


FIGURE 11. Pressures and Temperatures for Rod 4A During the MT-6A Transient

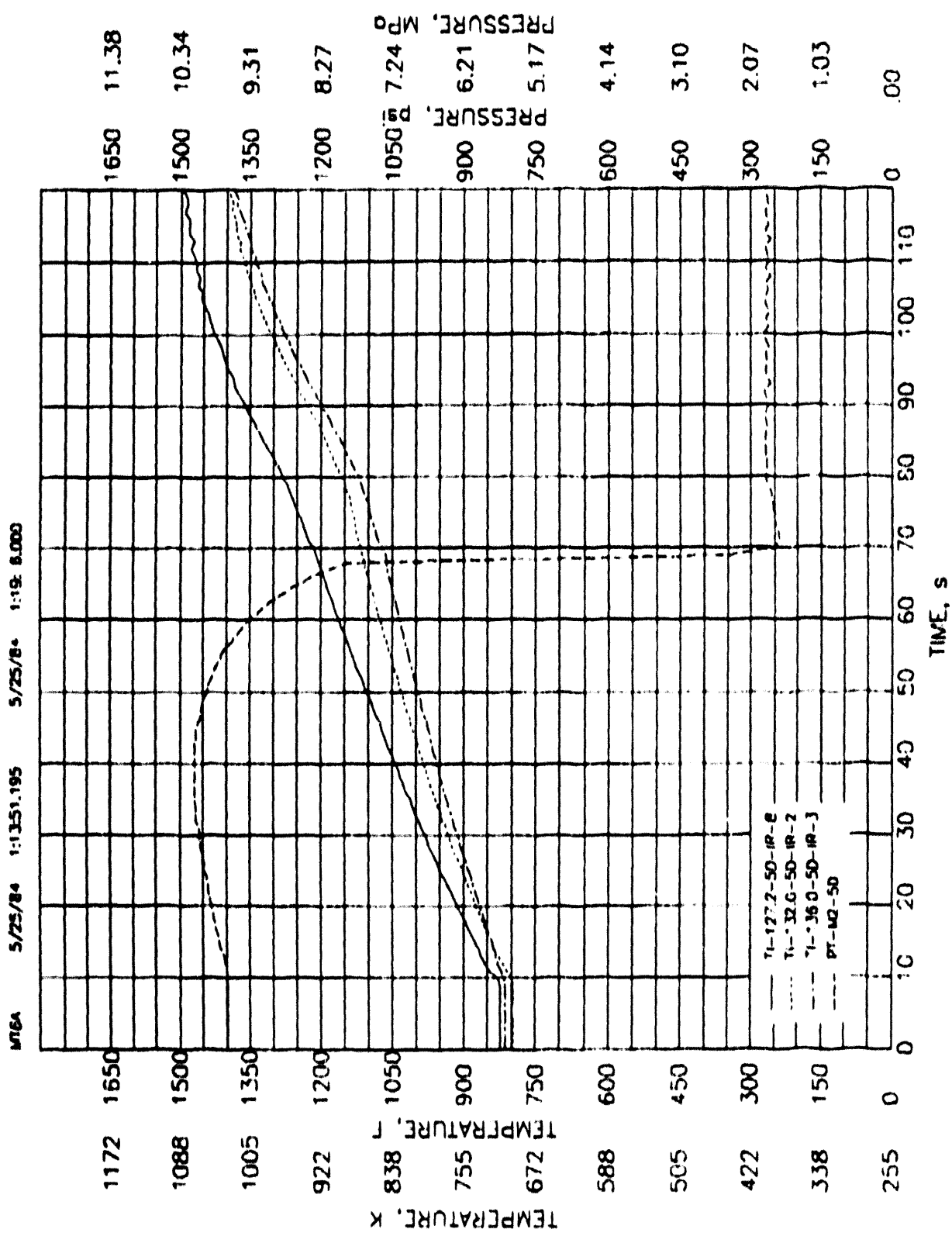


FIGURE 12. Pressures and Temperatures for Rod 5D During the MT-6A Transient

constant, the fuel heatup caused the pressure to increase. Because the fuel ballooned at higher temperatures, the pressure eventually decreased until rupture, which was followed by a rapid decrease in pressure. As shown in Figure 11, the fuel temperature was constant prior to the transient. After the steam cooling was shut off, the fuel temperature increased until just prior to rupture. Just before rupture, cladding temperatures dropped near the rupture location, perhaps because of cladding liftoff near the rupture zone. The temperature and corresponding pressure for a rod that has one TC hot junction located close to the rupture region are shown in Figure 11. A similar trace where the TCs are not close to the rupture region is shown in Figure 12. Peak fuel temperatures near a rupture region tend to be lower than those away from the rupture region, which tends to confirm that ballooning has no deleterious effect on heat transfer and may even enhance it.

AXIAL POWER DISTRIBUTION

Prior to the MT-6A test, the axial power distribution in the fuel assembly was evaluated using normalized local heatup rates, assembly self-powered neutron detector (SPND) measurements, assembly flux wire data, and a series of measurements taken by a transient flux probe during the preconditioning phase of the experiments in the NRU reactor. Local axial powers were calculated using the adiabatic period heatup rates and the fuel rod mass and specific heat. These normalized results are plotted against a computed power profile based on core physics calculations for the MT-4 test (Figure 13).

For the MT-6A experiment, a technique was devised that permitted insertion of a flux wire into the test train between the preconditioning and transient phases of the test. Thus, the flux wire data represent only the flux distribution that existed during the low-power operation of the transient. The axial scan data from this wire are shown in Figure 14, which represents the activity of the wire as a function of axial position along the test assembly. As shown, cyclic localized neutron flux increases of about $\pm 4\%$ with a spacing of about 18 cm (7 in.) are superimposed on the normal axial profile.

The stainless steel shroud used for the MT-6A experiment was a modification of the shroud design used in all previous NRU LOCA tests. In that design, the shroud was split lengthways, and 3-in. long flats were cut on the outside surface of the stainless steel shroud on 7-in. centers to accommodate clips that held the two halves together during the tests and permitted easy disassembly after the tests. The modification of existing shrouds for MT-6A and MT-6B consisted of removing some material from the inside surface of the shroud, welding the two halves together, and eliminating the clips. Stainless steel is a mild neutron absorber, and the reduced mass of metal at the flats resulted in an increased neutron flux at these locations. In the original shroud design, the mass in the region of the flats was reduced by 17%. After modifying the shroud for MT-6A, the localized mass was reduced by 21% of the cross section. The axial locations of these flats, as well as the location of the spacer grids, are shown in Figure 14. The correspondence of the flats and the localized flux increases is not exact; there is a 1- to

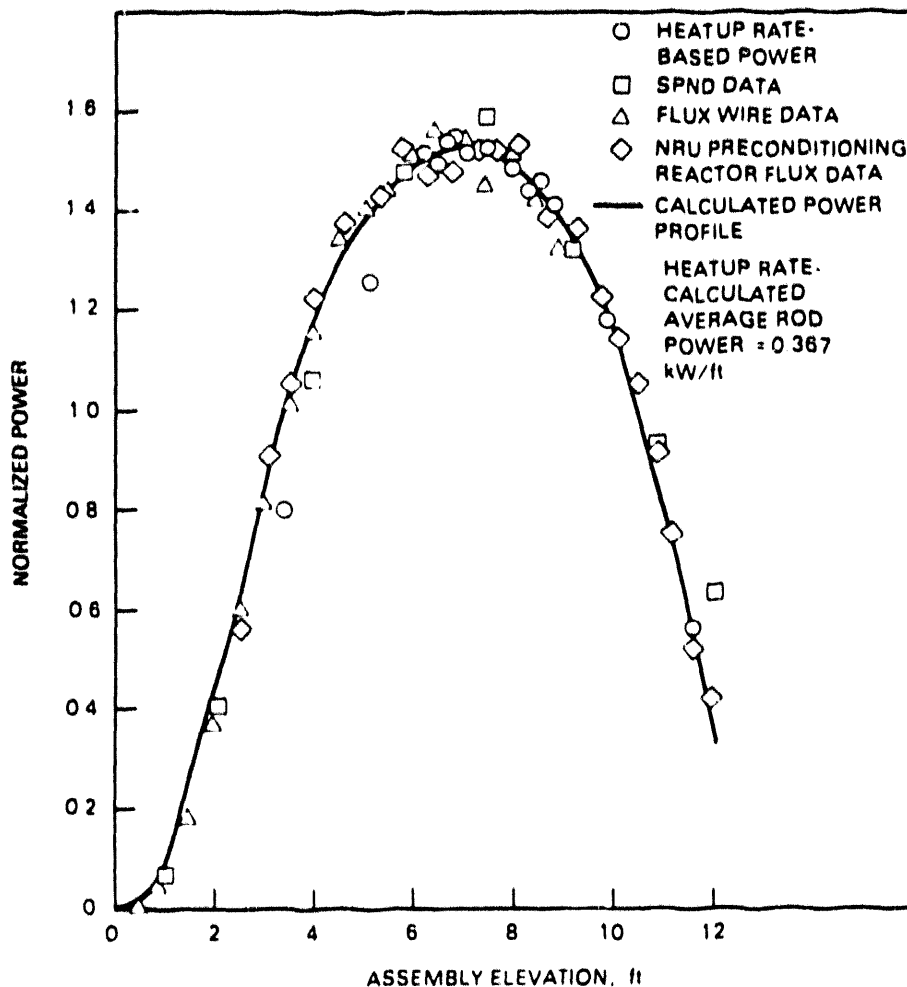


FIGURE 13. Comparison of MT-4 Heatup Rate-Based, SPND, Flux Wire, NRU Reactor Preconditioning, and Calculated Axial Power Profiles

1-1/2-in. offset between the activity increases and the locations of the flats. This offset is probably due to a lack of correspondence between the zero locations of the fuel rods and the flux wire.

The effects of the localized neutron flux and the resulting power and cladding temperature variations on the measured cladding strain for the MT-4 rods are shown in Figures 15 and 16. There is a correspondence between the locations of the flats on the shroud and the localized strain effects in the cladding. The large decrease in strain in the middle of the middle span is coincident with a nonflat region in the shroud. The effect of the mechanical restraint provided by the spacer grids on cladding strain is also clearly shown. There are no indications of significant cladding strain reductions between the other spacer grid spans, as was noted in MT-1 and MT-2. However,

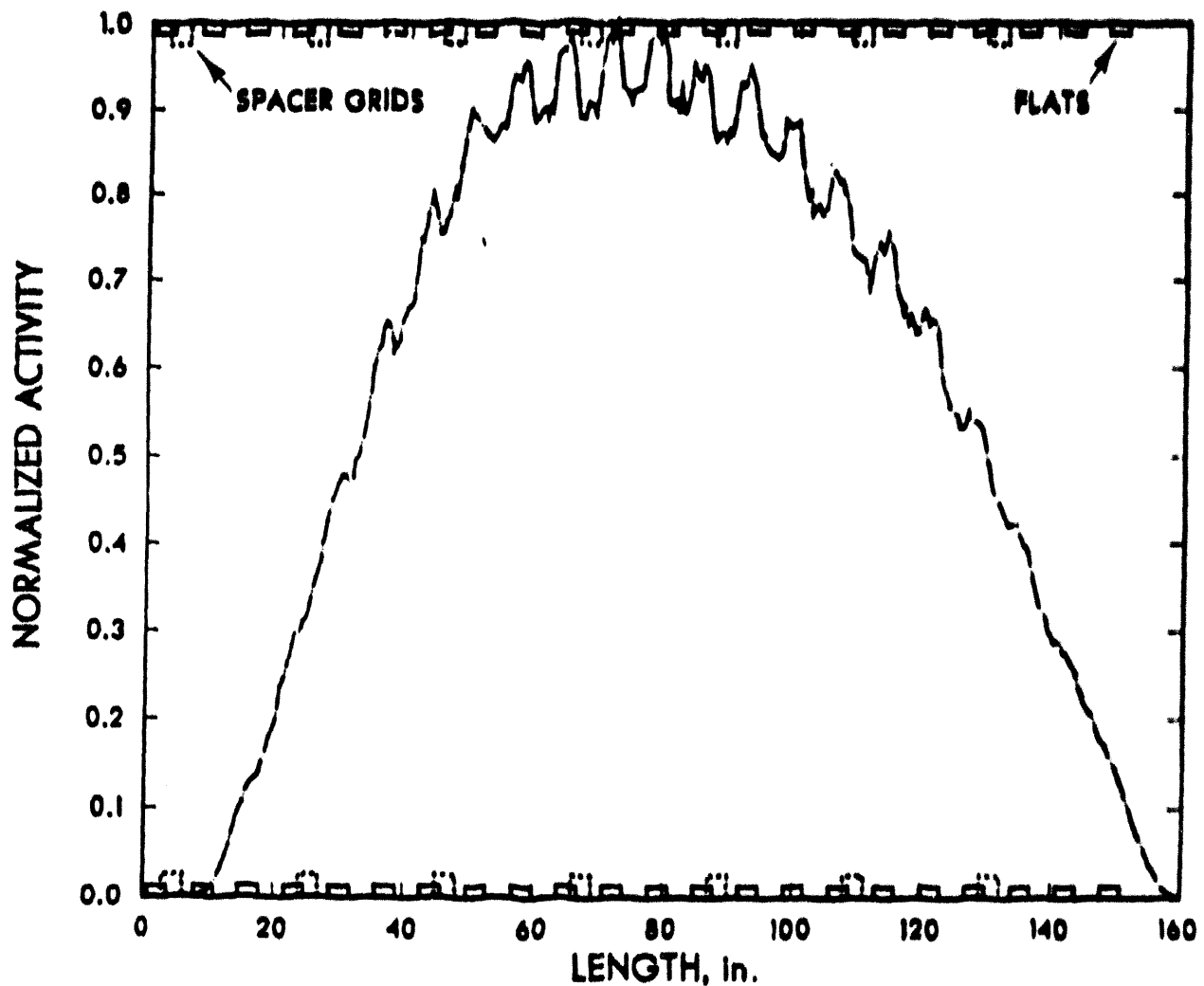


FIGURE 14. Axial Neutron Flux Distribution During the MT-6A Transient

a change in the shape of the strain profile is evident at locations associated with the flat regions in the shroud. This strain behavior is indicative of a temperature effect associated with the localized flux variations at these elevations.

An approximation of the effect of the localized flux and power increases on cladding temperature for the MT-4 tests can be deduced. The flux wire data for MT-6A show a minimum-to-maximum difference in local power of about 8%. Adjusting this value to account for the difference in the fraction of metal removed from the MT-4 shroud results in a local power variation of about 6%. For MT-4, the cladding strains occurred during the adiabatic heatup in which the cladding temperature ramp rates were controlled almost exclusively by the local power. The local temperature variations were very small at the start of the transient because they were primarily established

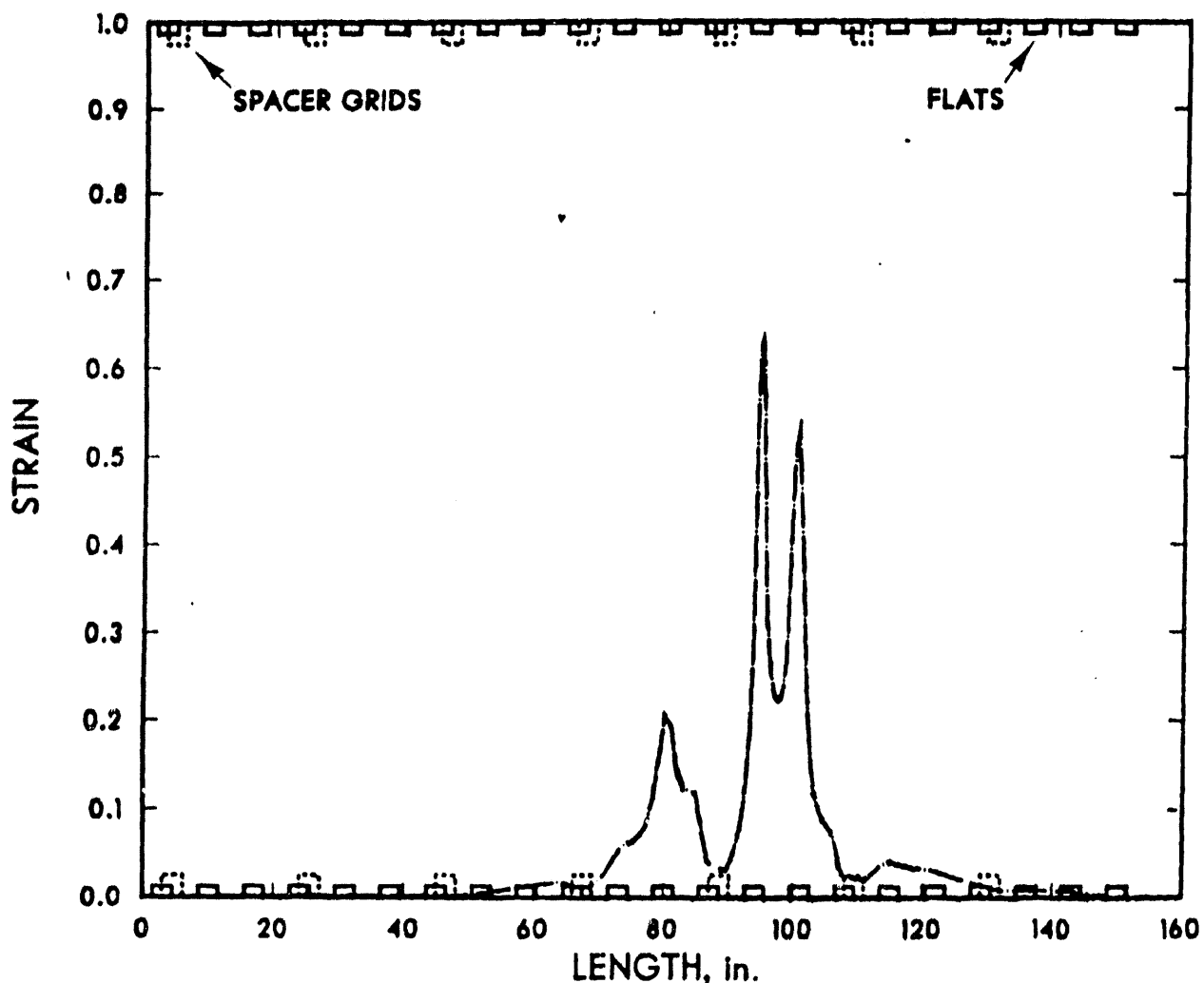


FIGURE 15. Axial Strain Profile for MT-4

by the temperature of the steam coolant. Thus, the local temperature variations in the region of maximum strain was estimated to be 6% of the 615K (650°F) temperature increase from the start of the transient to the time of rupture, or about 20K (40°F). Thus, the MT-4 data dramatically illustrate the extreme sensitivity of the cladding strain behavior to temperature.

Consideration of the effects of the localized flux and power variations on the cladding strain behavior for MT-4 is speculative. If the cladding strain behavior that occurred in the MT-4 rods had not been perturbed by the localized temperature effects, it is expected that the rate of volume increase in the rods would have been greater and the internal gas pressure decrease later in the transient prior to rupture would have been larger than what occurred. These effects would have delayed rupture and would have resulted in rupture at a somewhat lower pressure and higher temperature. However, once plastic instability was reached, the strain rate would have

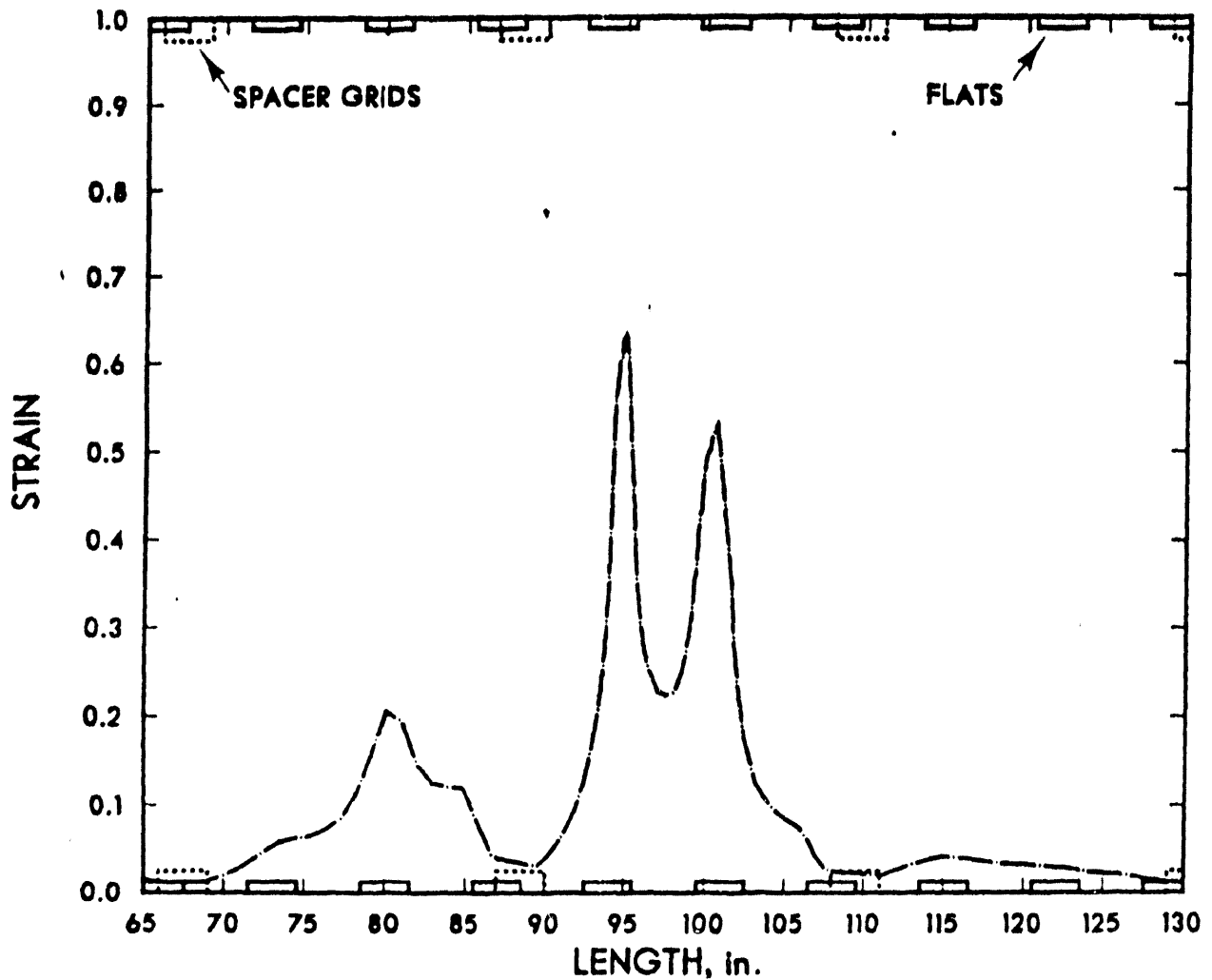


FIGURE 16. Partial Axial Strain Profile for MT-4

been sufficiently high that these effects would probably not have been large. The rupture hoop stress would still be expected to follow the temperature correlation. Because the rupture temperature data from the experiment are slightly higher than the alpha phase peak strain predicted by NUREG-0630,⁽¹¹⁾ use of this prediction would lead to the conclusion of a somewhat lower average rupture strain than was found. Thus, it may be concluded that the removal of metal to form the flats on the stainless steel shroud affected the local power, which in turn affected the local strain if the strains occurred during the adiabatic heatup period. This resulted in a modification of the axial strain pattern, probably a small increase in the peak rupture strain, and no change in the coolability conclusions.

EFFECT OF STEAM COOLING VERSUS WATER COOLING ON TEST ASSEMBLY POWER

A test was performed prior to the MT-6A transient to determine the effect of steam cooling versus water cooling on test assembly power. For this test, the NRU reactor power was maintained at a constant level. Calorimetry measurements showed that the test assembly power was 86.8 kW when filled with water and 94.5 kW when filled with steam, indicating an approximate 8% decrease in power as the reflood completely fills the test assembly. These results can be used to improve the interpretation of the MT-6A and MT-6B test data, which has a similar 21-rod test assembly, as well as all prior test data.

REFERENCES

1. Hann, C. R. 1979. Program Plan for LOCA Simulation in the National Research Universal (NRU) Reactor. PNL-3056, Pacific Northwest Laboratory, Richland, Washington.
2. Mohr, C. L., G. M. Hesson, G. E. Russcher, R. K. Marshall, and L. L. King. April 1981. Prototypic Thermal-Hydraulic Experiment in NRU to Simulate Loss-of-Coolant Accidents. NUREG/CR-1882, PNL-3681, Pacific Northwest Laboratory, Richland, Washington.
3. Russcher, G. E., L. W. Cannon, R. L. Goodman, G. M. Hesson, and L. L. King. September 1981. Experiment Operations Plan for Loss-of-Coolant Accident Simulation in the National Research Universal Reactor, Addendum 1: Materials Tests 1 and 2. NUREG/CR-1735, PNL-3765, Pacific Northwest Laboratory, Richland, Washington.
4. Russcher, G. E., R. K. Marshall, G. M. Hesson, N. J. Wildung, and W. N. Rausch. October 1981. LOCA Simulation in the NRU Reactor - Materials Test-1. NUREG/CR-2152, Vol. 1, PNL-3835, Pacific Northwest Laboratory, Richland, Washington.
5. Barner, J. O., G. M. Hesson, L. L. King, R. K. Marshall, L. J. Parchen, J. P. Pilger, W. N. Rausch, G. E. Russcher, B. J. Webb, N. J. Wildung, C. L. Wilson, M. D. Wismer, and C. L. Mohr. March 1982. LOCA Simulation in the NRU Reactor - Materials Test-2. NUREG/CR-2509, PNL-4155, Pacific Northwest Laboratory, Richland, Washington.
6. Wilson, C. L., C. L. Mohr, G. M. Hesson, N. J. Wildung, G. E. Russcher, B. J. Webb, and M. D. Freshley. July 1983. LOCA Simulation in NRU Program - Data Report for the Fourth Materials Experiment (MT-4). NUREG/CR-3272, PNL-4669, Pacific Northwest Laboratory, Richland, Washington.
7. Hochreiter, L. E. 1983. "NRC/EPRI/W FLECHT-SEASET Program: Natural Circulation Results, 163 Blocked Bundle Results." 10th Water Reactor Safety Research Information Meeting, Gaithersburg, Maryland, October 12-15, 1982. NUREG/CP-0041, Vol. 1, January 1983. U.S. Nuclear Regulatory Commission, Washington, D.C.
8. Erbacher, F. J. 1981. "LWR Fuel Cladding Deformation in a LOCA and Its Interaction with the Emergency Core Cooling." ANS, ENS Topical Meeting on Reactor Safety Aspects of Fuel Behavior, Sun Valley, Idaho, August 1981.
9. NUREG-1230. December 1988. Compendium of ECCS Research for Realistic LOCA Analysis. Division of Systems Research, U.S. Nuclear Regulatory Commission, Washington, D.C.

10. Marshall, R. K., C. L. Mohr, P. N. McDuffie, and R. A. Scoggin. 1983. The Continuous Measurement of Coolant Liquid Level During the MT-4 LOCA Experiment in the NRU Reactor. NUREG/CR-3183, PNL-4650, Pacific Northwest Laboratory, Richland, Washington.
11. Powers, D. A., and R. O. Meyer. April 1980. Cladding Swelling and Rupture Models for LOCA Analysis. NUREG-0630, Pacific Northwest Laboratory, Richland, Washington.

APPENDIX A

TRANSIENT FUEL PRESSURES AND TEMPERATURES
DURING THE MT-6A TRANSIENT

APPENDIX A

TRANSIENT FUEL PRESSURES AND TEMPERATURES DURING THE MT-6A TRANSIENT

Summaries of transient fuel pressures and inside cladding temperatures for MT-6A are presented in this appendix. Figures A.1 through A.18 present both pressure and temperature traces for each rod. Figure A.19 presents pressure traces only for three rods that had no thermocouples.

The remainder of this appendix consists of the following figures:

A.1	Fuel Rod Interior Cladding Temperatures for Rod 1B at Levels 90.0 and 94.0, Rod 3B at Level 98.0, and Plenum Pressures for Rod 1B	A.3
A.2	Fuel Rod Interior Cladding Temperatures at Levels 127.2, 132.0, and 136.0, and Plenum Pressures for Rod 1C	A.4
A.3	Fuel Rod Interior Cladding Temperatures at Levels 127.2, 132.0, and 136.0, and Plenum Pressures for Rod 1D	A.5
A.4	Fuel Rod Interior Cladding Temperatures at Levels 56.0, 61.0, and 69.0, and Plenum Pressures for Rod 2A	A.6
A.5	Fuel Rod Interior Cladding Temperatures at Levels 102.0, 106.2, and 111.0, and Plenum Pressures for Rod 2B	A.7
A.6	Fuel Rod Interior Cladding Temperatures at Levels 56.0, 61.0, and 69.0, and Plenum Pressures for Rod 1C	A.8
A.7	Fuel Rod Interior Cladding Temperatures at Levels 115.0, 119.0, and 123.0, and Plenum Pressure for Rod 2D	A.9
A.8	Fuel Rod Interior Cladding Temperatures at Levels 56.0, 61.0, and 69.0, and Plenum Pressures for Rod 2E	A.10
A.9	Fuel Rod Interior Cladding Temperatures at Levels 102.0, 106.2, and 111.0, and Plenum Pressures for Rod 3A	A.11
A.10	Fuel Rod Interior Cladding Temperatures at Levels 98.0, 90.0, and 94.0, and Plenum Pressures for Rod 3B	A.12
A.11	Fuel Rod Interior Cladding Temperatures at Levels 115.0, 119.0, and 123.0, and Plenum Pressures for Rod 3E	A.13
A.12	Fuel Rod Interior Cladding Temperatures at Levels 74.0, 84.0 and 79.0, and Plenum Pressures for Rod 4A	A.14

A.13	Fuel Rod Interior Cladding Temperatures at Levels 102.0, 106.2, and 111.0, and Plenum Pressures for Rod 4B	A.15
A.14	Fuel Rod Interior Cladding Temperatures at Levels 115.0, 119.0, and 123.0, and Plenum Pressures for Rod	A.16
A.15	Fuel Rod Interior Cladding Temperatures at Levels 74.0, 79.0, and 84.0, and Plenum Pressures for Rod 4E	A.17
A.16	Fuel Rod Interior Cladding Temperatures at Levels 98.0, 94.0, and 90.0, and Plenum Pressures for Rod 5B	A.18
A.17	Fuel Rod Interior Cladding Temperature at Levels 74.0, 79.0, and 84.0, and Plenum Pressure for Rod 5C	A.19
A.18	Fuel Rod Interior Cladding Temperature at Levels 127.2, 132.0, and 136.0, and Plenum Pressures for Rod 5D	A.20
A.19	Fuel Rod Plenum Pressures for Rods 3C, 4C, and 3D	A.21

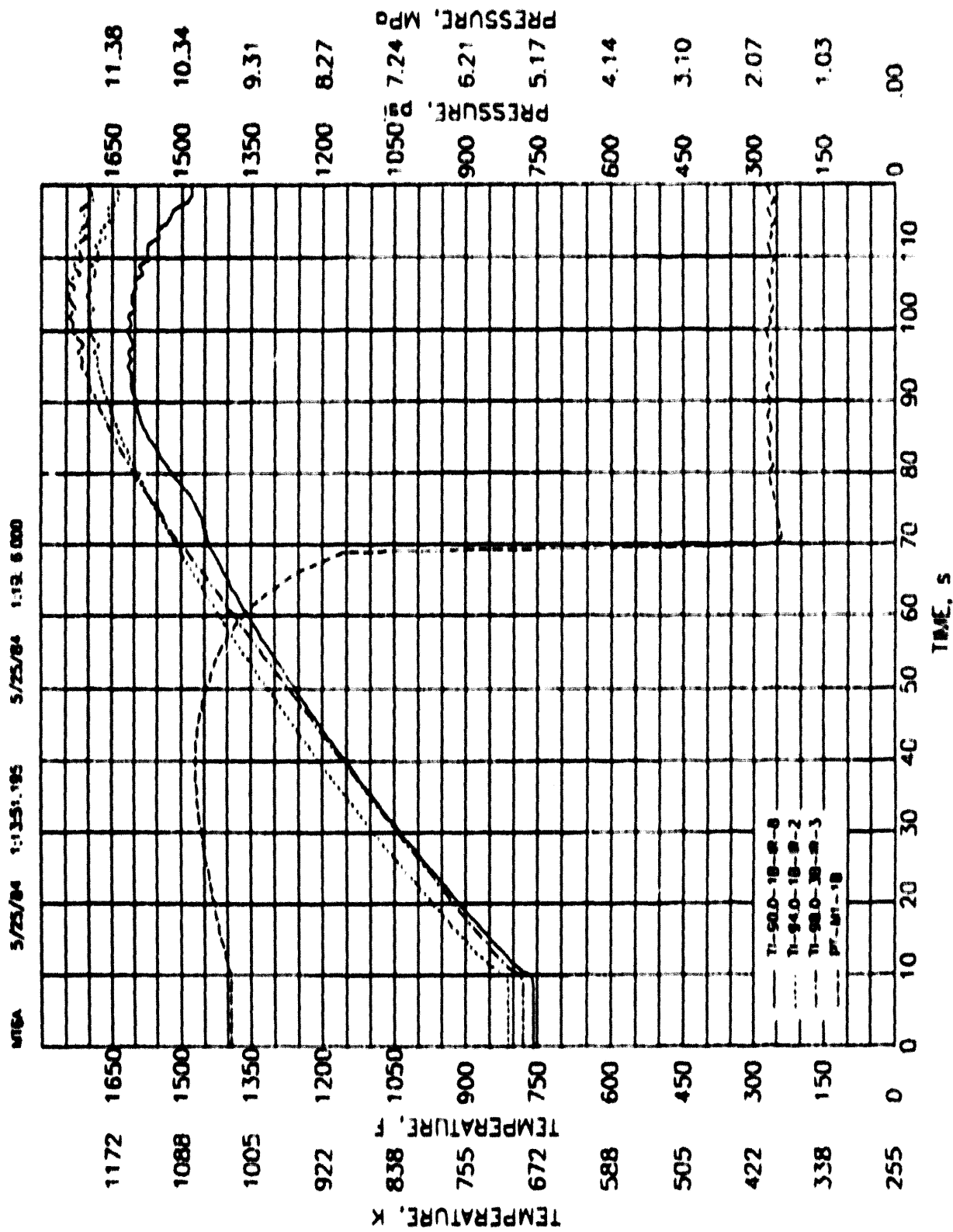


FIGURE A.1. Fuel Rod Interior Cladding Temperatures for Rod 1B at Levels 90.0 and 94.0, Rod 3B at Level 98.0, and Plenum Pressures for Rod 1B

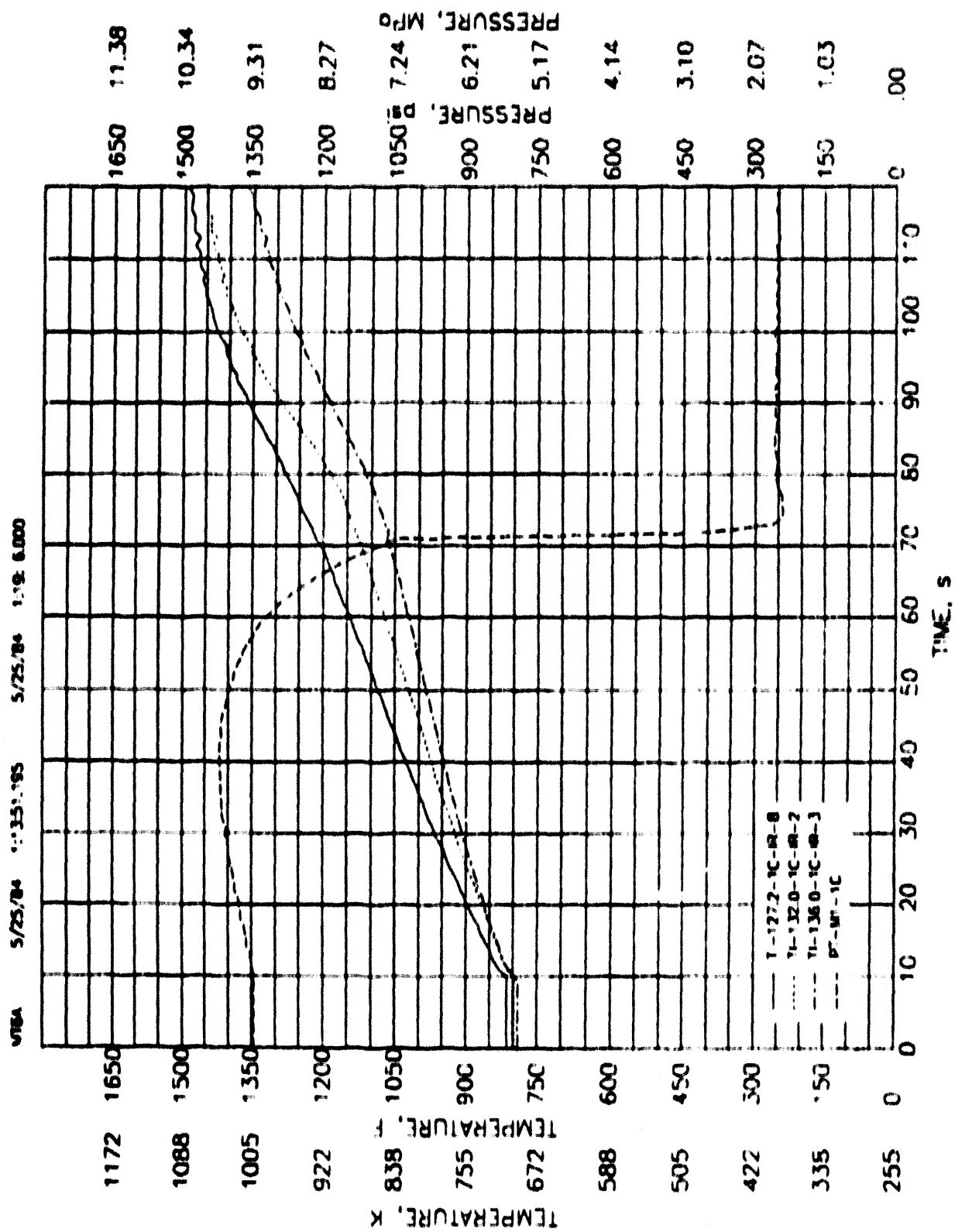


FIGURE A.2. Fuel Rod Interior Cladding Temperatures at Levels 127.2, 132.0, and 136.0, and Plenum Pressures for Rod IC

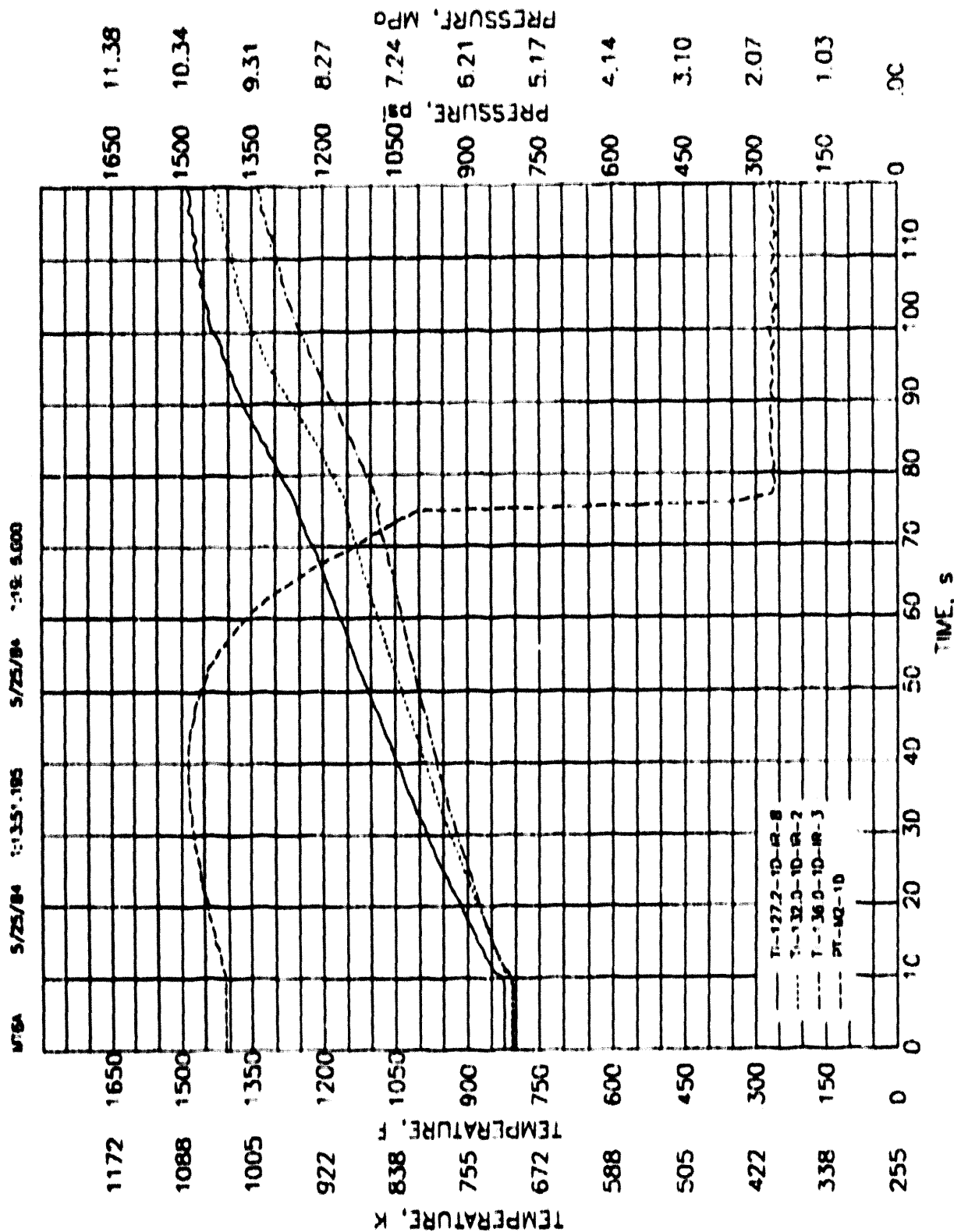


FIGURE A.3. Fuel Rod Interior Cladding Temperatures at Levels 127.2, 132.0, and 136.0, and Plenum Pressures for Rod 10

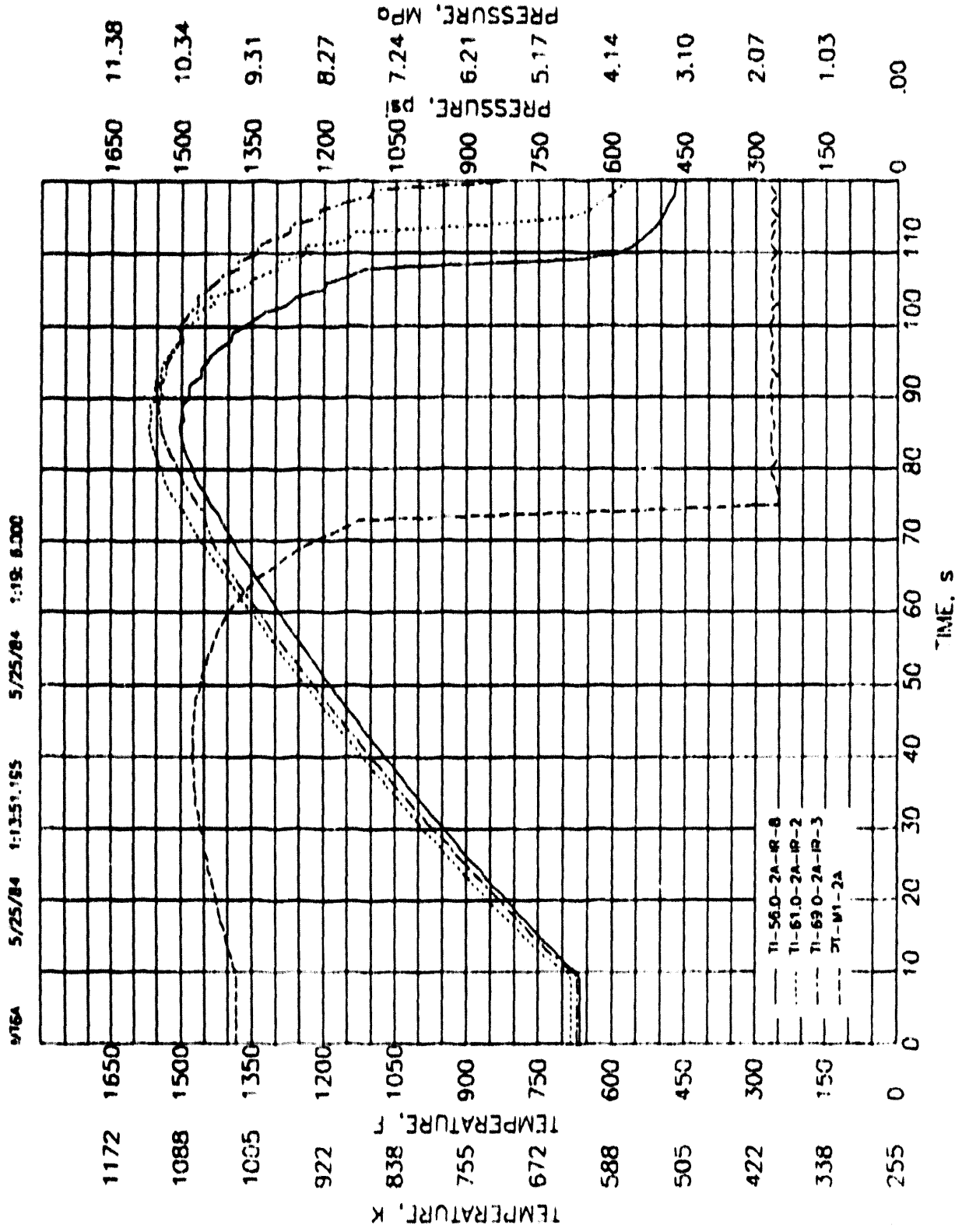


FIGURE A.4. Fuel Rod Interior Cladding Temperatures at Levels 56.0, 61.0, and 69.0, and Planum Pressures for Rod 2A

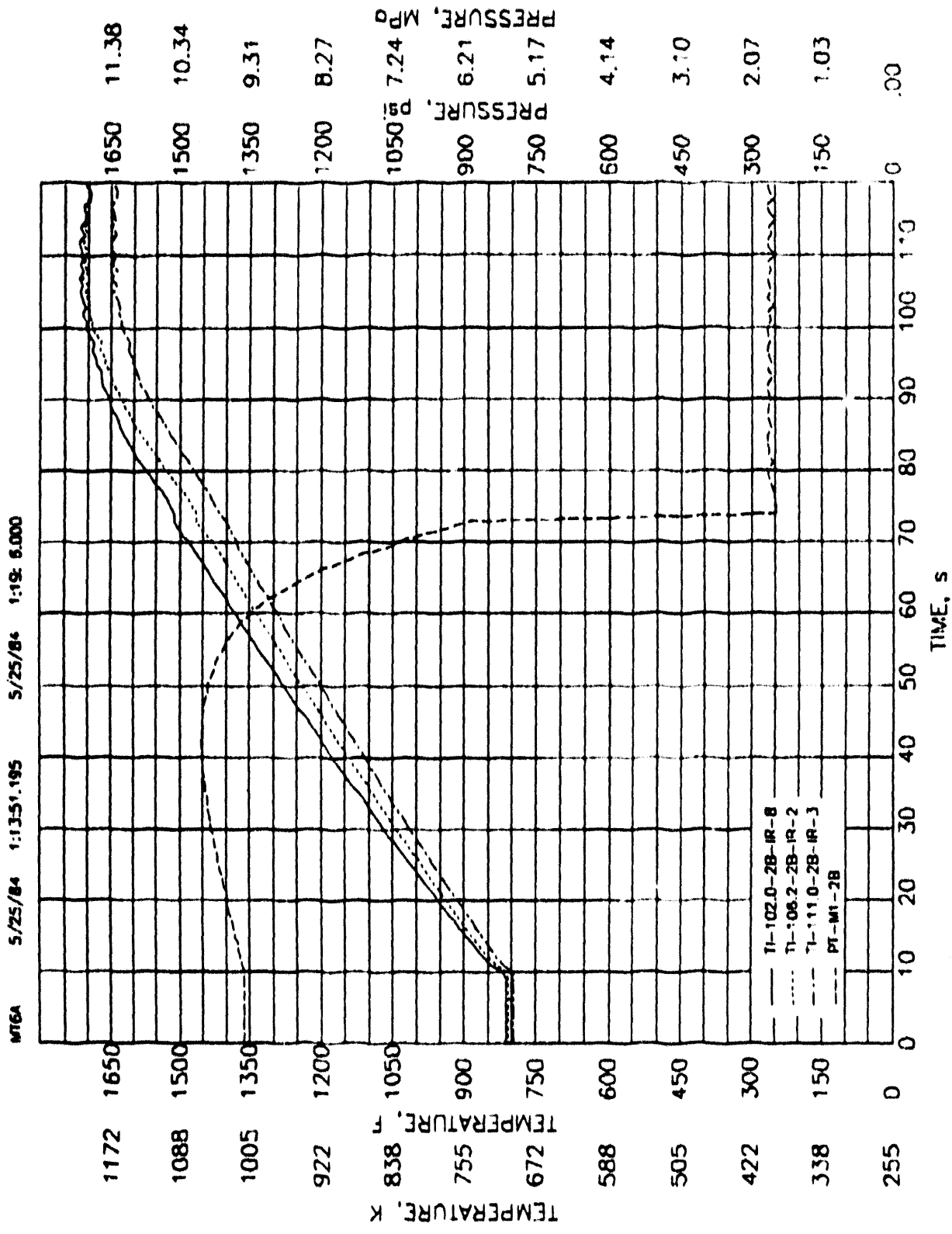


FIGURE A.5. Fuel Rod Interior Cladding Temperatures at Levels 102.0, 106.2, and 111.0, and Planum Pressures for Rod 2B

MT6A 5/25/84 1:13.51.195 5/25/84 1:19:6.000

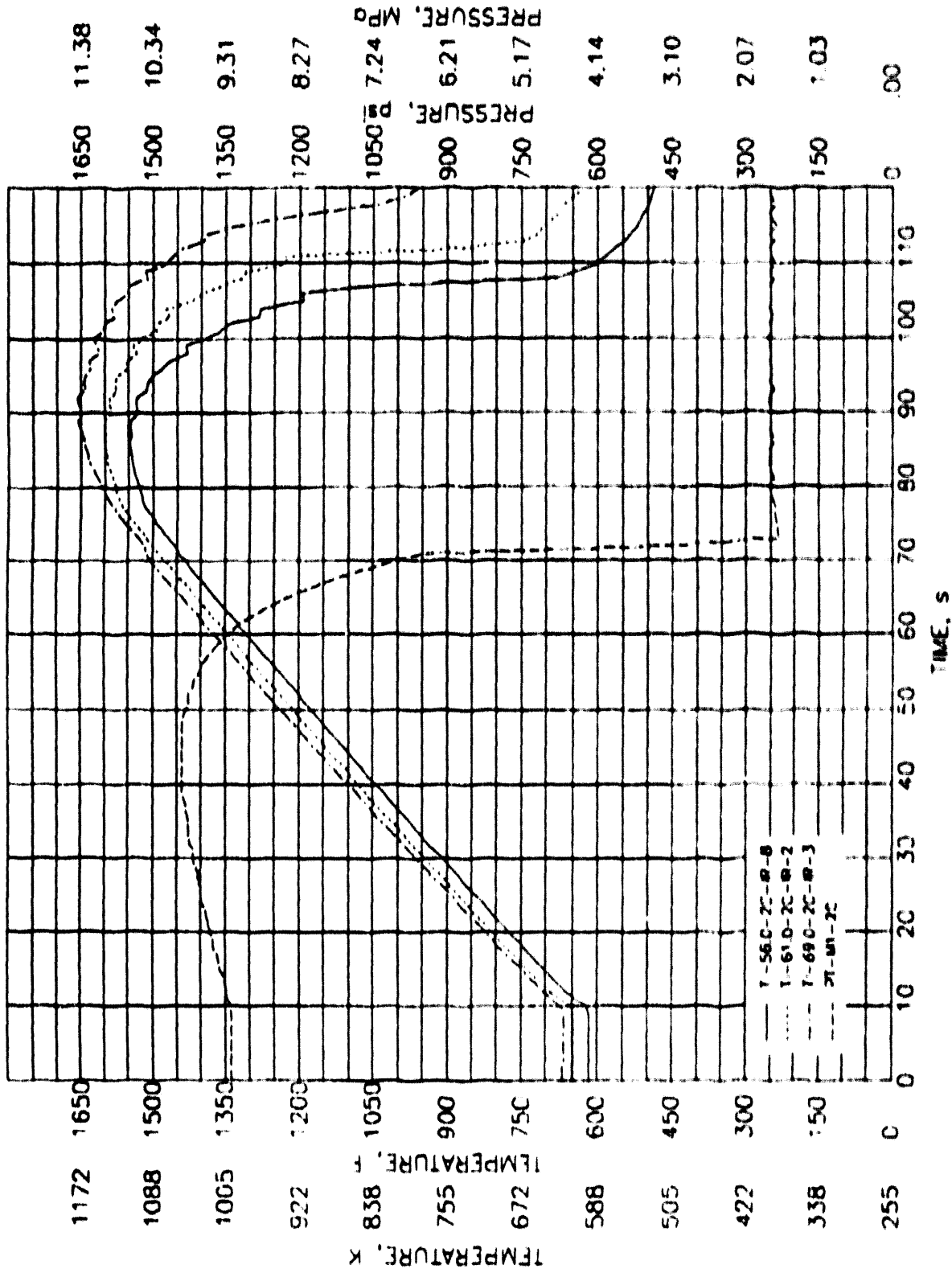


FIGURE A.6. Fuel Rod Interior Cladding Temperatures at Levels 56.0, 61.0, and 69.0, and Plenum Pressures for Rod IC

MF6A 5/25/84 11:35:19.5 5/25/84 1:19:6.000

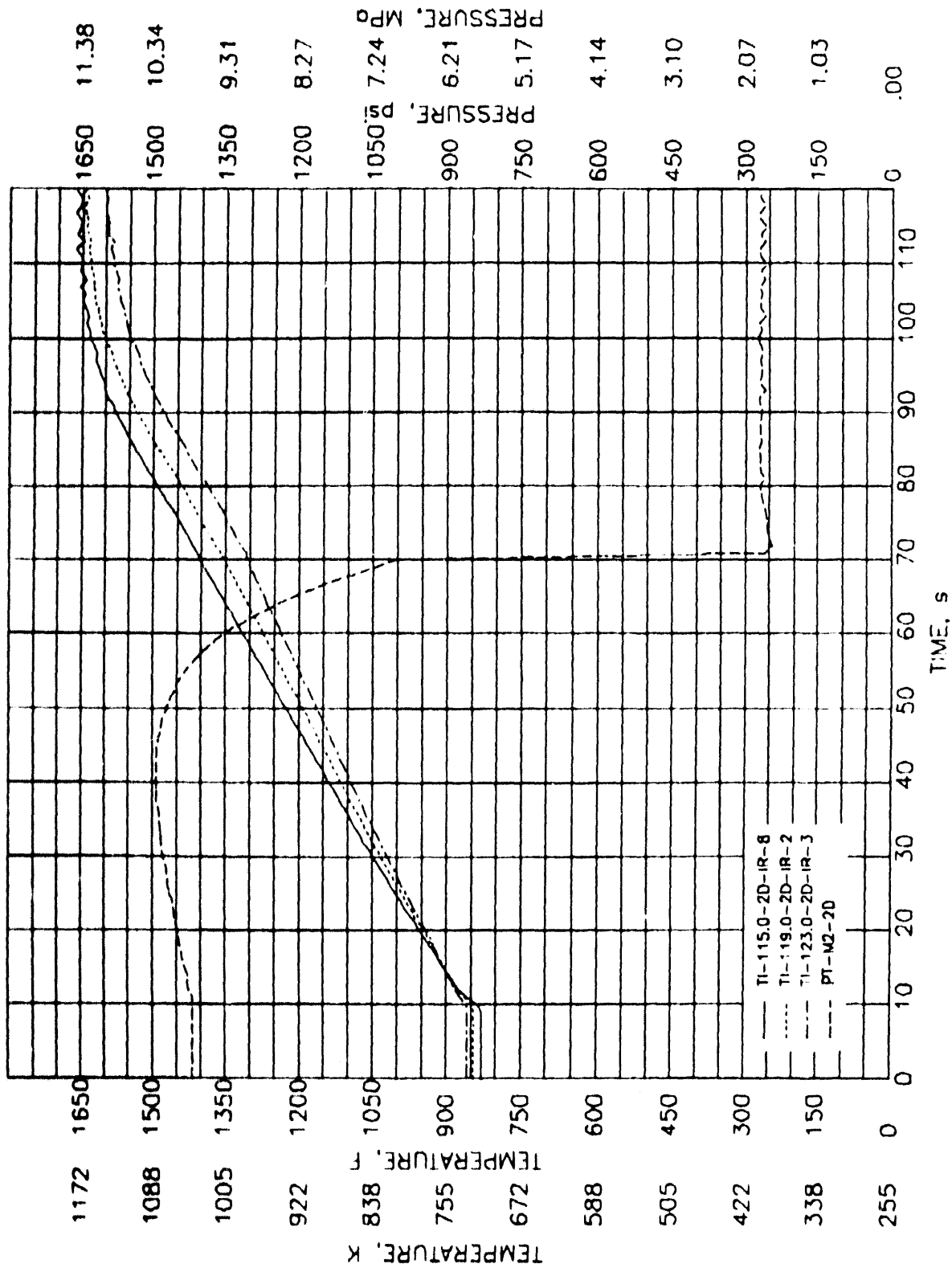


FIGURE A.7. Fuel Rod Interior Cladding Temperatures at Levels 115.0, 119.0, and 123.0, and Plenum Pressure for Rod 2D

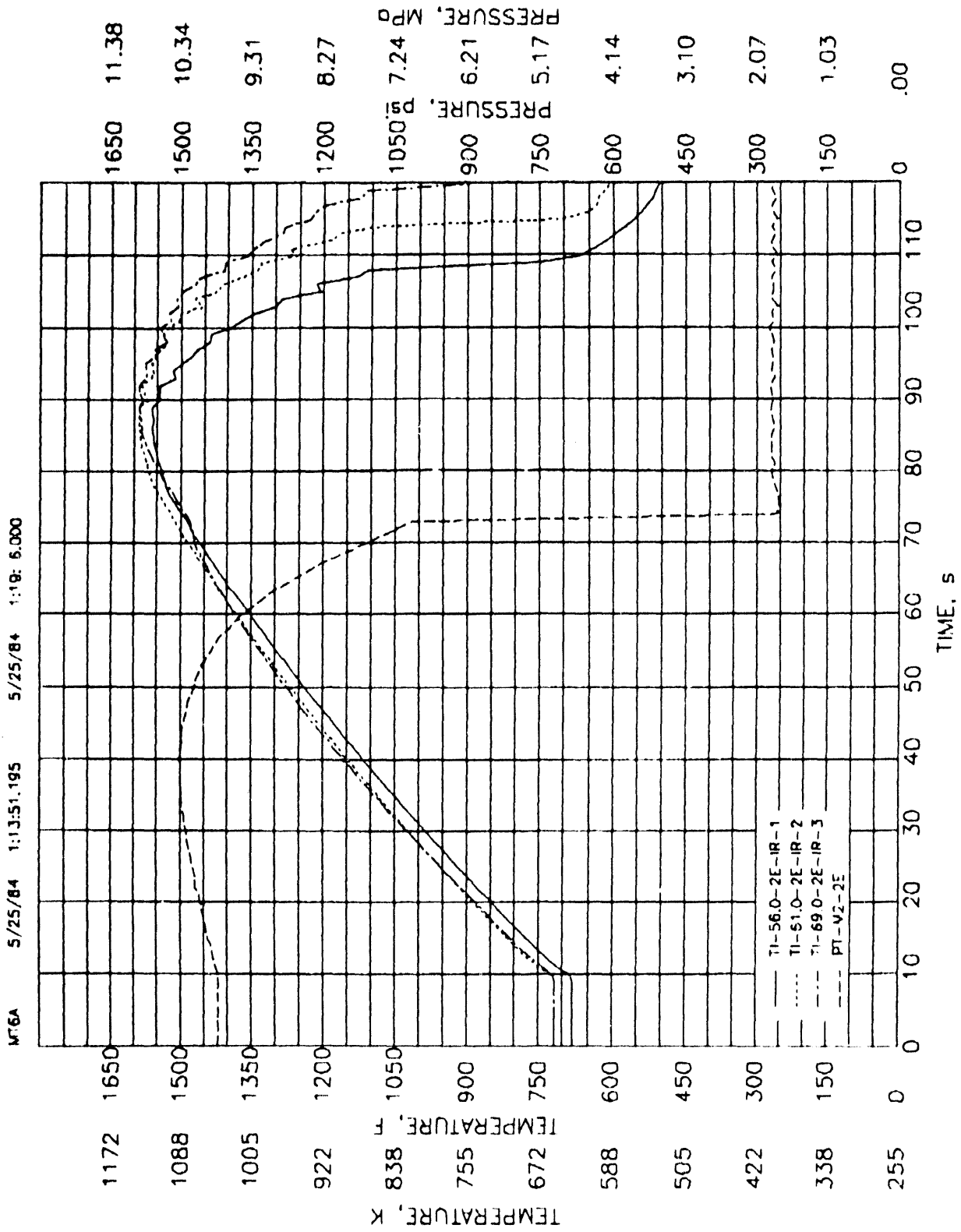


FIGURE A.8. Fuel Rod Interior Cladding Temperatures at Levels 56.0, 61.0, and 69.0, and Plenum Pressures for Rod 2E

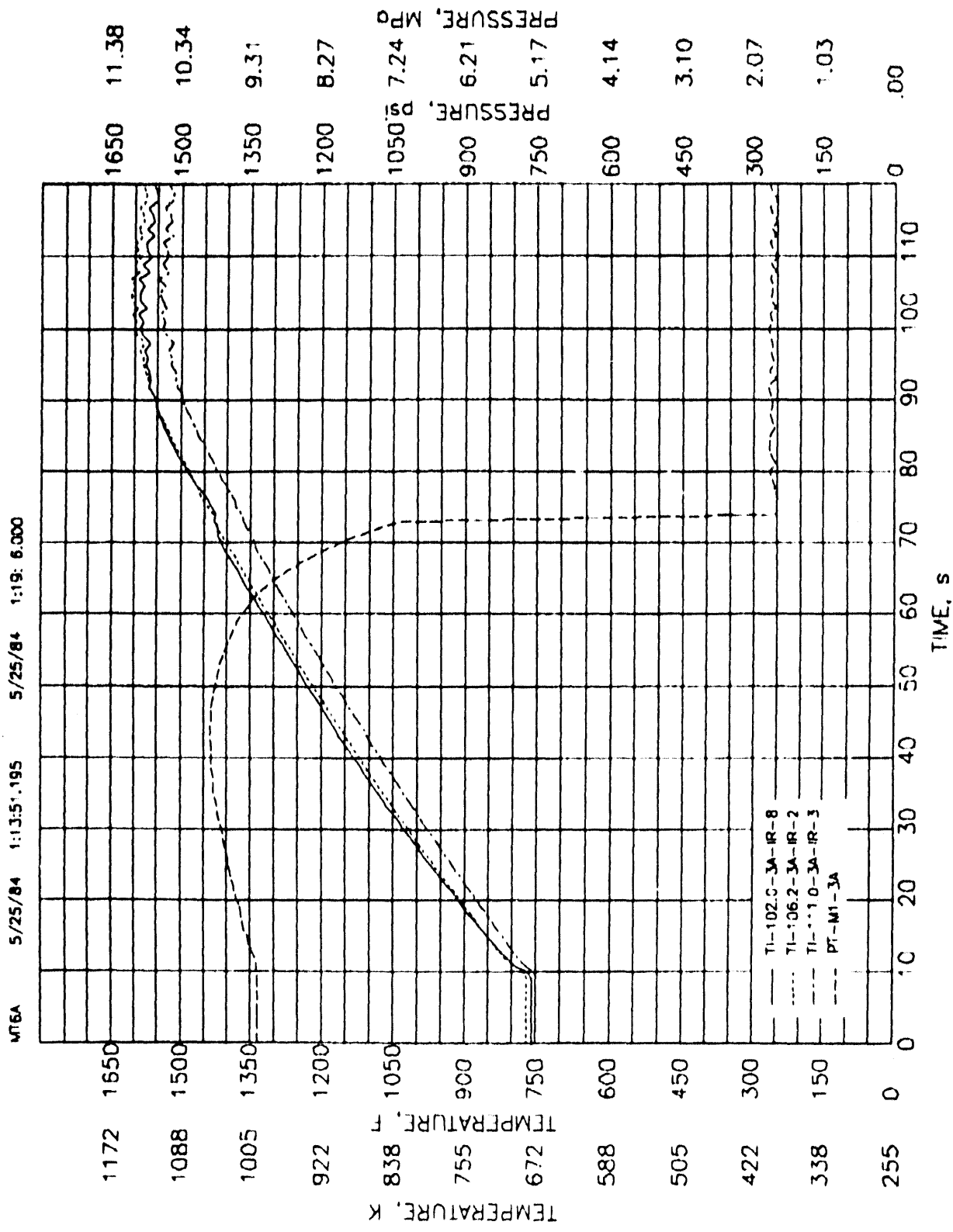


FIGURE A.9. Fuel Rod Interior Cladding Temperatures at Levels 102.0, 106.2, and 111.0, and Plenum Pressures for Rod 3A

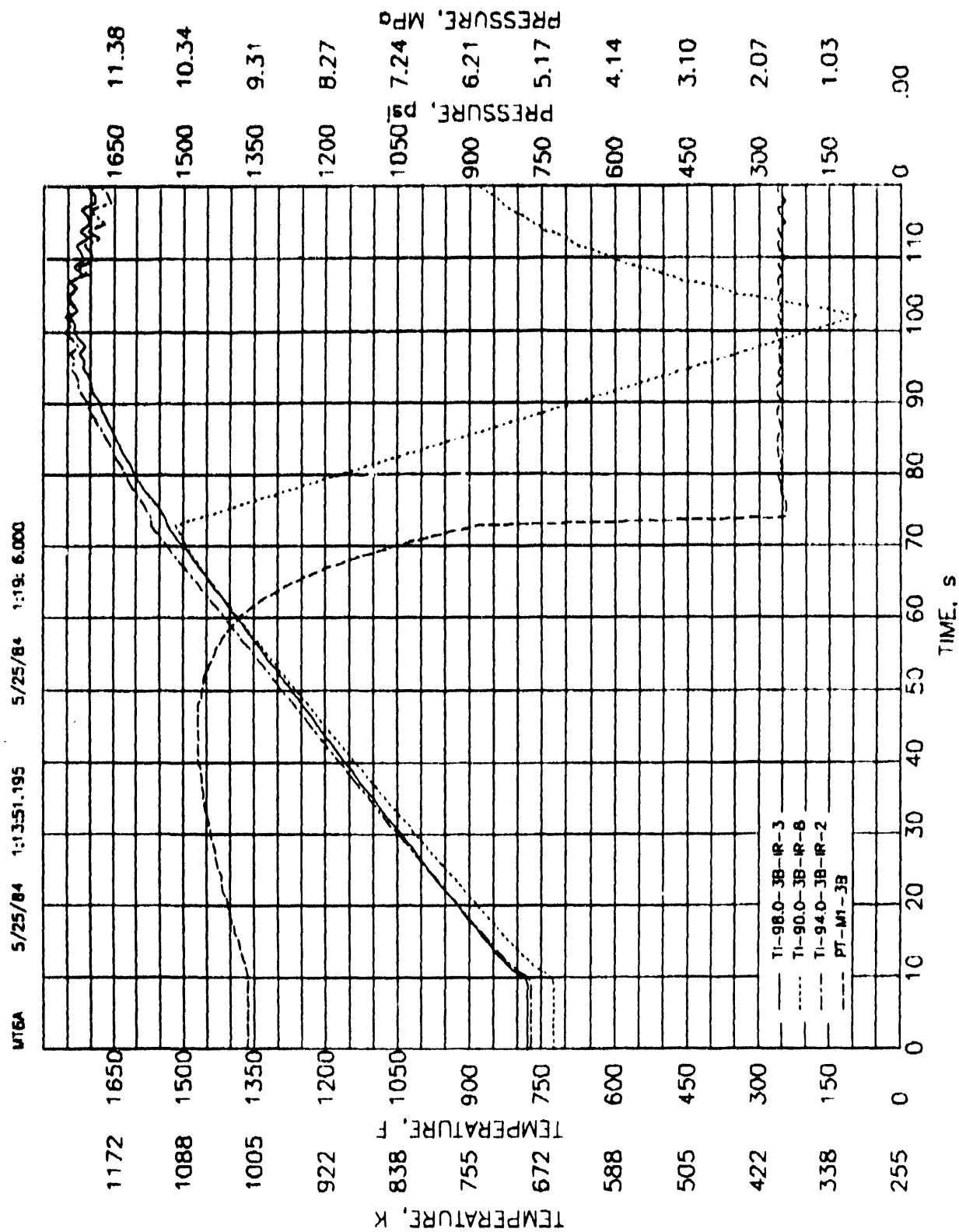


FIGURE A.10. Fuel Rod Interior Cladding Temperatures at Levels 98.0, 90.0, and 94.0, and Plenum Pressures for Rod 3B

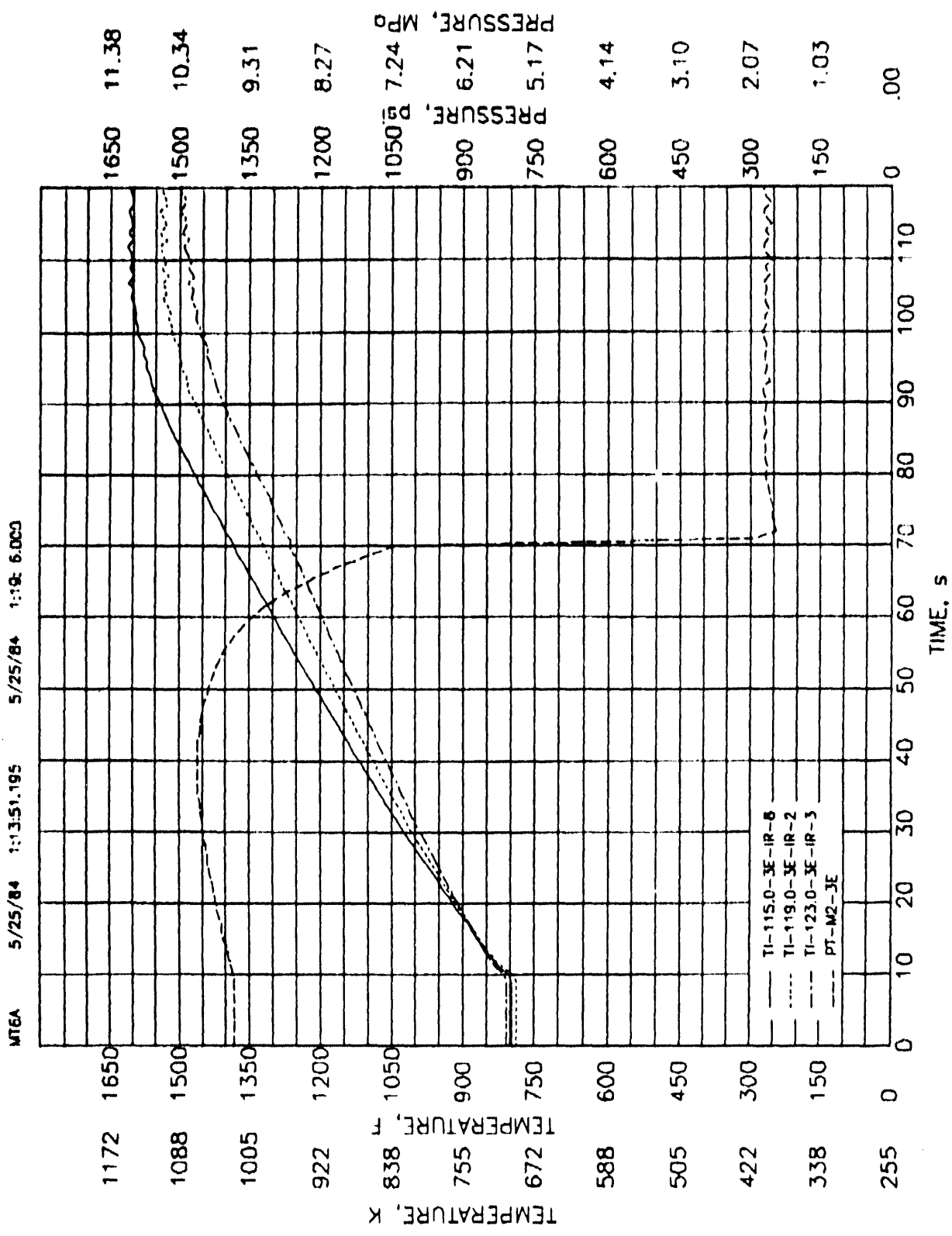


FIGURE A.11: Fuel Rod Interior Cladding Temperatures at Levels 115.0, 119.0, and 123.0, and Plenum Pressures for Rod 3E

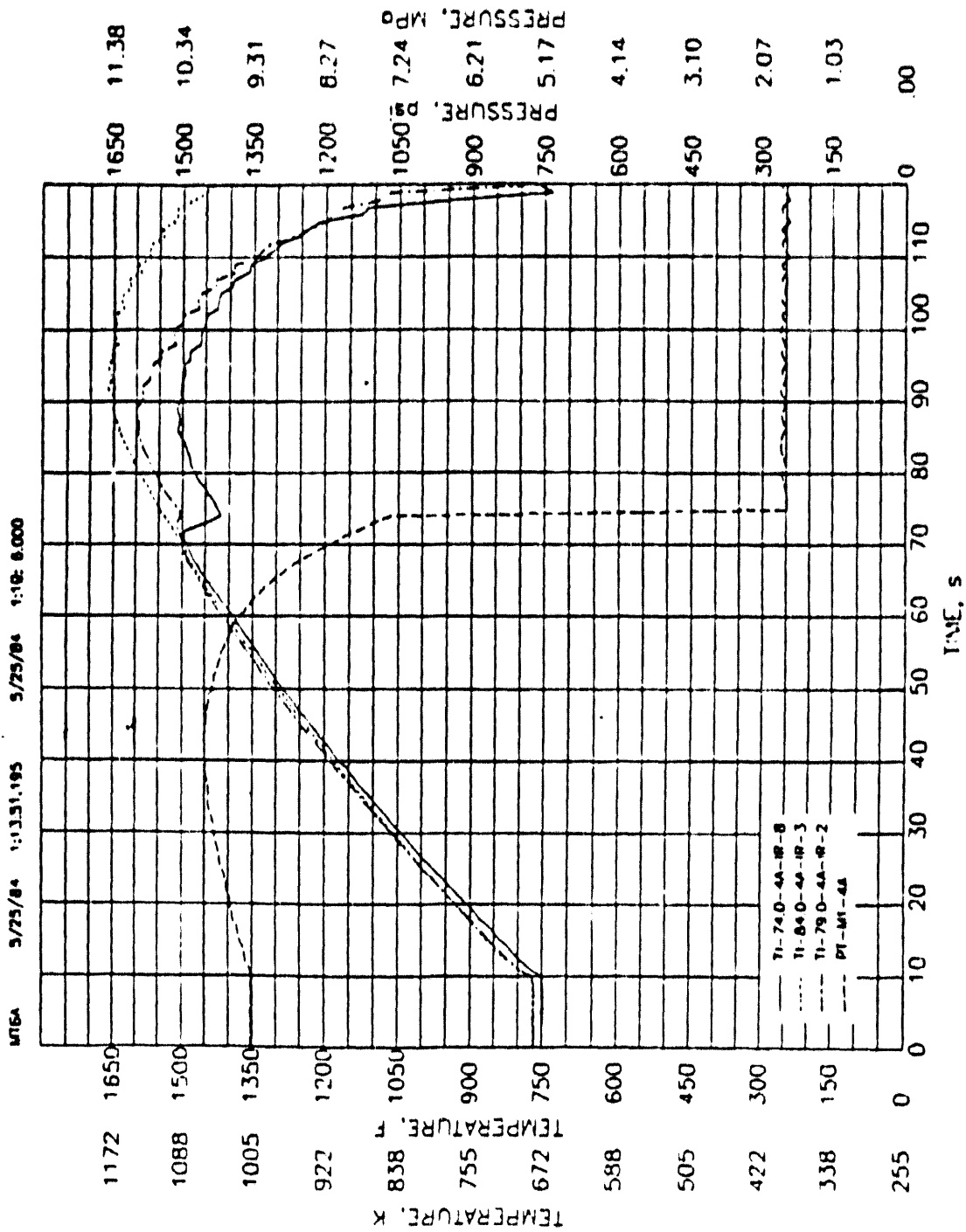


FIGURE A.12. Fuel Rod Interior Cladding Temperatures at Levels 74.0, 84.0 and 79.0, and Plenum Pressures for Rod 4A

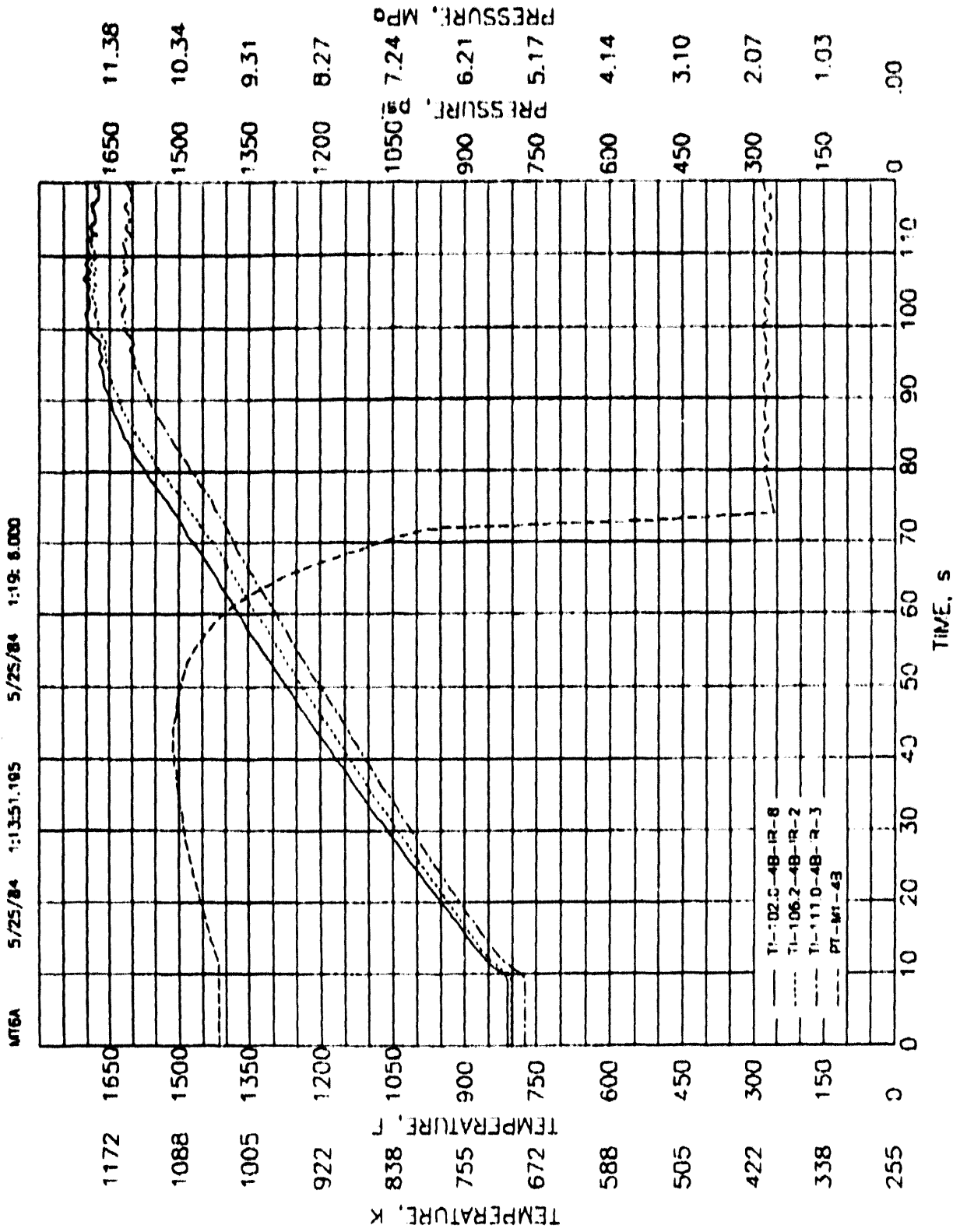


FIGURE A.13. Fuel Rod Interior Cladding Temperatures at Levels 102.0, 106.2, and 111.0, and Plenum Pressures for Rod 48

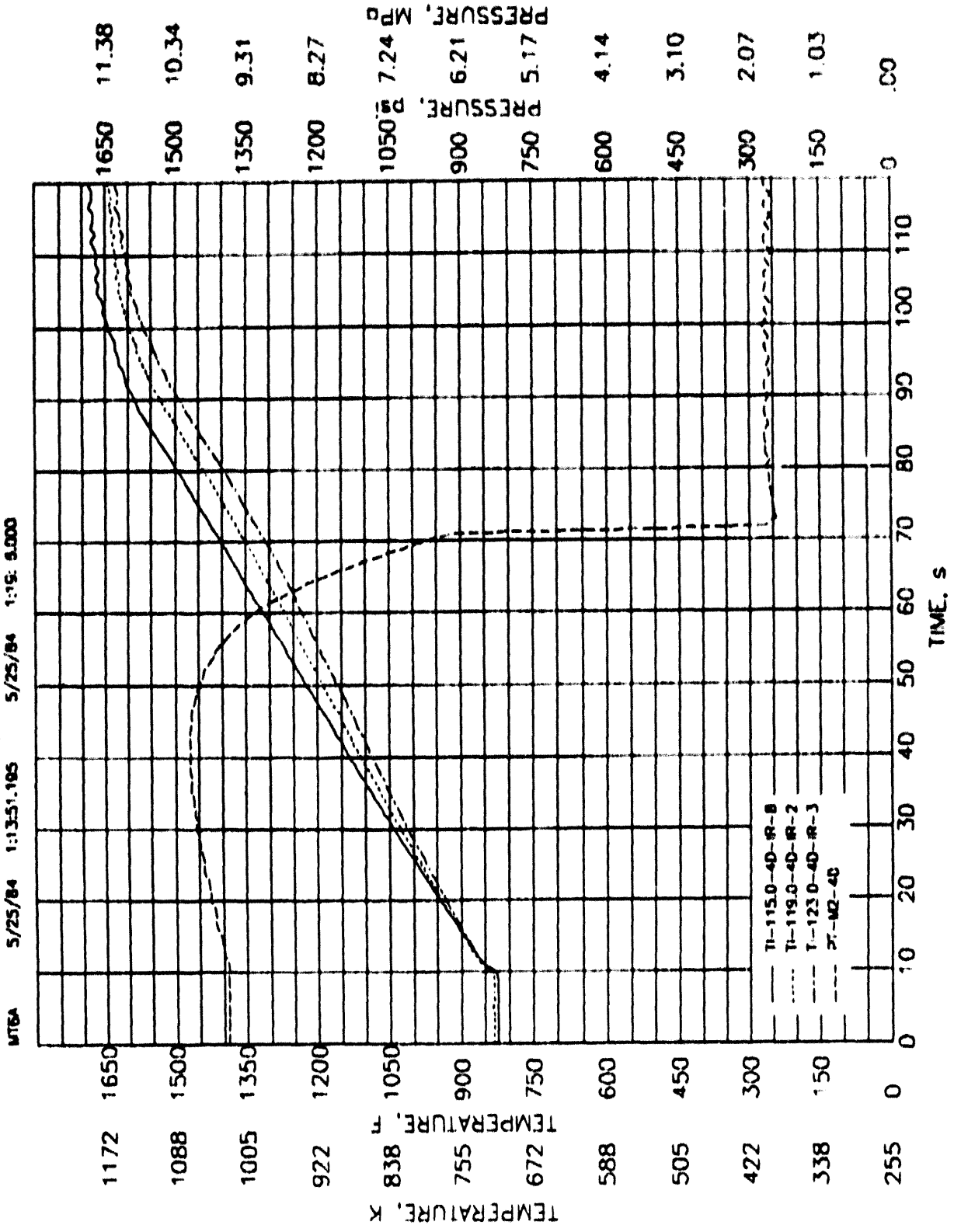


FIGURE A.14. Fuel Rod Interior Cladding Temperatures at Levels 115.0, 119.0, and 123.0, and Plenum Pressures for Rod 4D

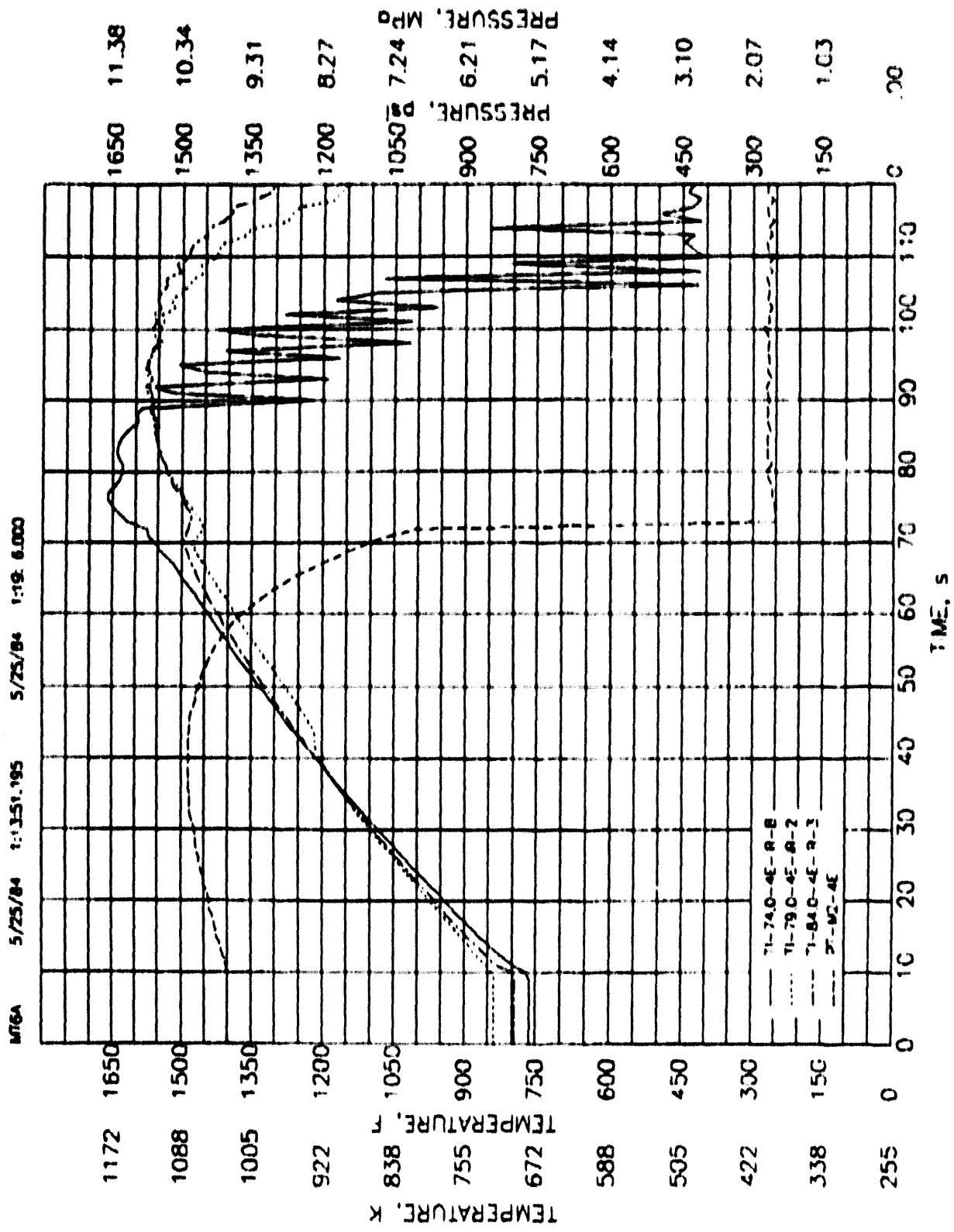


FIGURE A.15. Fuel Rod Interior Cladding Temperatures at Levels 74.0, 79.0, and 84.0, and Plenum Pressures for Rod 4E

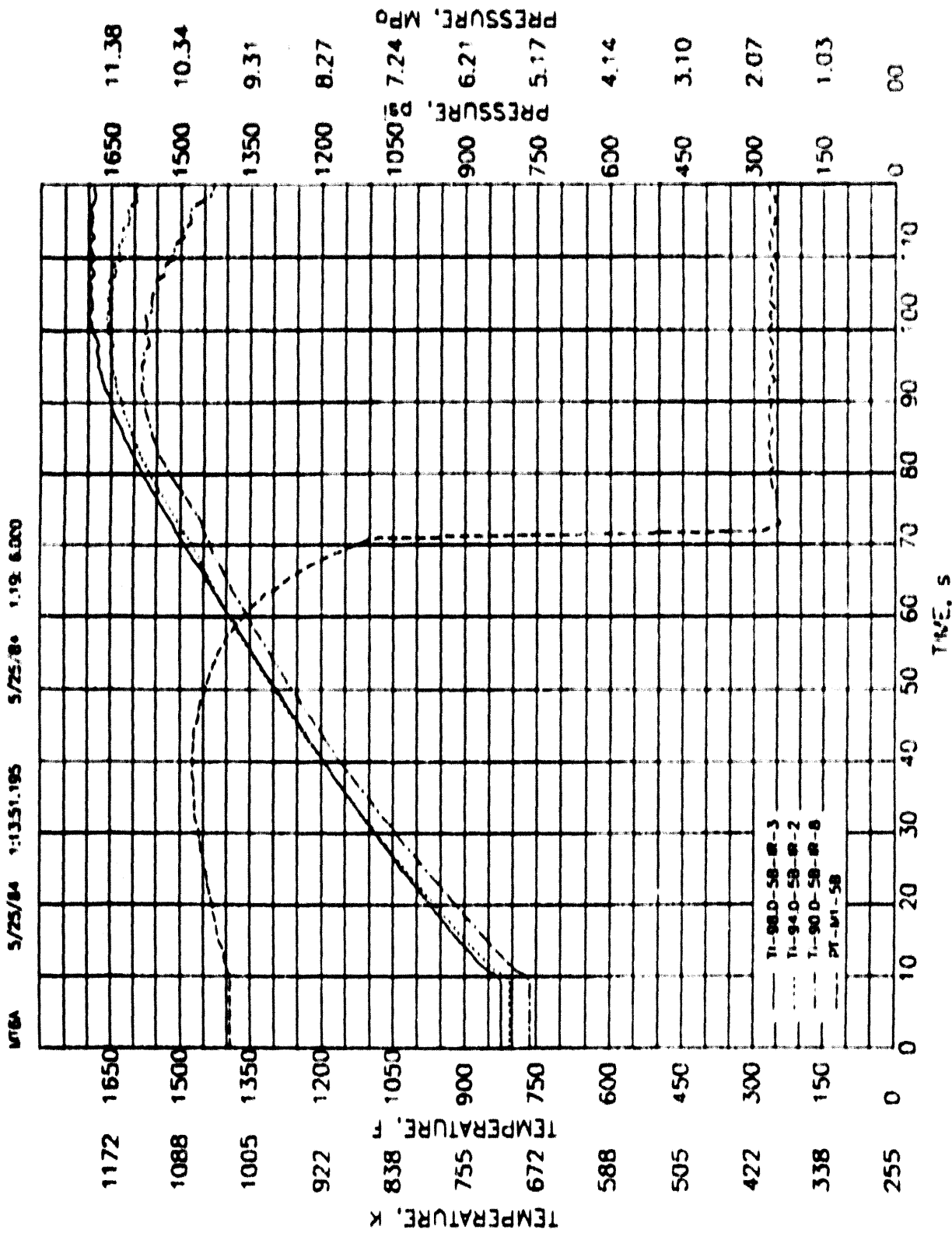


FIGURE A.16. Fuel Rod Interior Cladding Temperatures at Levels 98.0, 94.0, and 90.0, and Plenum Pressures for Rod 58

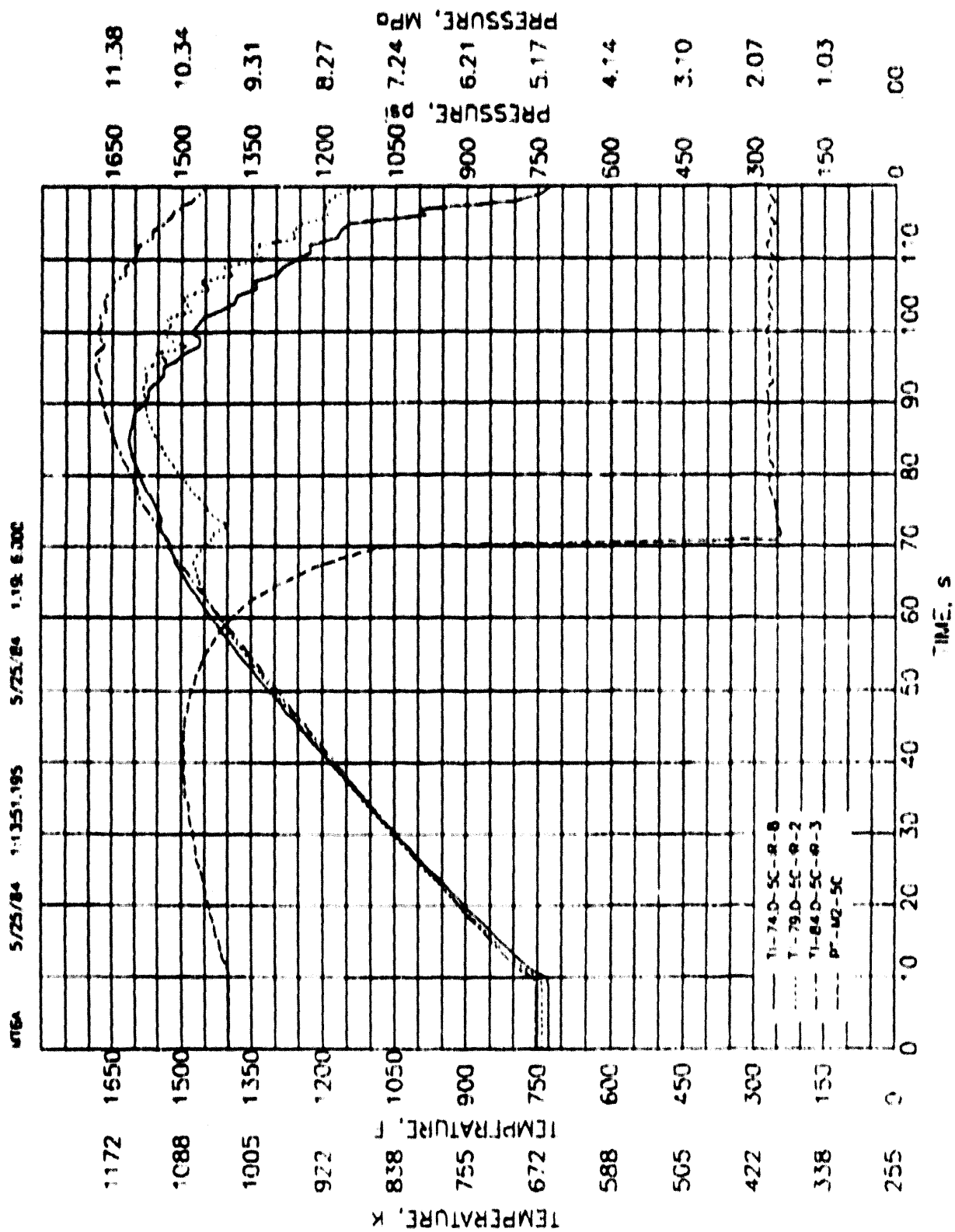


FIGURE A.17. Fuel Rod Interior Cladding Temperature at Levels 74.0, 79.0, and 84.0, and Plenum Pressure for Rod 5C

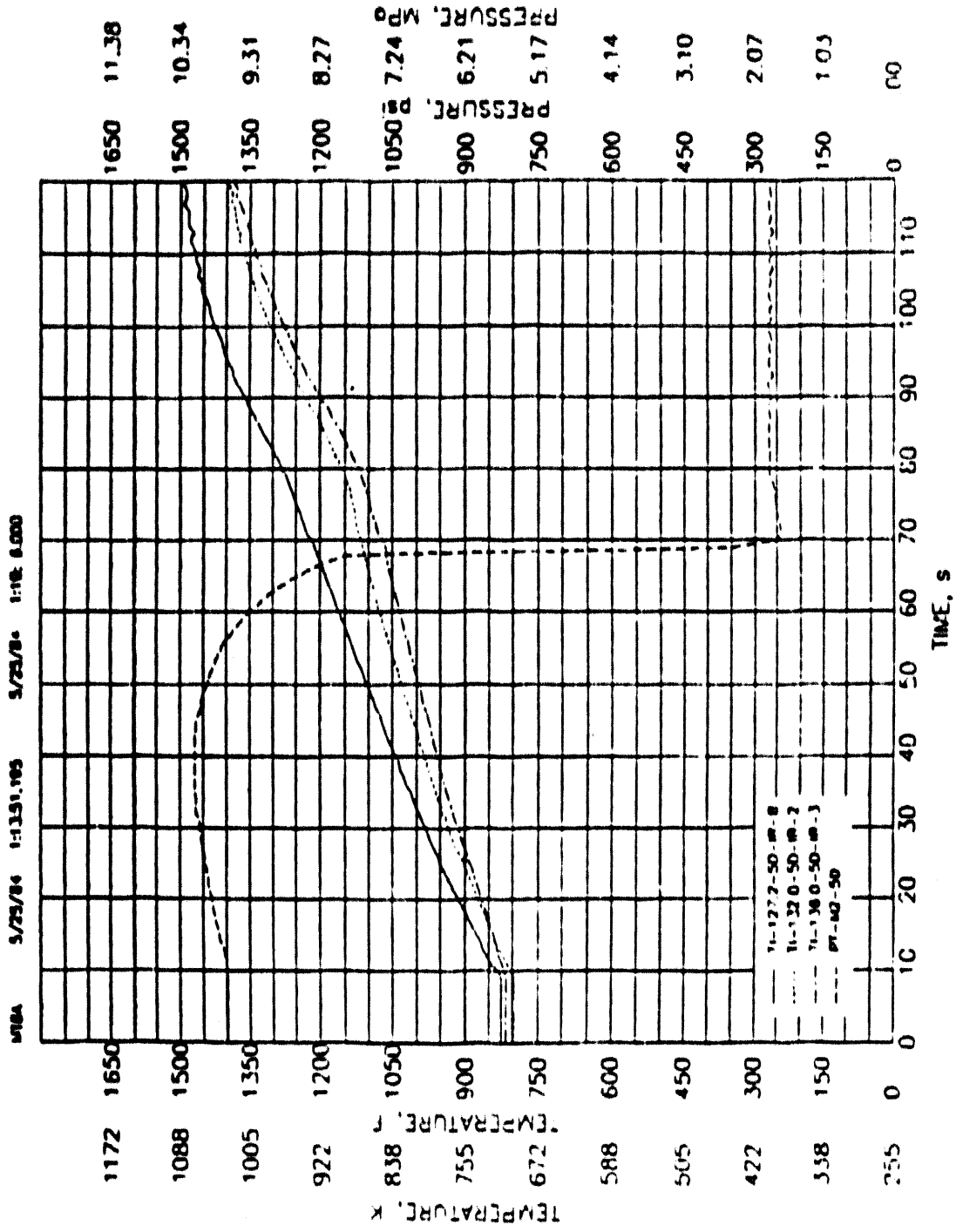


FIGURE A.18. Fuel Rod Interior Cladding Temperature at Levels 127.2, 132.0, and 136.0, and Plenum Pressures for Rod 50

MT&A 5/25/84 1:13:51.195 5/25/84 1:19: 6.000

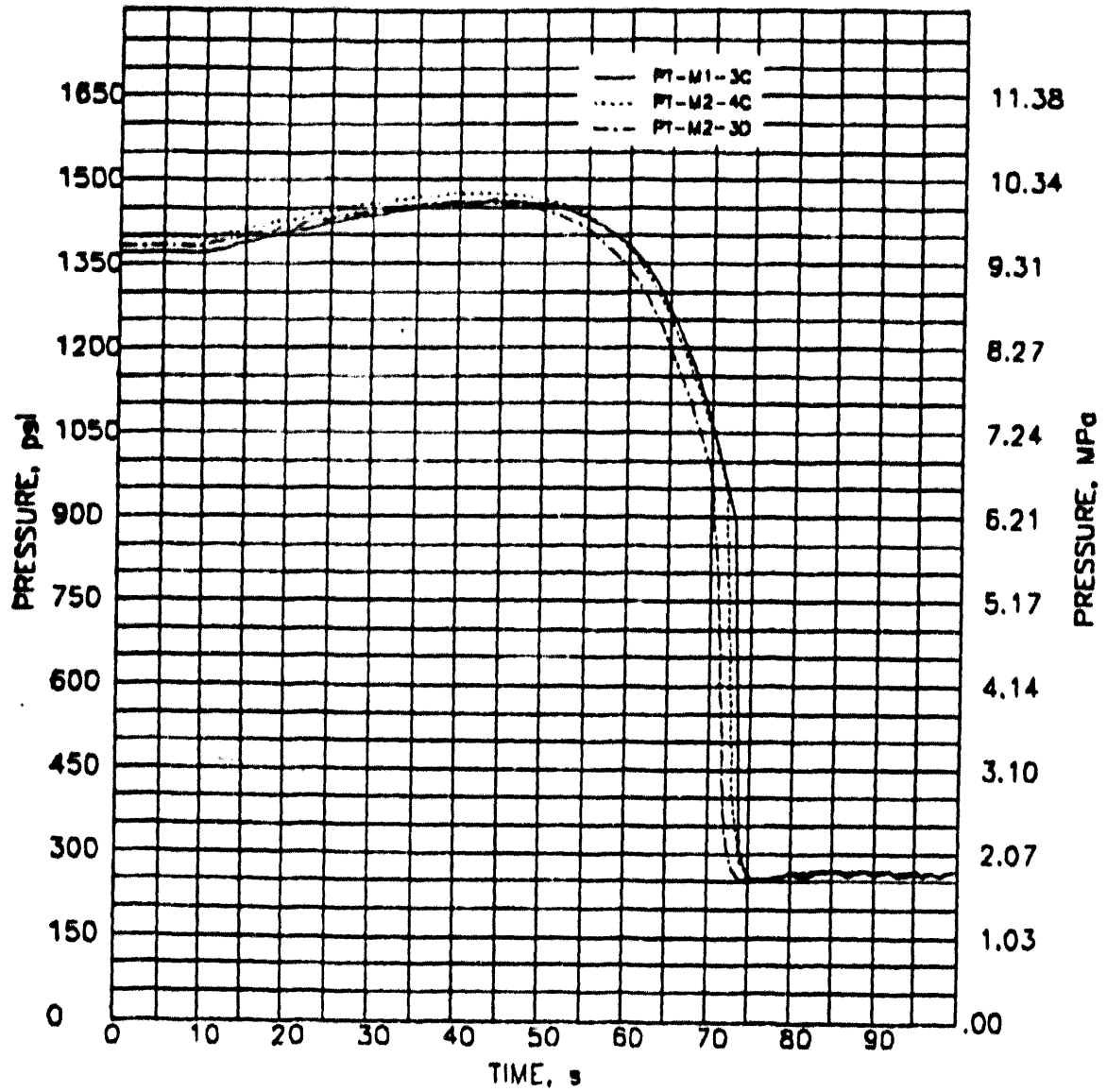


FIGURE A.19. Fuel Rod Plenum Pressure for Rods 3C, 4C, and 3D

APPENDIX B

TRANSIENT FUEL CLADDING TEMPERATURES
DURING THE MT-6A TRANSIENT

APPENDIX B

TRANSIENT FUEL CLADDING TEMPERATURES
DURING THE MT-6A TRANSIENT

Fuel cladding thermocouples were welded to the inside of the fuel cladding. Temperature curves for these thermocouples for the MT-6A transient are presented in this appendix. These curves demonstrate how the fuel heats up almost adiabatically until the reflood water starts to cool the fuel at the thermocouple elevation. These curves demonstrate that the rods can be cooled, even though all 21 rods ballooned and ruptured and were constrained by the shroud.

The remainder of this appendix consists of the following figures:

B.1	Fuel Rod Interior Cladding Temperatures for Rods 2E, 2A, and 2C at Level 56	B.3
B.2	Fuel Rod Interior Cladding Temperatures for Rods 2C, 2E, and 2A at Level 61	B.4
B.3	Fuel Rod Interior Cladding Temperatures for Rods 2E, 2A, and 2C at Level 69.0	B.5
B.4	Fuel Rod Interior Cladding Temperatures for Rods 5C, 4E, and 4A at Level 74.0	B.6
B.5	Fuel Rod Interior Cladding Temperatures for Rods 4E, 5C, and 4A at Level 79.0	B.7
B.6	Fuel Rod Interior Cladding Temperatures for Rods 5C, 4A, and 4E at Level 84.0	B.8
B.7	Fuel Rod Interior Cladding Temperatures for Rods 3B, 5B, and 1B at Level 90	B.9
B.8	Fuel Rod Interior Cladding Temperatures for Rods 3B, 5B, and 1B at Level 94.0	B.10
B.9	Fuel Rod Interior Cladding Temperatures for Rods 5B, 3B, and 1B at Level 98	B.11
B.10	Fuel Rod Interior Cladding Temperatures for Rods 3A, 4B, and 2B at Level 102	B.12
B.11	Fuel Rod Interior Cladding Temperatures for Rods 2B, 4B, and 3A at Level 106.2	B.13

B.12	Fuel Rod Interior Cladding Temperatures for Rods 3A, 2B, and 4B at Level 111.0	B.14
B.13	Fuel Rod Interior Cladding Temperature for Rods 4D, 3E, and 2D at Level 115.0	B.15
B.14	Fuel Rod Interior Cladding Temperatures for Rods 4D, 2D, and 3E at Level 119.0	B.16
B.15	Fuel Rod Interior Cladding Temperatures for Rods 3E, 4D, and 2D at Level 123.0	B.17
B.16	Fuel Rod Interior Cladding Temperatures for Rods 1D, 1C, and 5D at Level 127.2	B.18
B.17	Fuel Rod Interior Cladding Temperatures for Rods 1D, 5D, and 1C at Level 127.2	B.19
B.18	Fuel Rod Interior Cladding Temperatures for Rods 1D, 5D, and 1C at Level 136.0	B.20

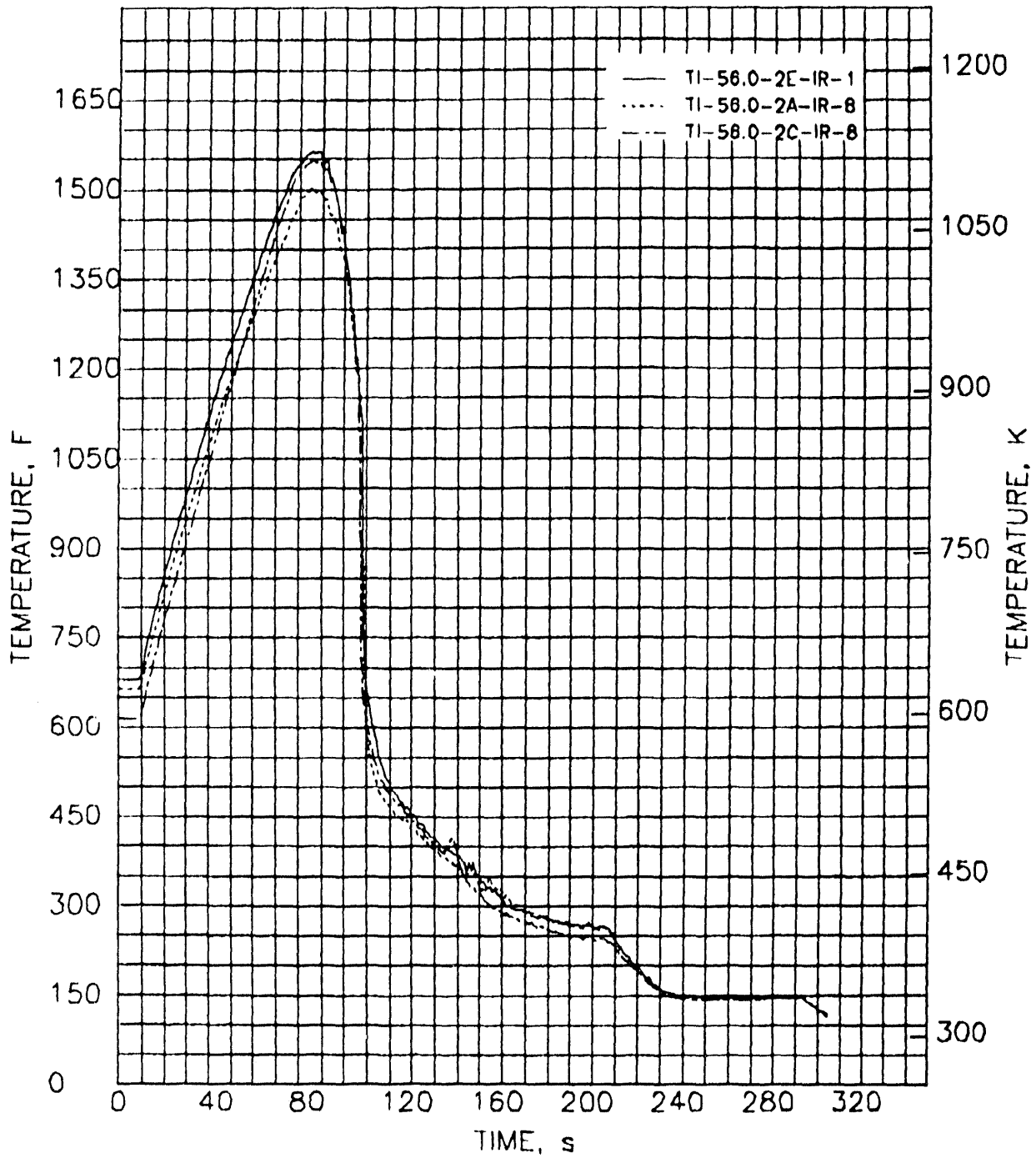


FIGURE B.1. Fuel Rod Interior Cladding Temperatures for Rods 2E, 2A, and 2C at Level 56

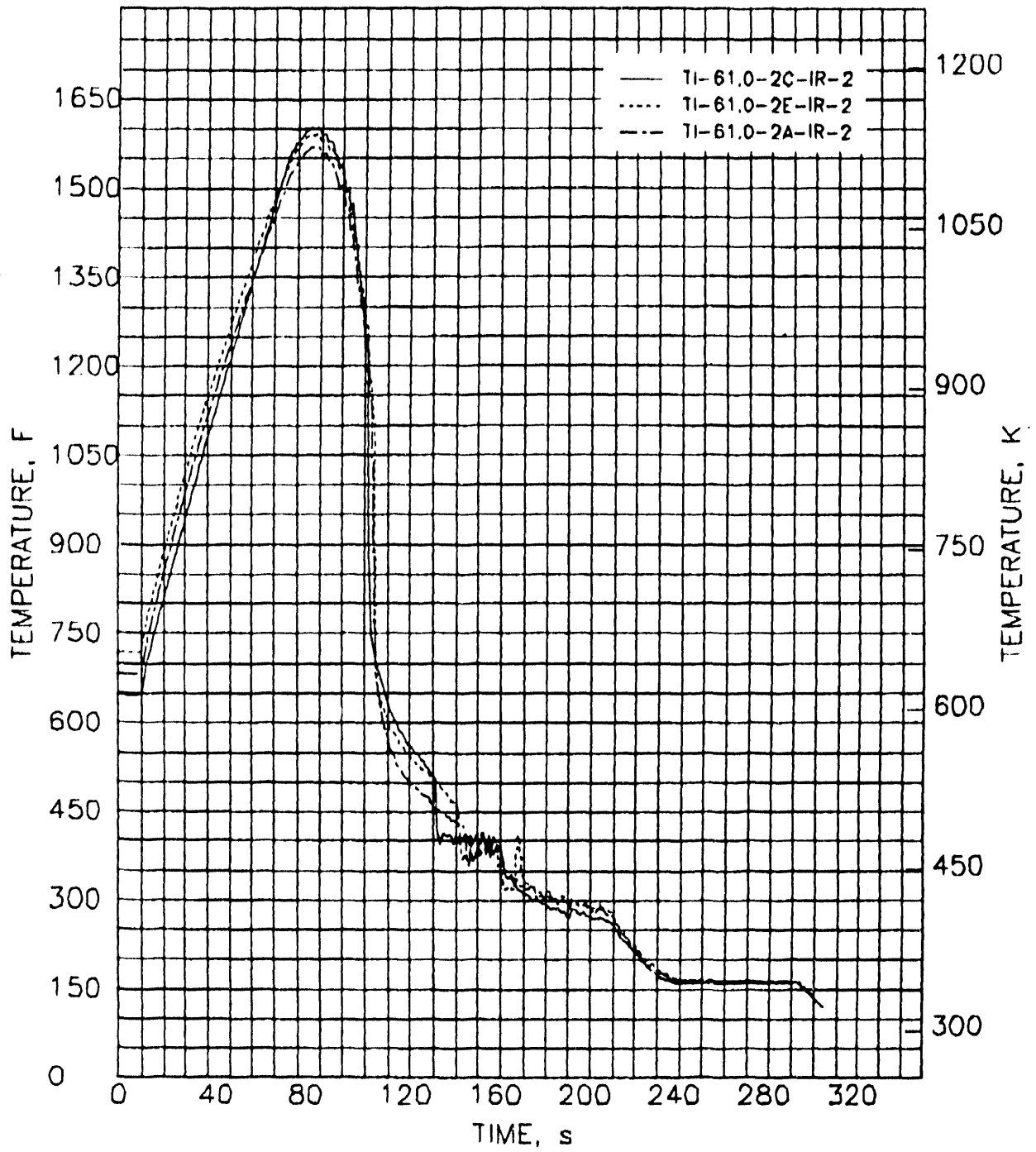


FIGURE B.2. Fuel Rod Interior Cladding Temperatures for Rods 2C, 2E, and 2A at Level 61

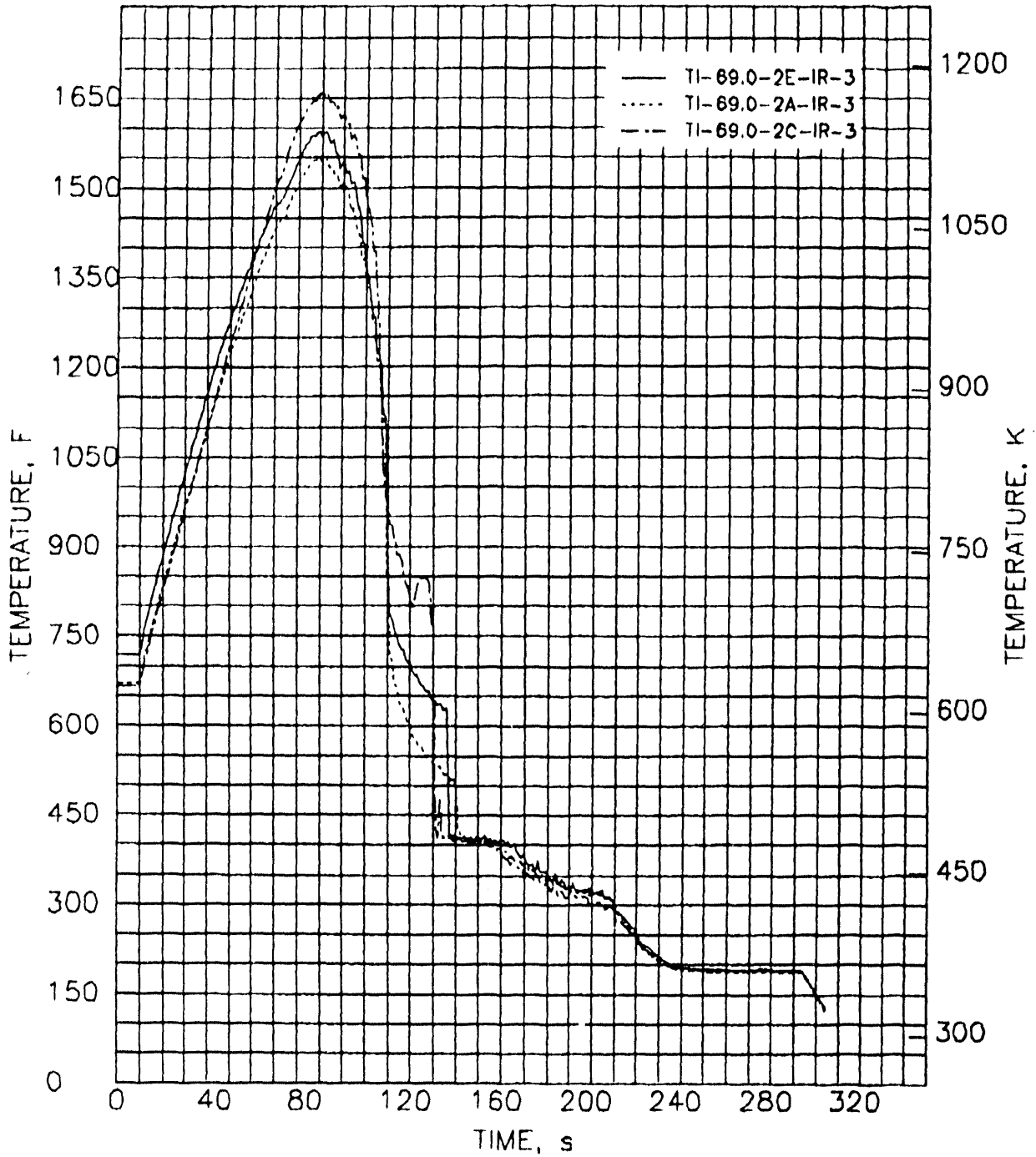


FIGURE B.3. Fuel Rod Interior Cladding Temperatures for Rods 2E, 2A, and 2C at Level 69.

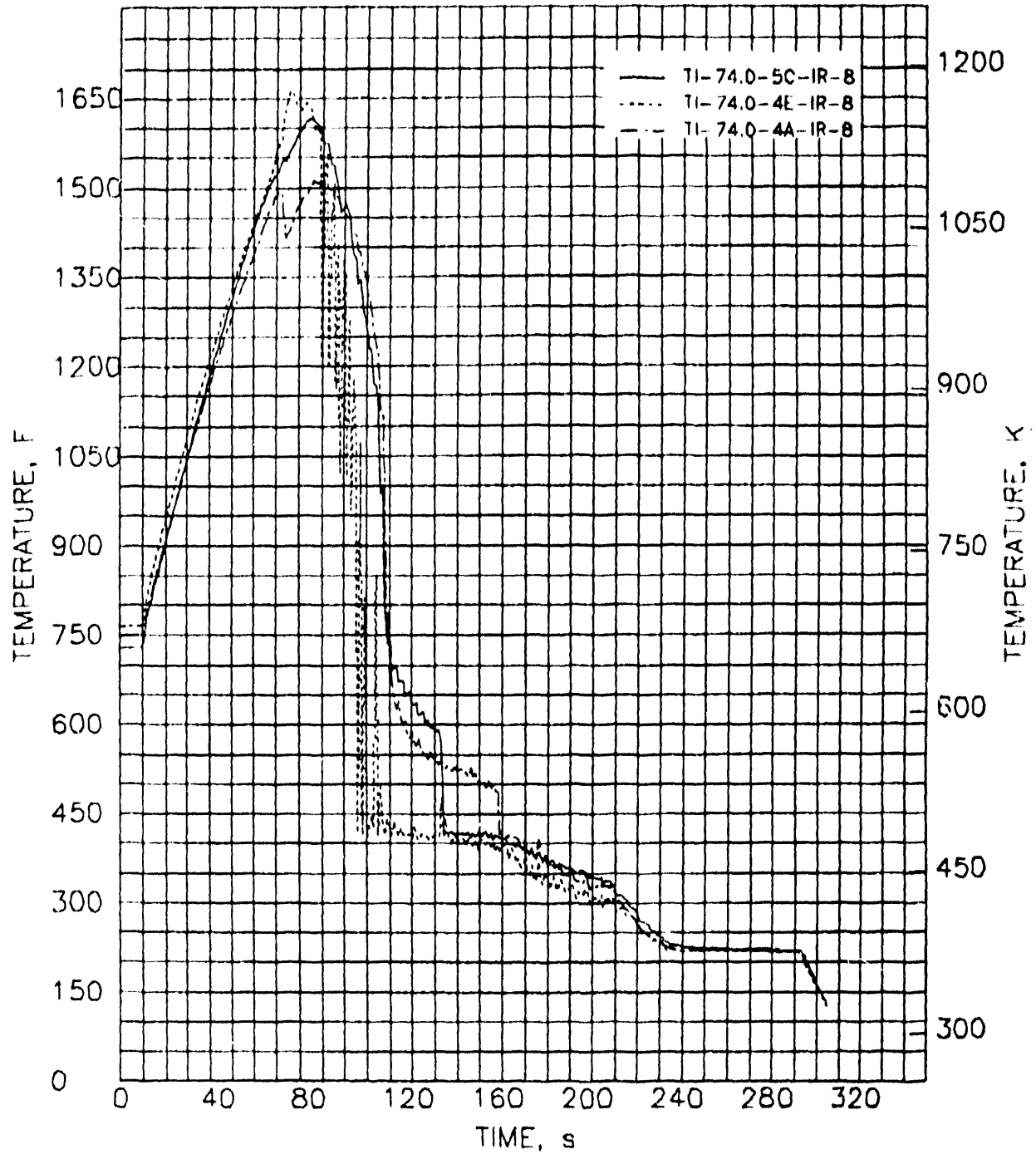


FIGURE B.4. Fuel Rod Interior Cladding Temperatures for Rods 5C, 4E, and 4A at Level 74.0

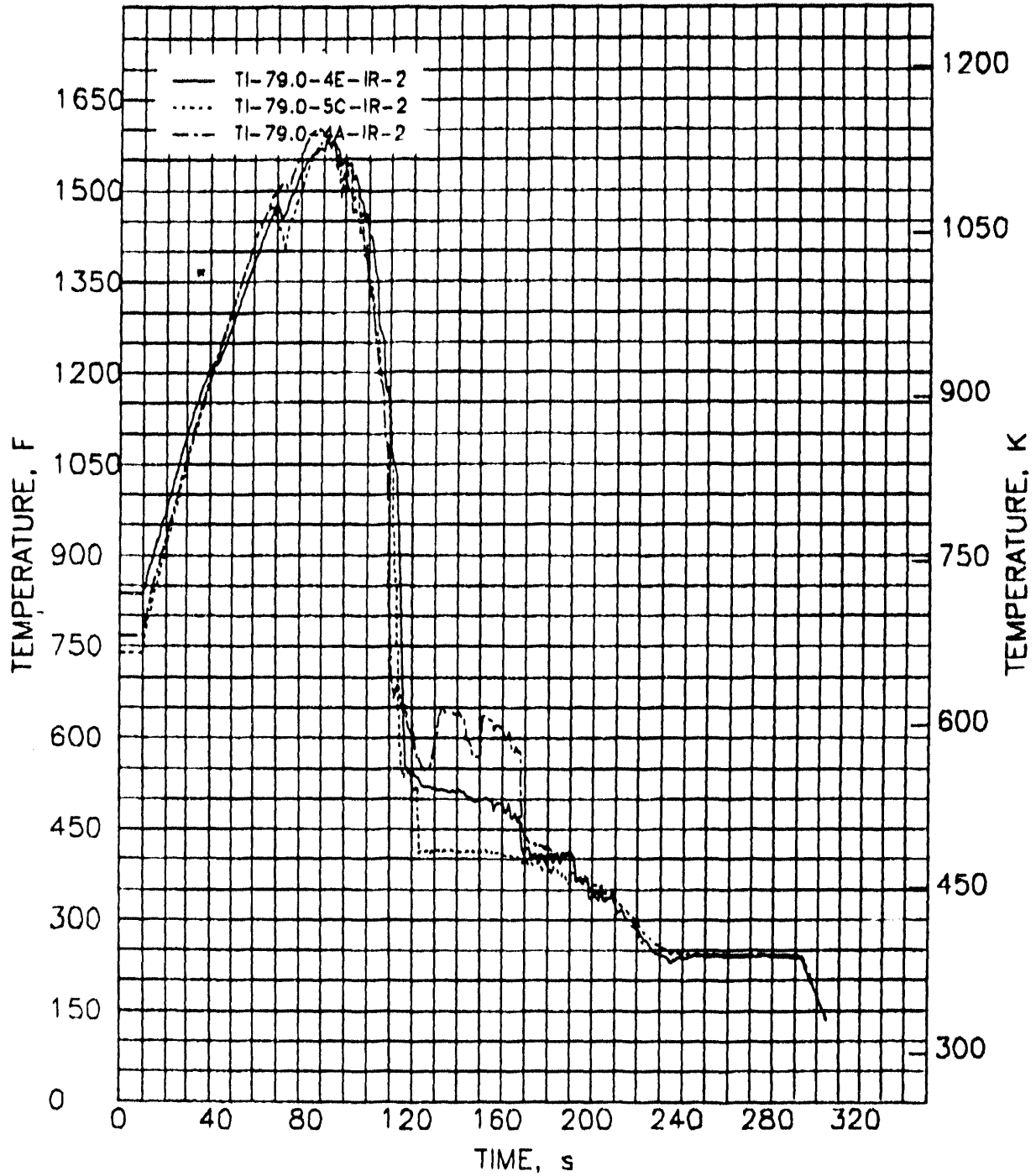


FIGURE B.5. Fuel Rod Interior Cladding Temperatures for Rods 4E, 5C, and 4A at Level 79.0

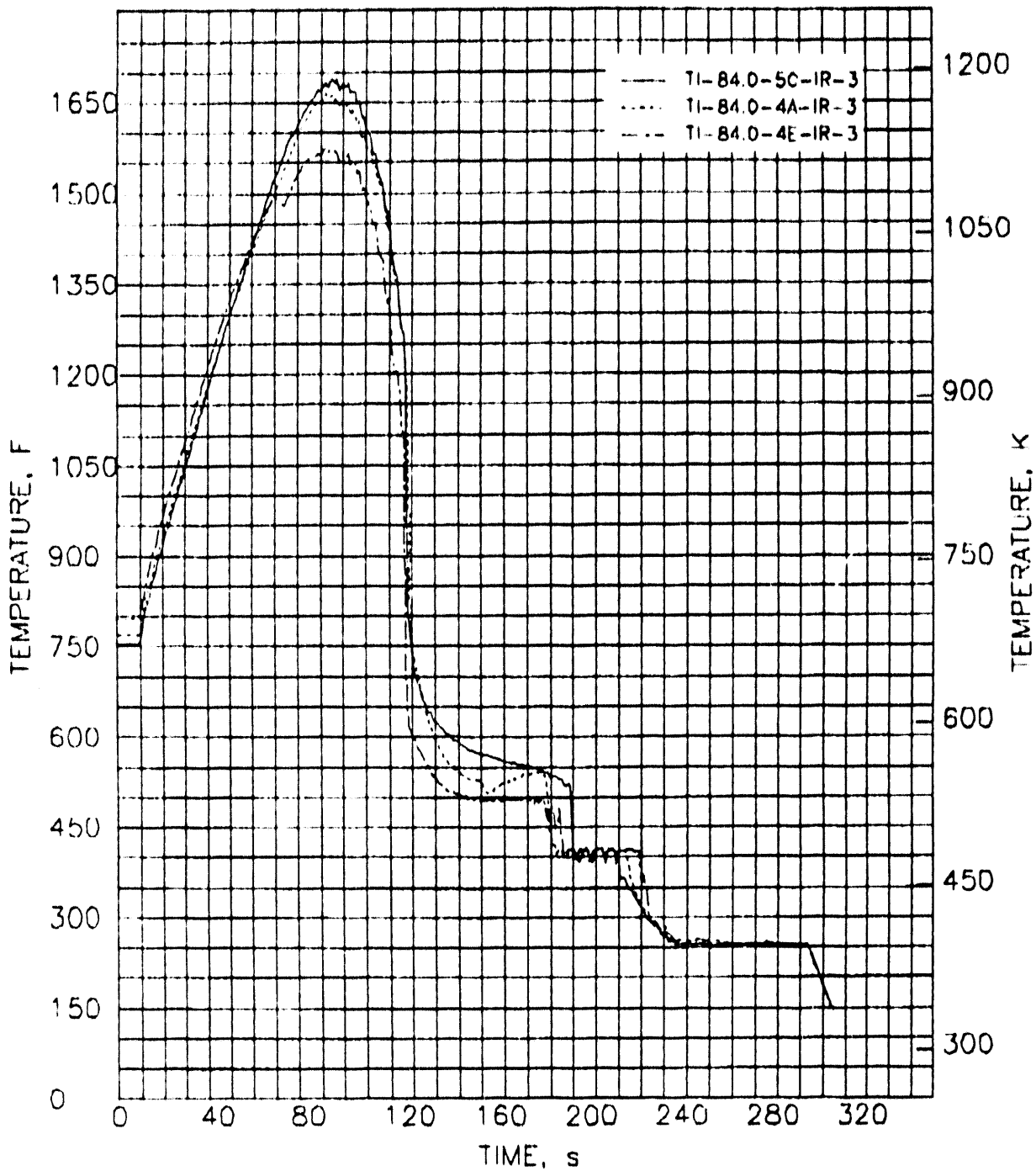


FIGURE B.6. Fuel Rod Interior Cladding Temperatures for Rods 5C, 4A, and 4E at Level 84.0

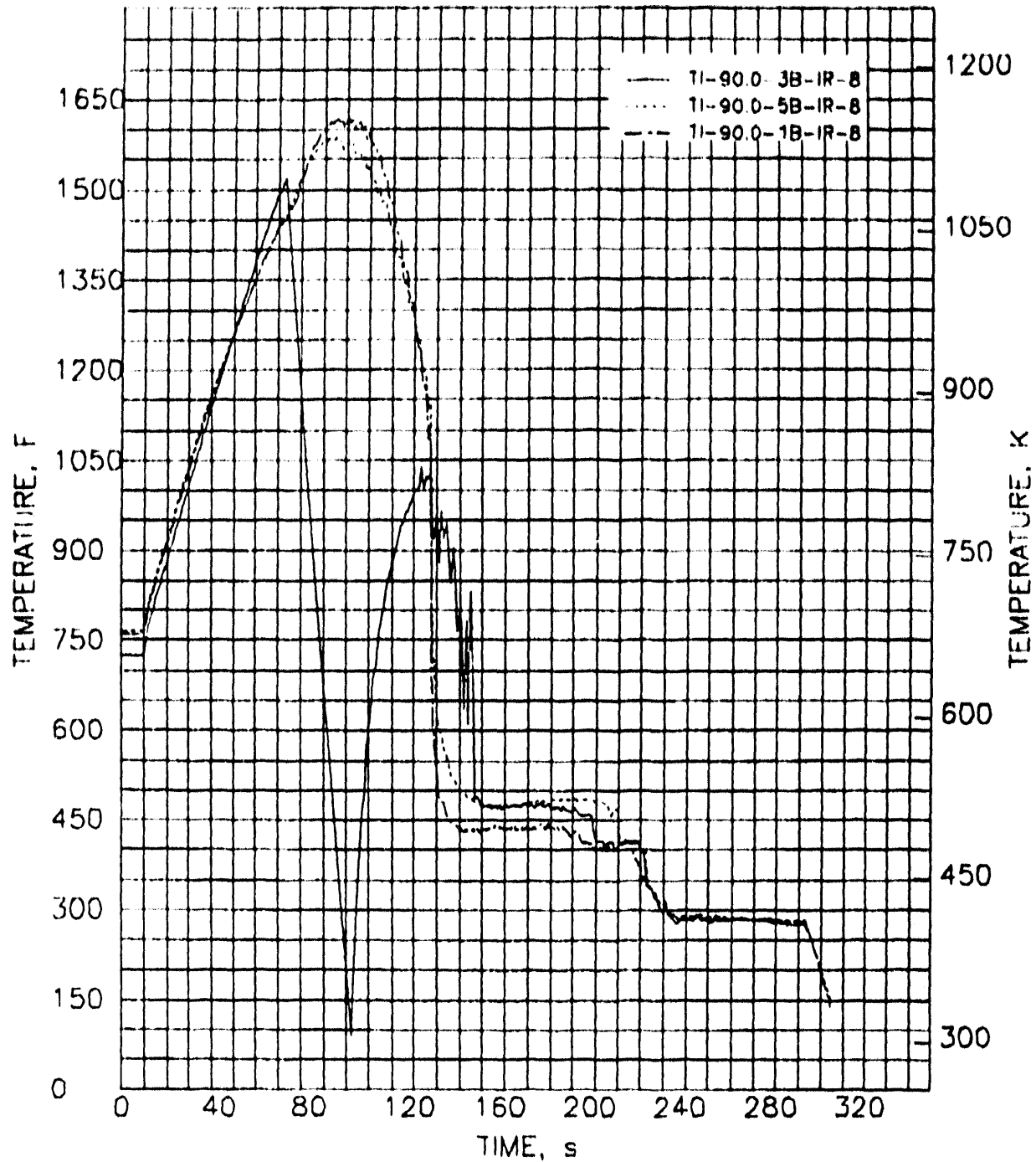


FIGURE B.7. Fuel Rod Interior Cladding Temperatures for Rods 3B, 5B and 1B at Level 90.0

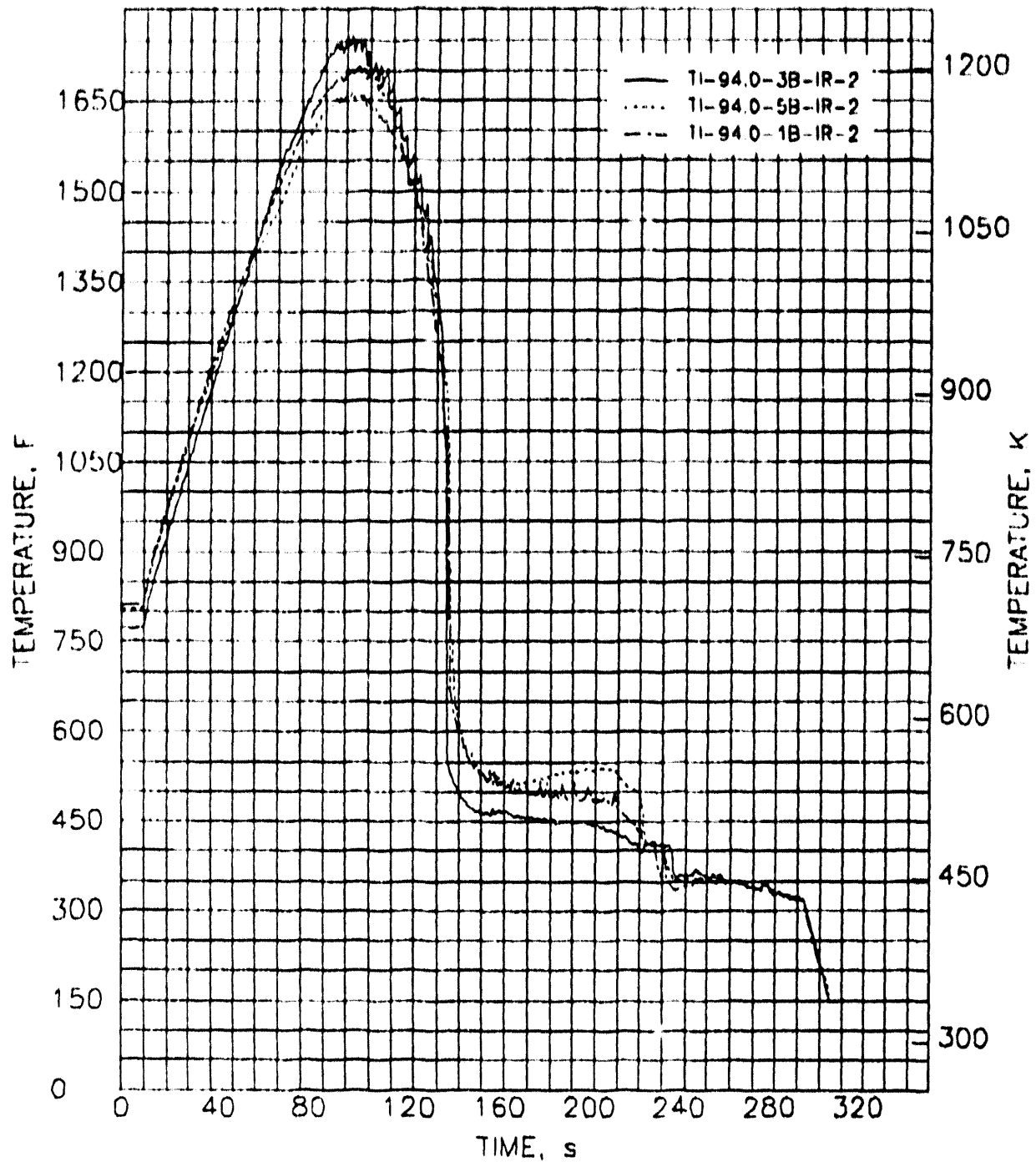


FIGURE B.8. Fuel Rod Interior Cladding Temperatures for Rods 3B, 5B, and 1B at Level 94.0

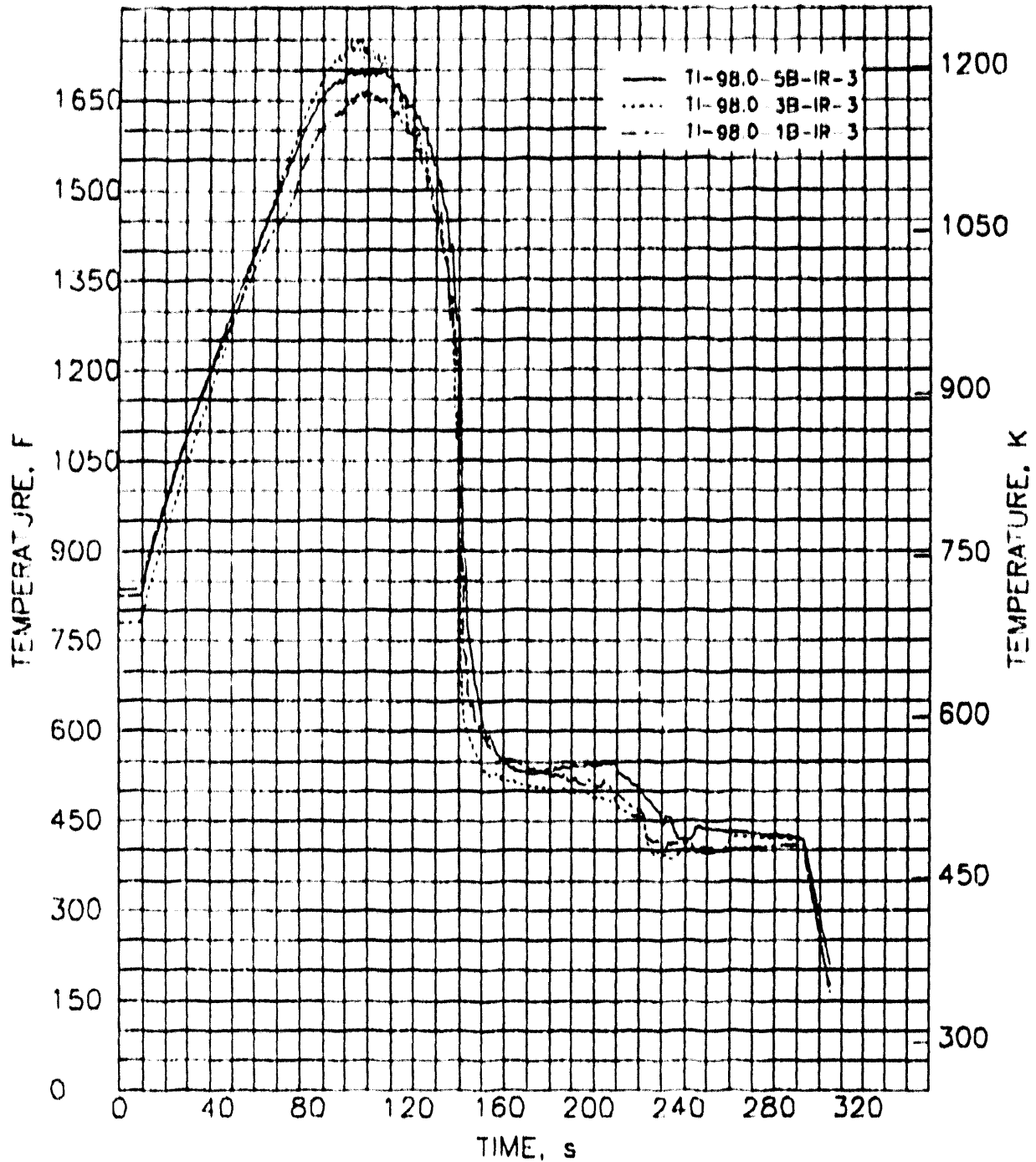


FIGURE B.9. Fuel Rod Interior Cladding Temperatures for Rods 5B, 3B, and 1B at Level 98.0

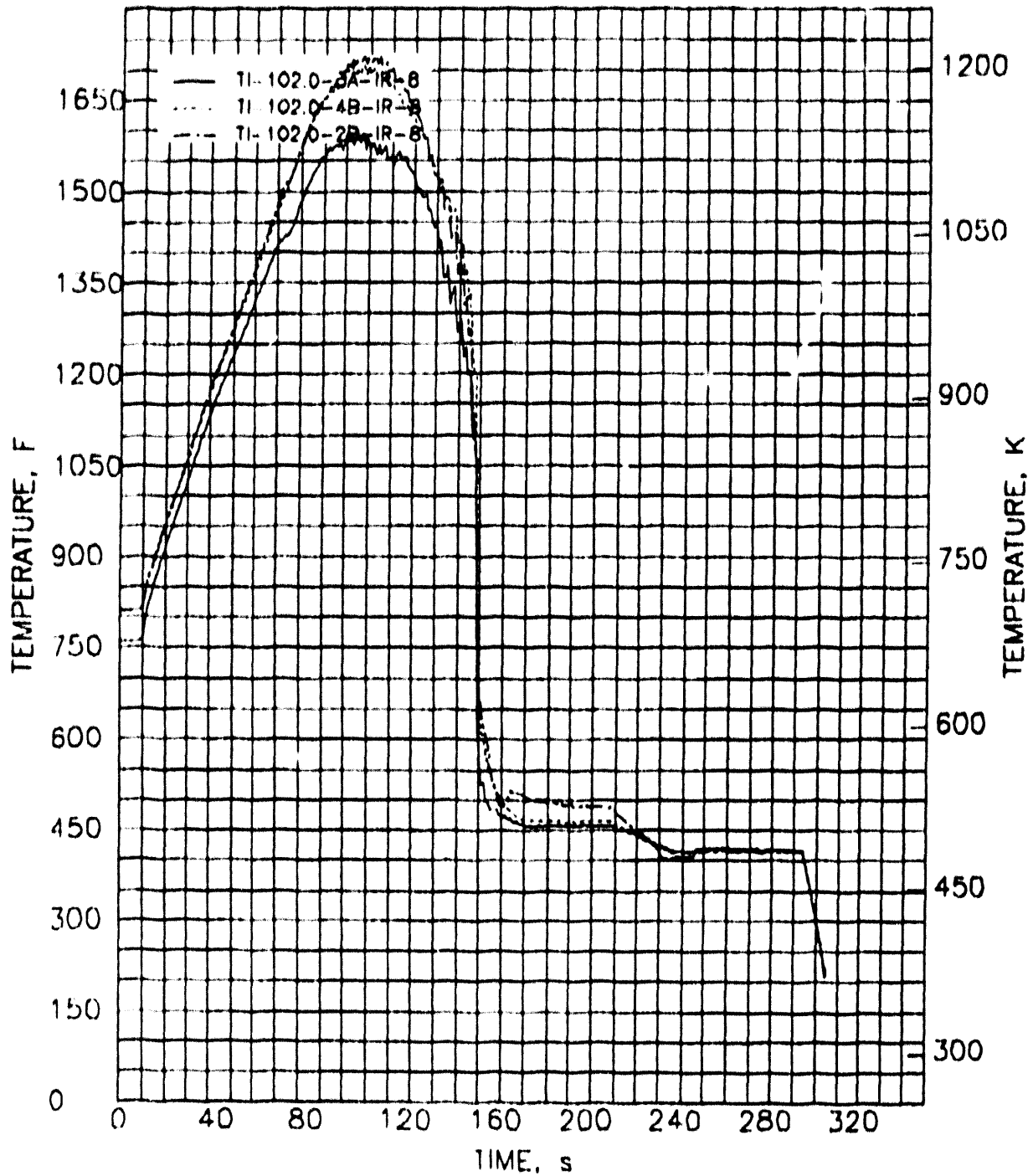


FIGURE B.10. Fuel Rod Interior Cladding Temperatures for Rods 3A, 4B, and 2B at Level 102.0

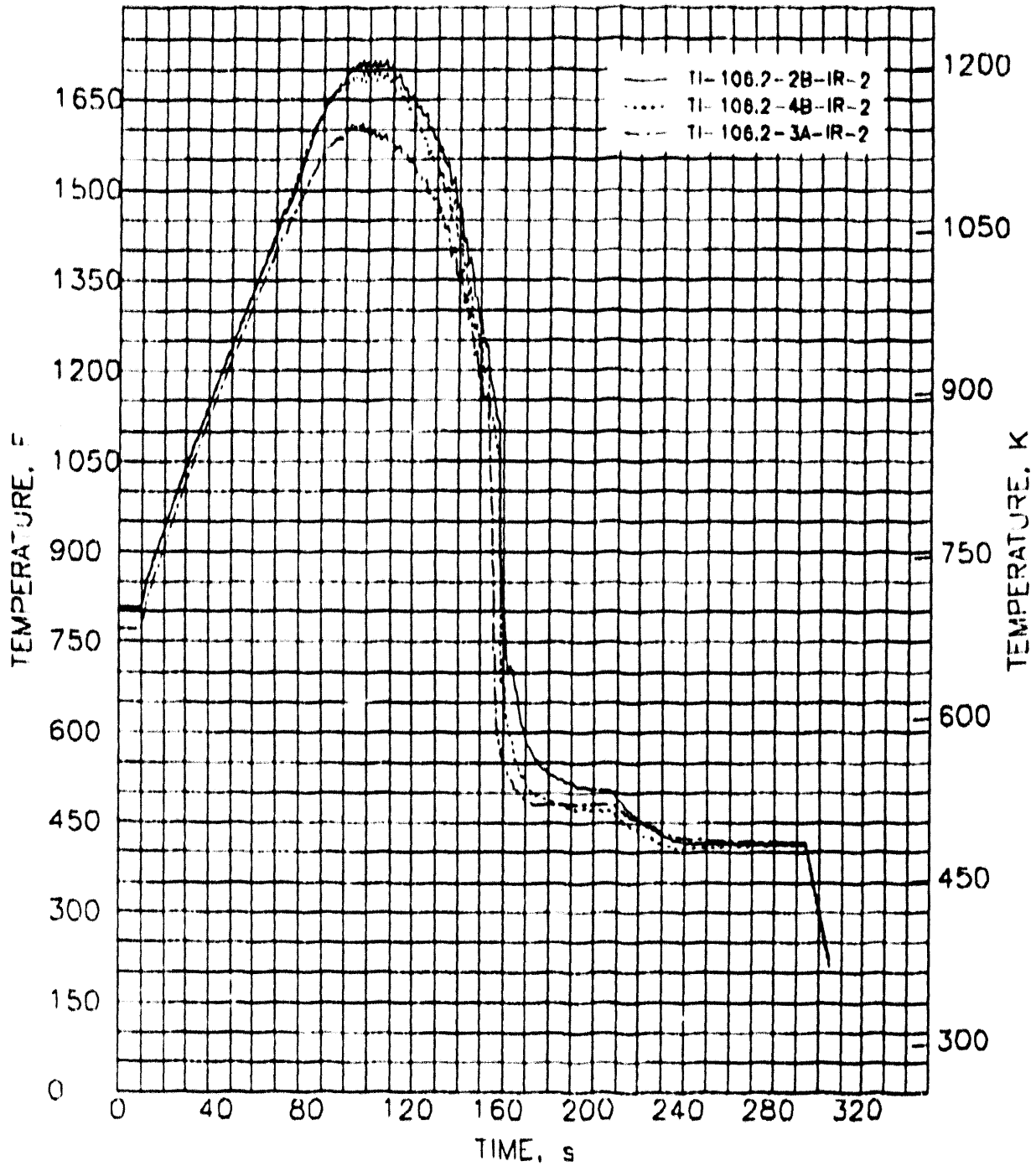


FIGURE B.11. Fuel Rod Interior Cladding Temperatures for Rods 2B, 4B, and 3A at Level 106.2

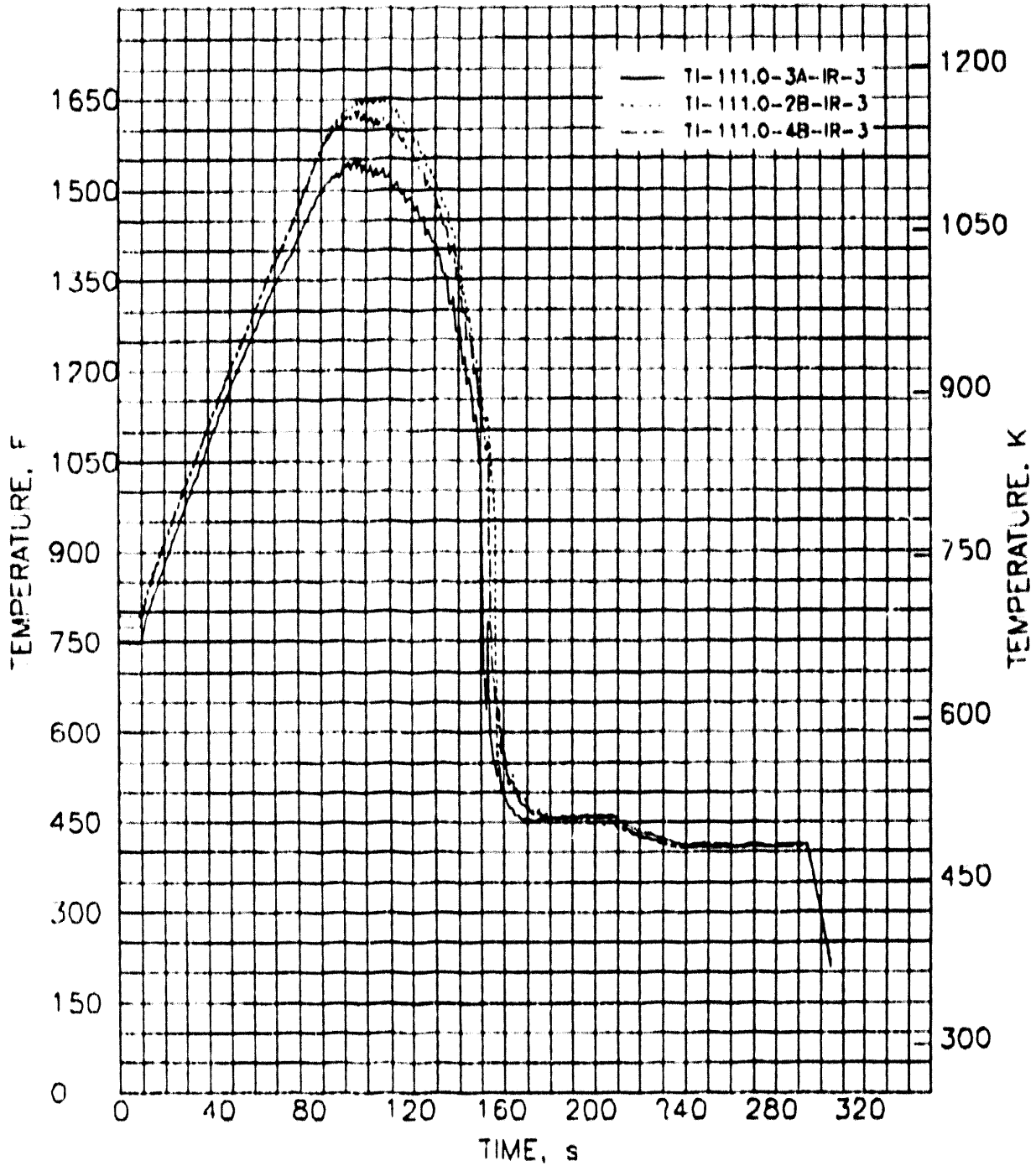


FIGURE B.12. Fuel Rod Interior Cladding Temperatures for Rods 3A, 2B, and 4B at Level 111.0

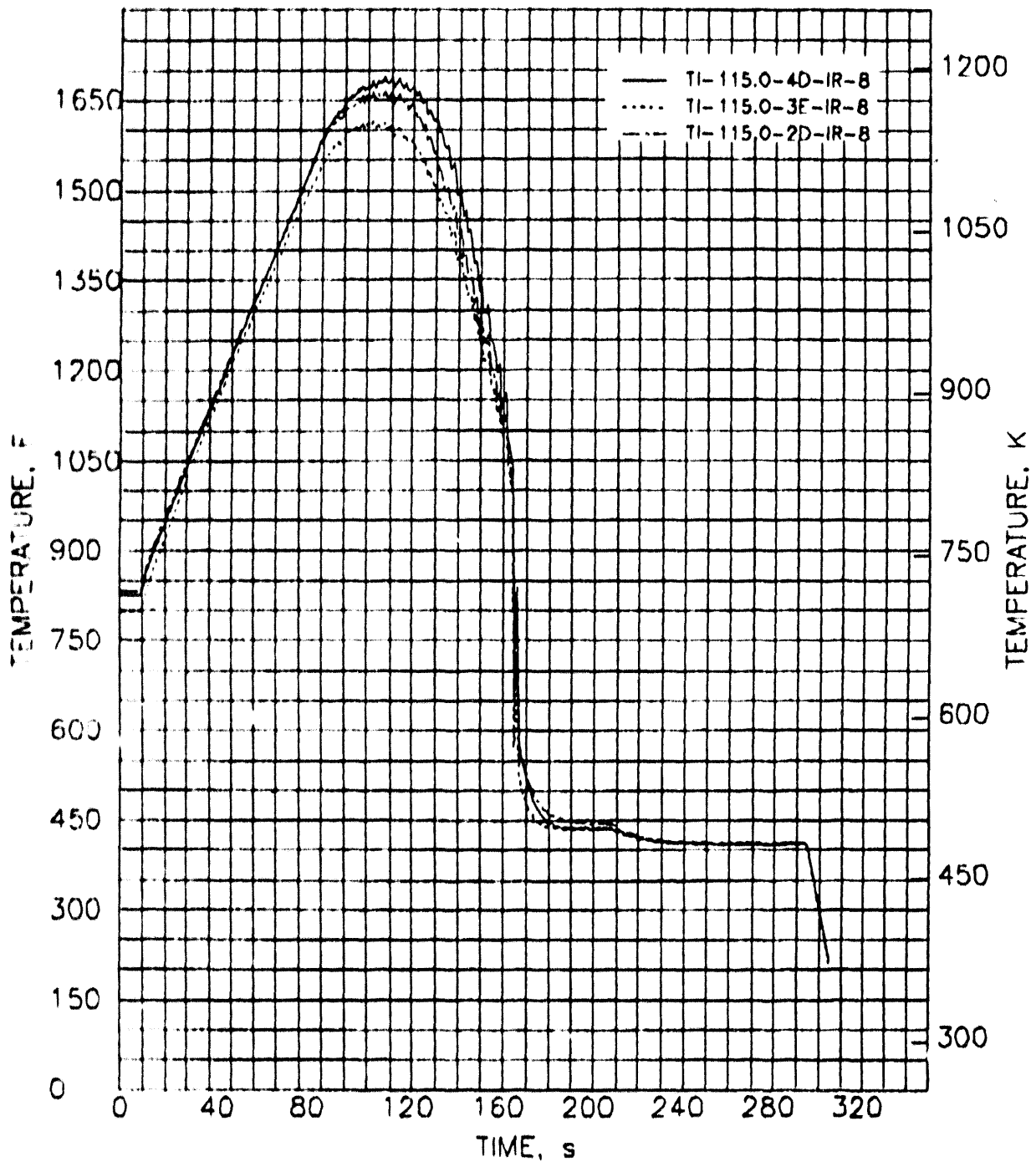


FIGURE B.13. Fuel Rod Interior Cladding Temperatures for Rods 4D, 3E, and 2D at Level 115.0

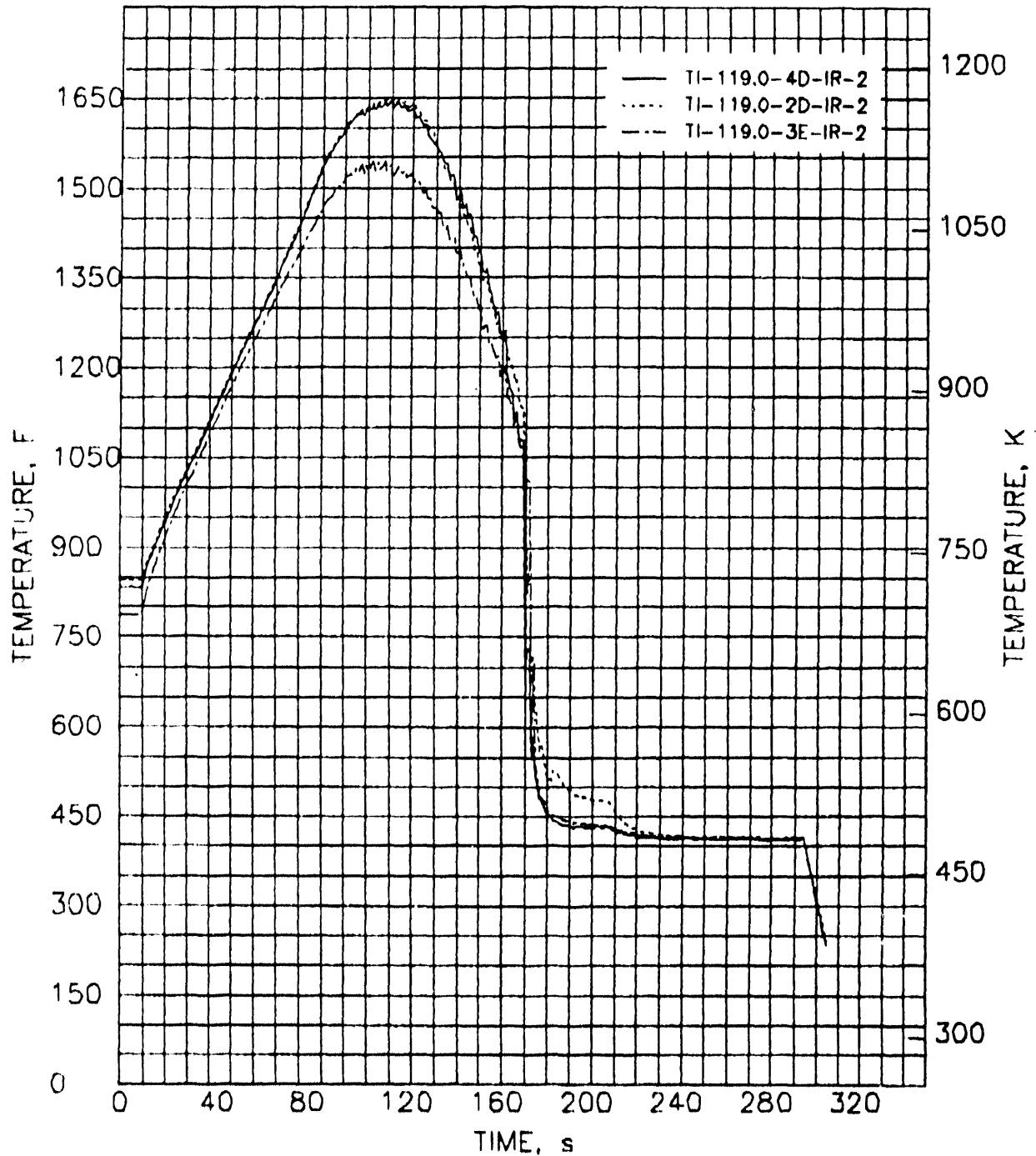


FIGURE B.14. Fuel Rod Interior Cladding Temperatures for Rods 4D, 2D, and 3E at Level 119.0

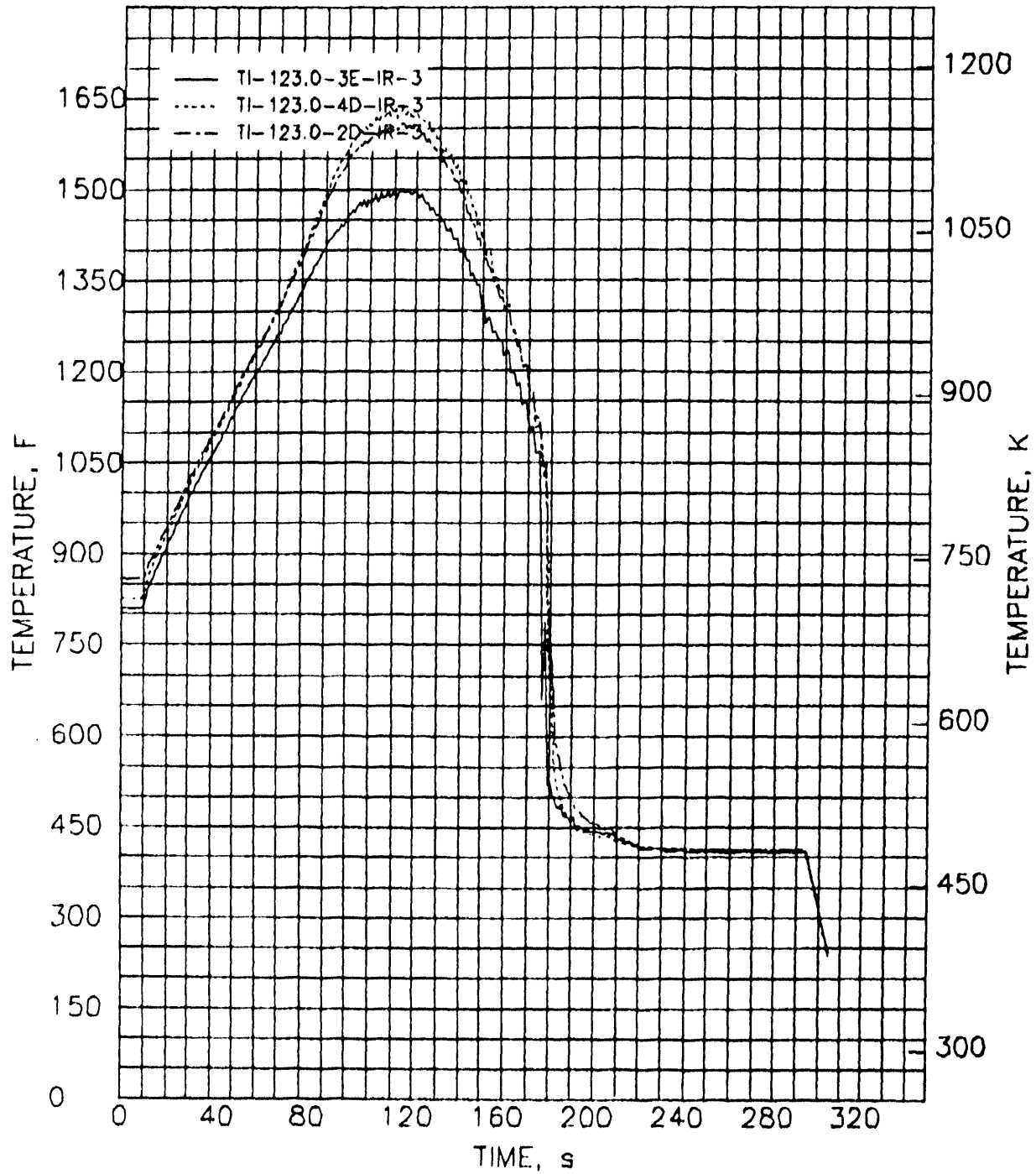


FIGURE B.15. Fuel Rod Interior Cladding Temperatures for Rods 3E, 4D, and 2D at Level 123.0

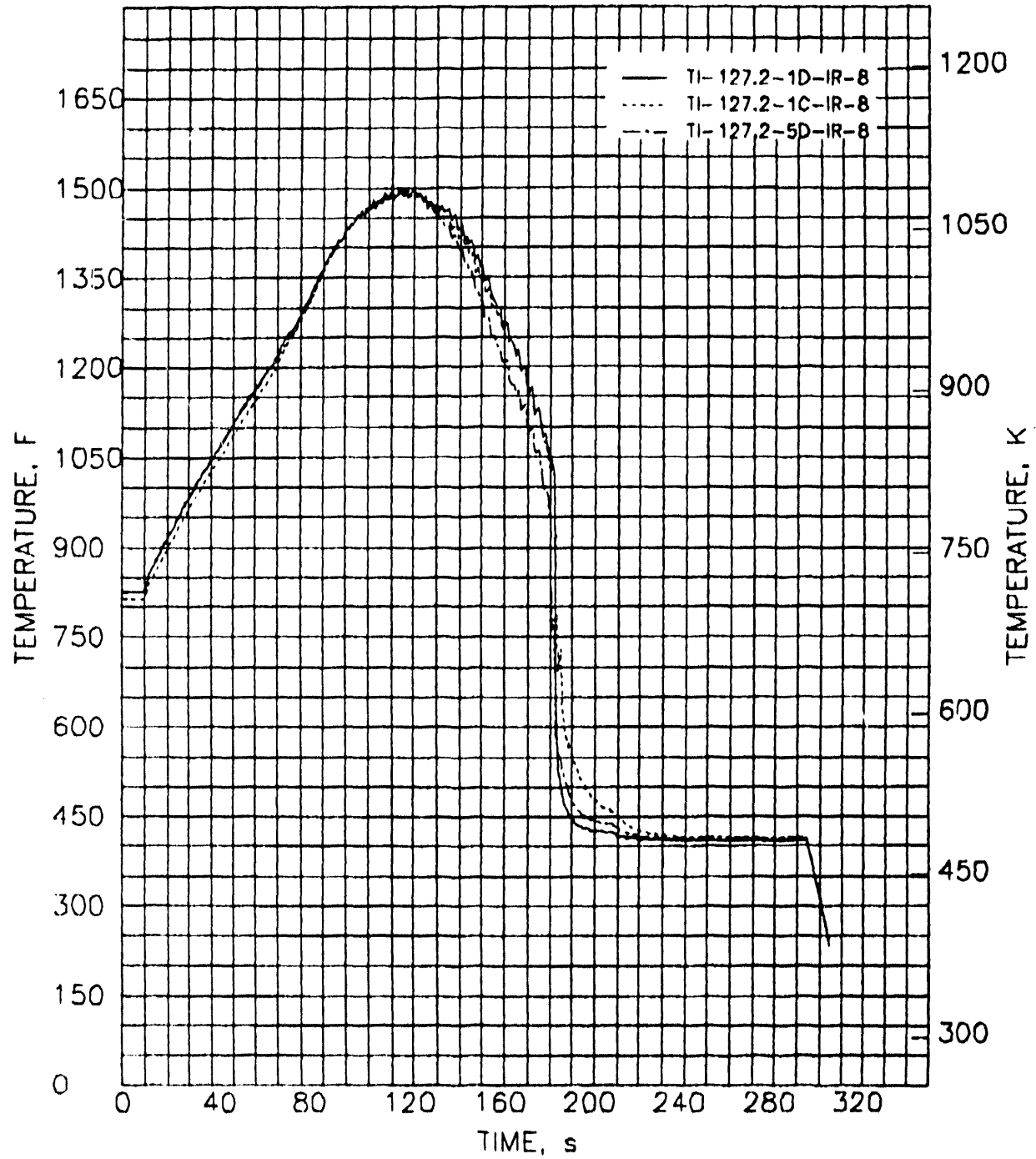


FIGURE B.16. Fuel Rod Interior Cladding Temperatures for Rods 1D, 1C, and 5D at Level 127.2

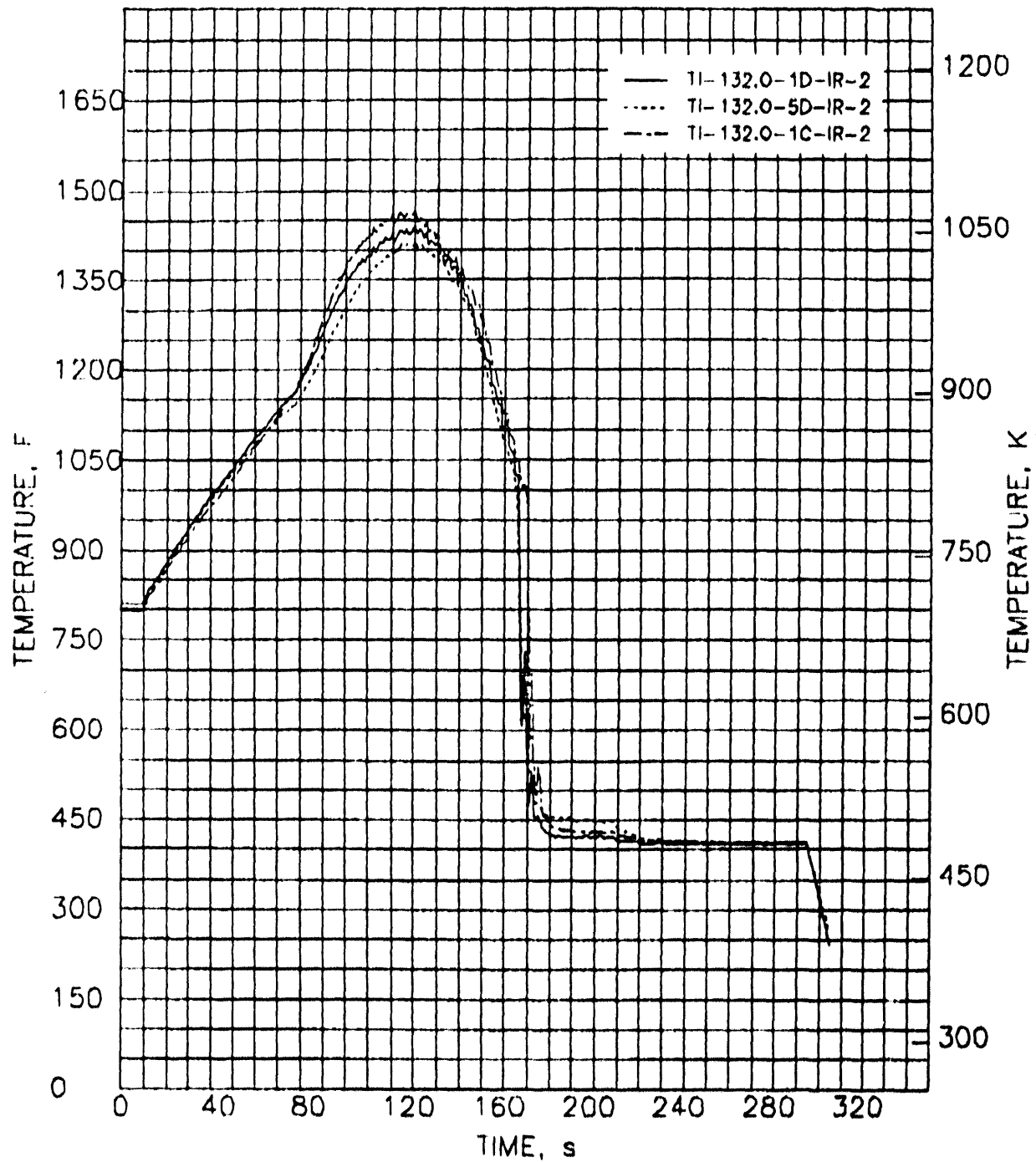


FIGURE B.17. Fuel Rod Interior Cladding Temperatures for Rods 1D, 5D, and 1C at Level 132.0

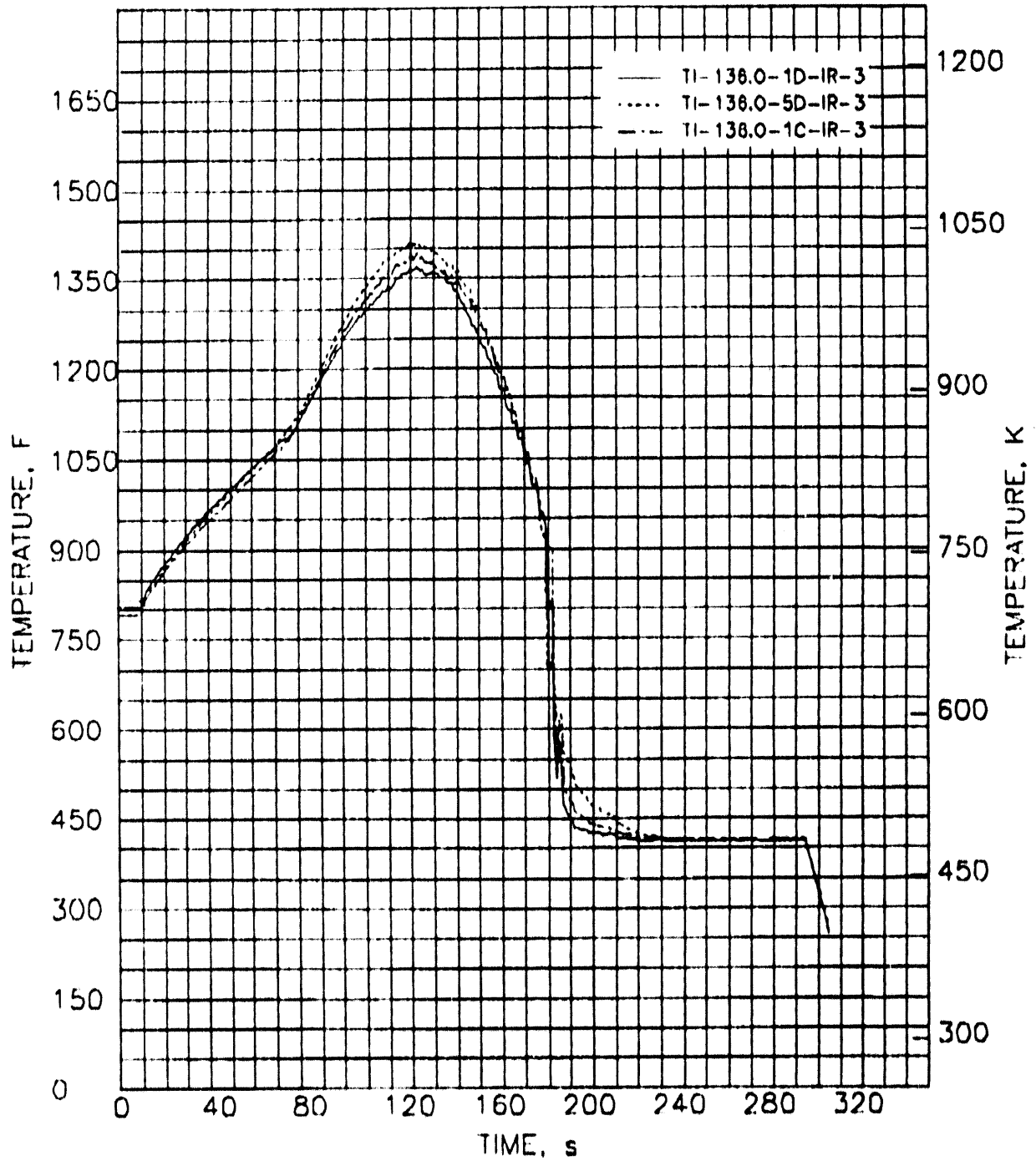


FIGURE B.18. Fuel Rod Interior Cladding Temperatures for Rods 1D, 5D, and 1C at Level 136.0

APPENDIX C

TRANSIENT FUEL CLADDING AND SHROUD INSIDE AND OUTSIDE TEMPERATURES
DURING THE MT-6A TRANSIENT

APPENDIX C

TRANSIENT FUEL CLADDING AND SHROUD INSIDE AND OUTSIDE TEMPERATURES
DURING THE MT-6A TRANSIENT

Fuel cladding temperatures and shroud inside and outside temperatures are compared in this appendix. These curves demonstrate how effectively the shroud insulates the hot fuel rods from the pressure tube.

The remainder of this appendix consists of the following figures:

- | | | |
|-----|---|-----|
| C.1 | Comparison of Fuel Rod Interior Cladding, Shroud Inner Liner,
and Shroud Outside Temperatures at Level 79 | C.2 |
| C.2 | Comparison of Fuel Rod Interior Cladding, Shroud Inner Liner,
and Shroud Outside Temperatures at Level 102 | C.3 |
| C.3 | Comparison of Fuel Rod Interior Cladding, Shroud Inner Liner,
and Shroud Outside Temperatures at Level 123 | C.4 |

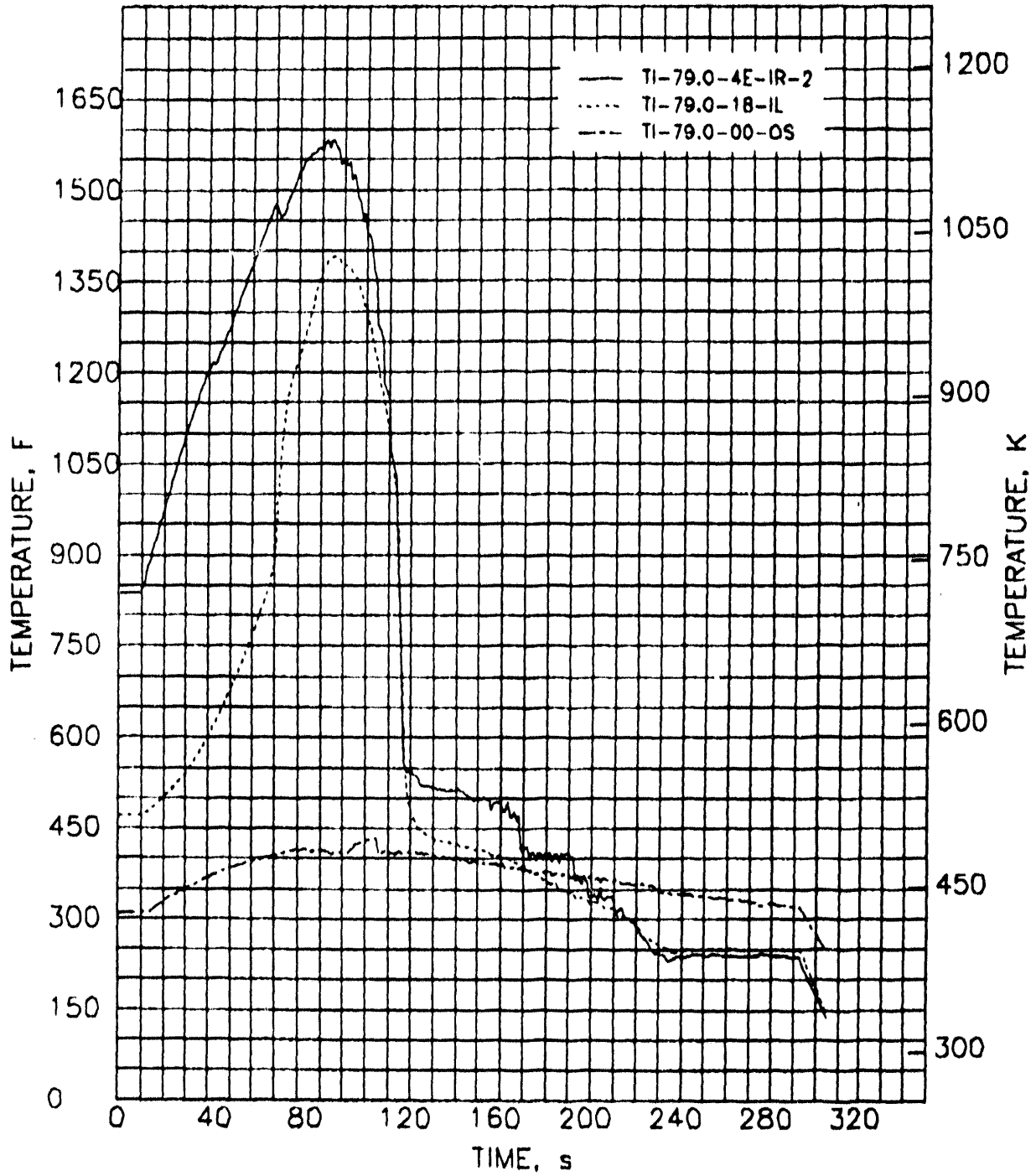


FIGURE C.1. Comparison of Fuel Rod Interior Cladding, Shroud Inner Liner, and Shroud Outside Temperatures at Level 79

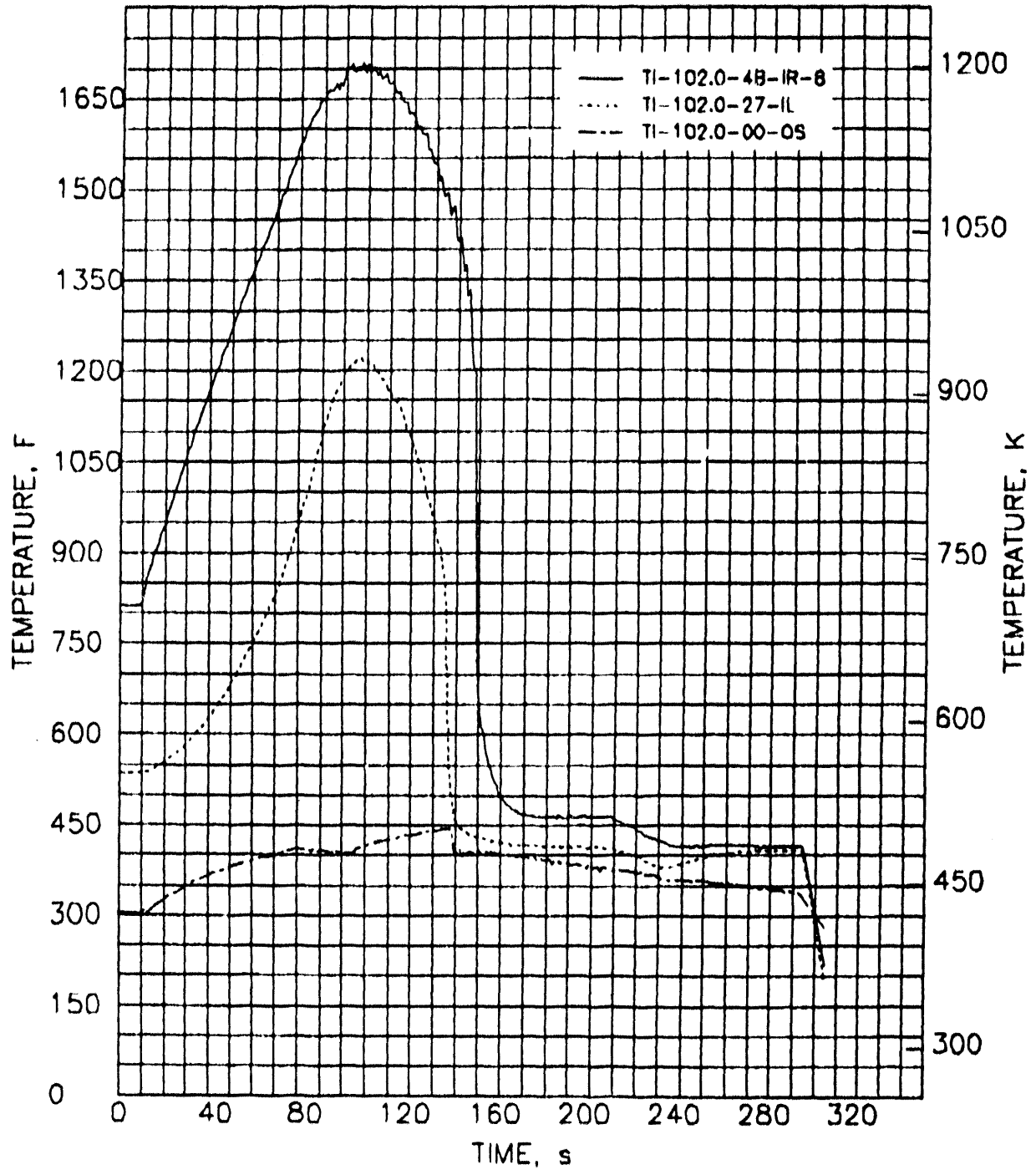


FIGURE C.2. Comparison of Fuel Rod Interior Cladding Shroud Inner Liner, and Shroud Outside Temperatures at Level 102

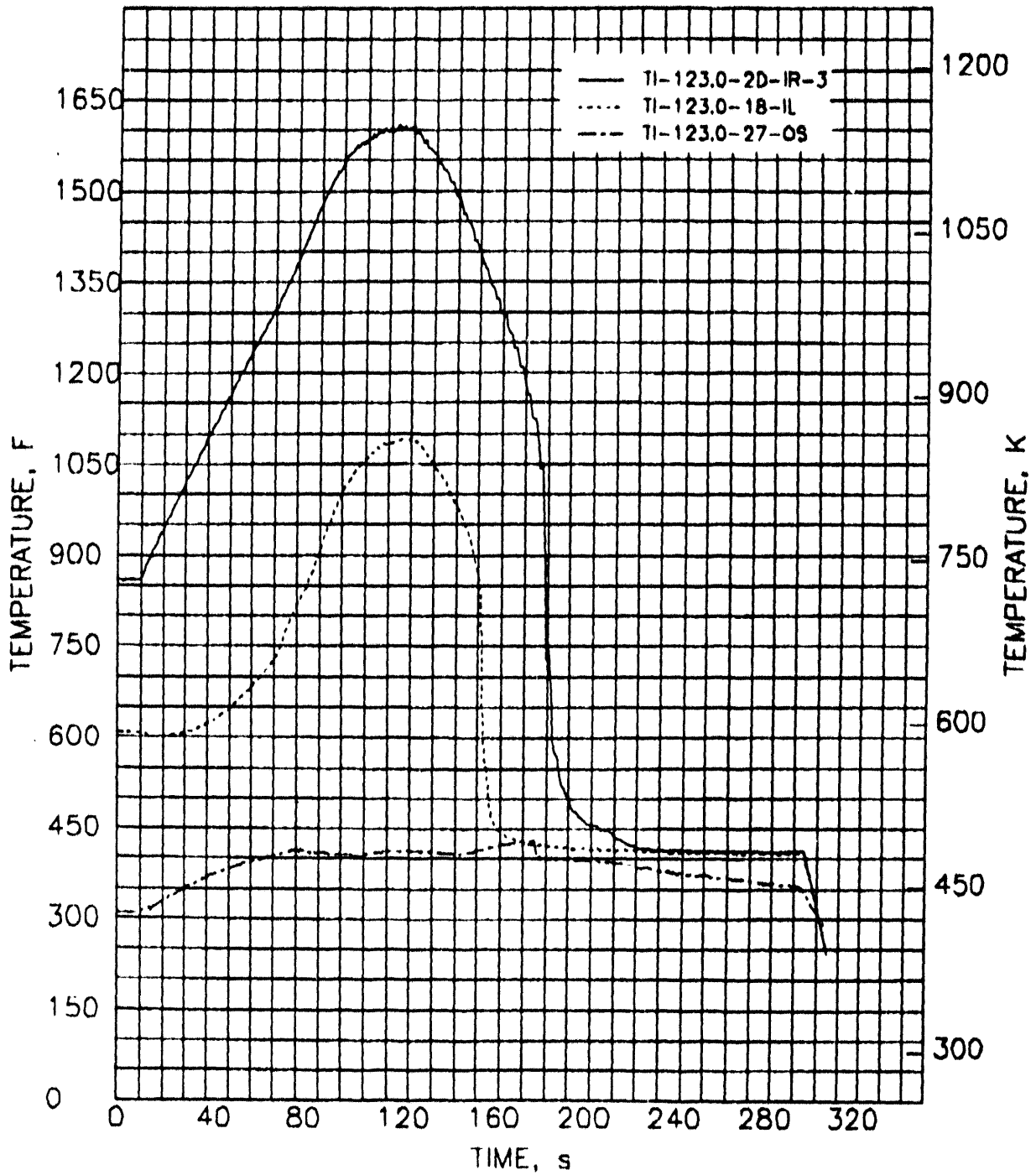


FIGURE C.3. Comparison of Fuel Rod Interior Cladding, Shroud Inner Liner, and Shroud Outside Temperatures at Level 123

APPENDIX D

TRANSIENT SHROUD LINER TEMPERATURES
DURING THE MT-6A TRANSIENT

APPENDIX D

TRANSIENT SHROUD LINER TEMPERATURES
DURING THE MT-6A TRANSIENT

Shroud liner thermocouples were located on the insulation side of the inner liner. Shroud liner temperatures for the transient are presented in this appendix.

The remainder of this appendix consists of the following figures:

D.1	Shroud Inner Liner Temperatures at Level 79	D.2
D.2	Shroud Inner Liner Temperatures at Level 102	D.3
D.3	Shroud Inner Liner Temperatures at Level 123	D.4
D.4	Shroud Inner Liner Temperatures at Level 144	D.5
D.5	Shroud Inner Liner Temperature at Level 156	D.6

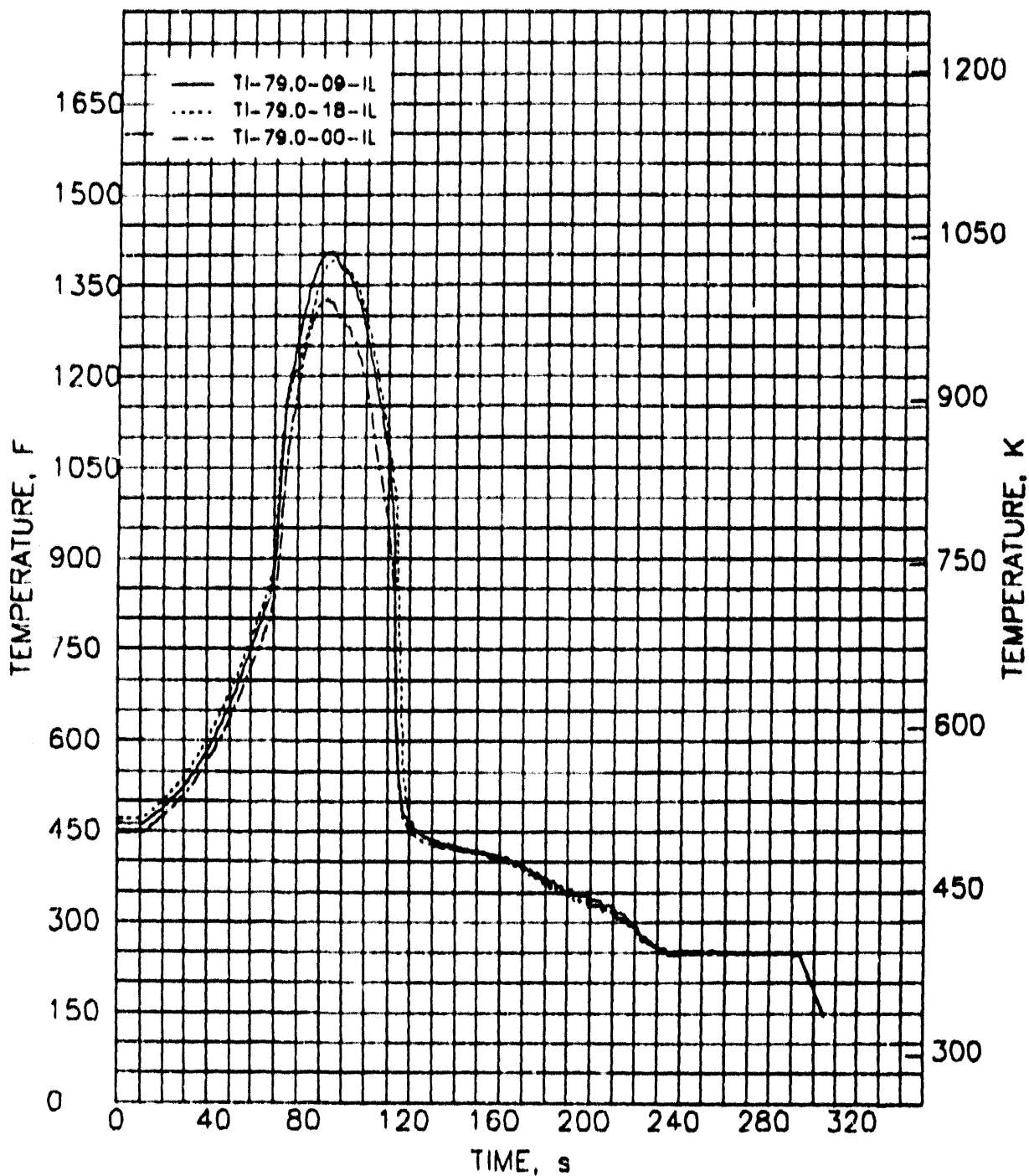
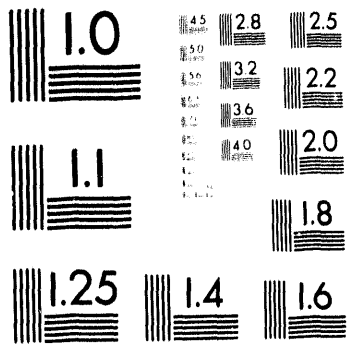


FIGURE D.1. Shroud Inner Liner Temperatures at Level 79



2 of 2

NT6A

5/25/84

1:13:51.195

5/25/84

1:19: 6.000

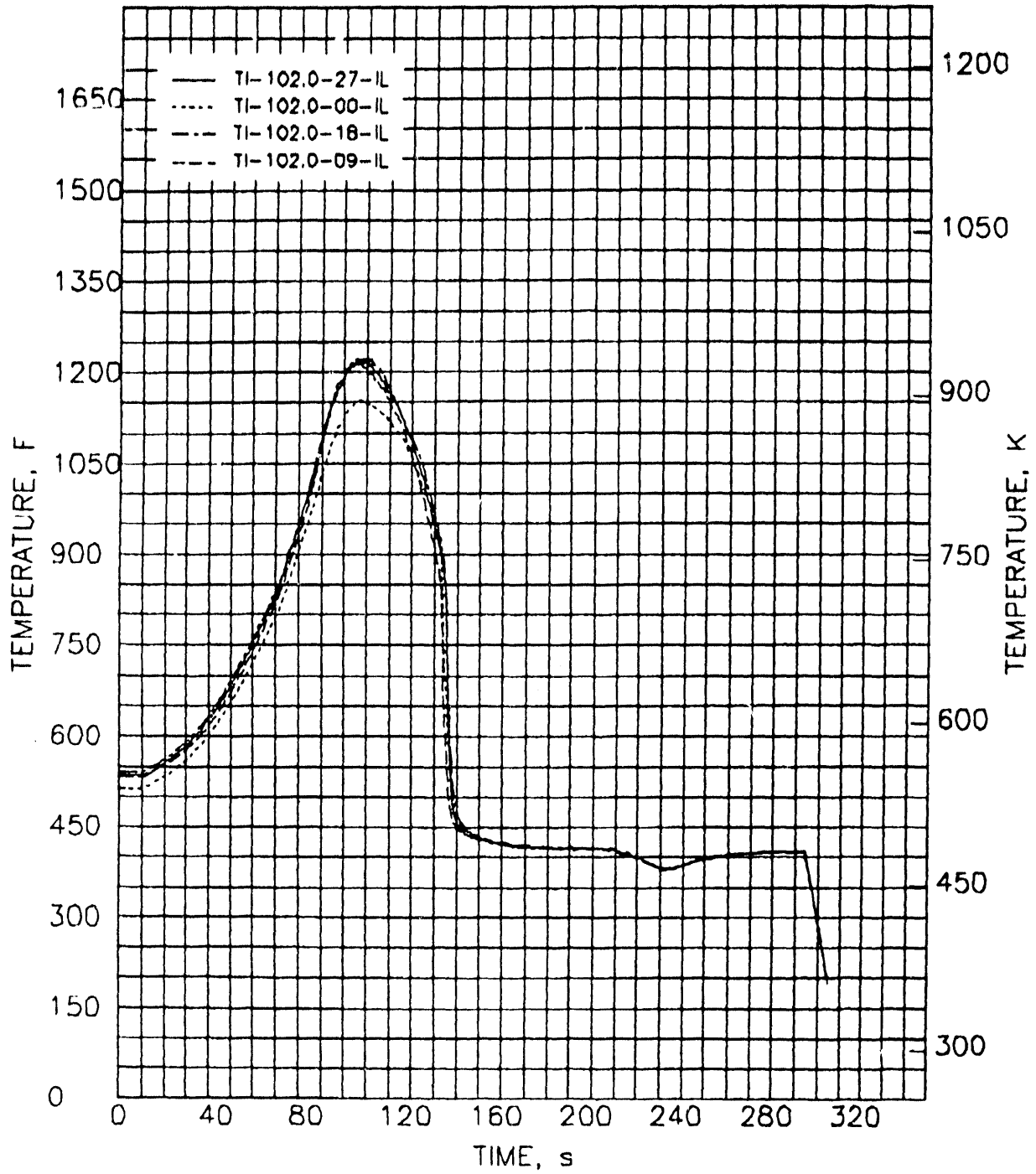


FIGURE D.2. Shroud Inner Liner Temperatures at Level 102

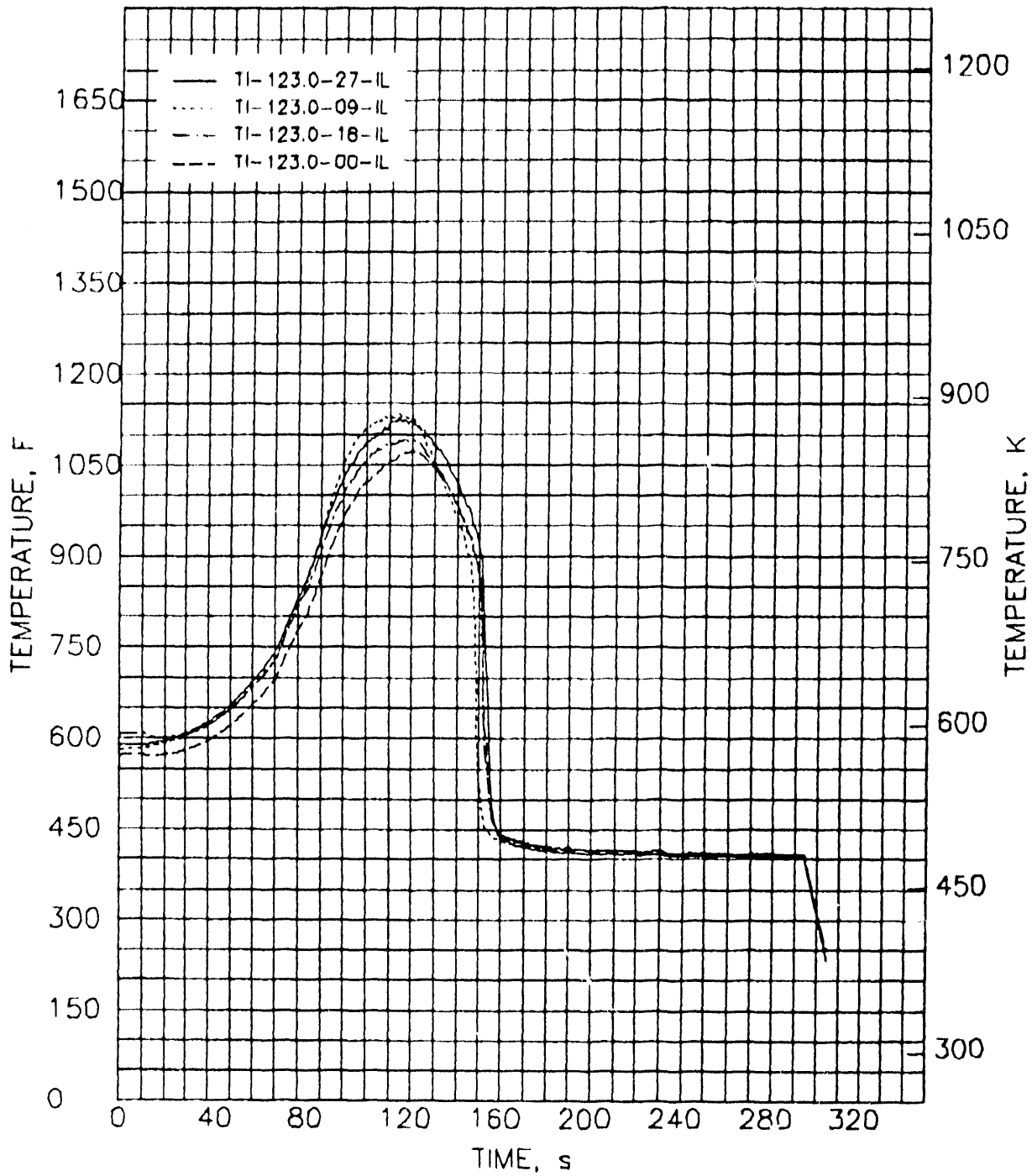


FIGURE D.3. Shroud Inner Liner Temperatures at Level 123

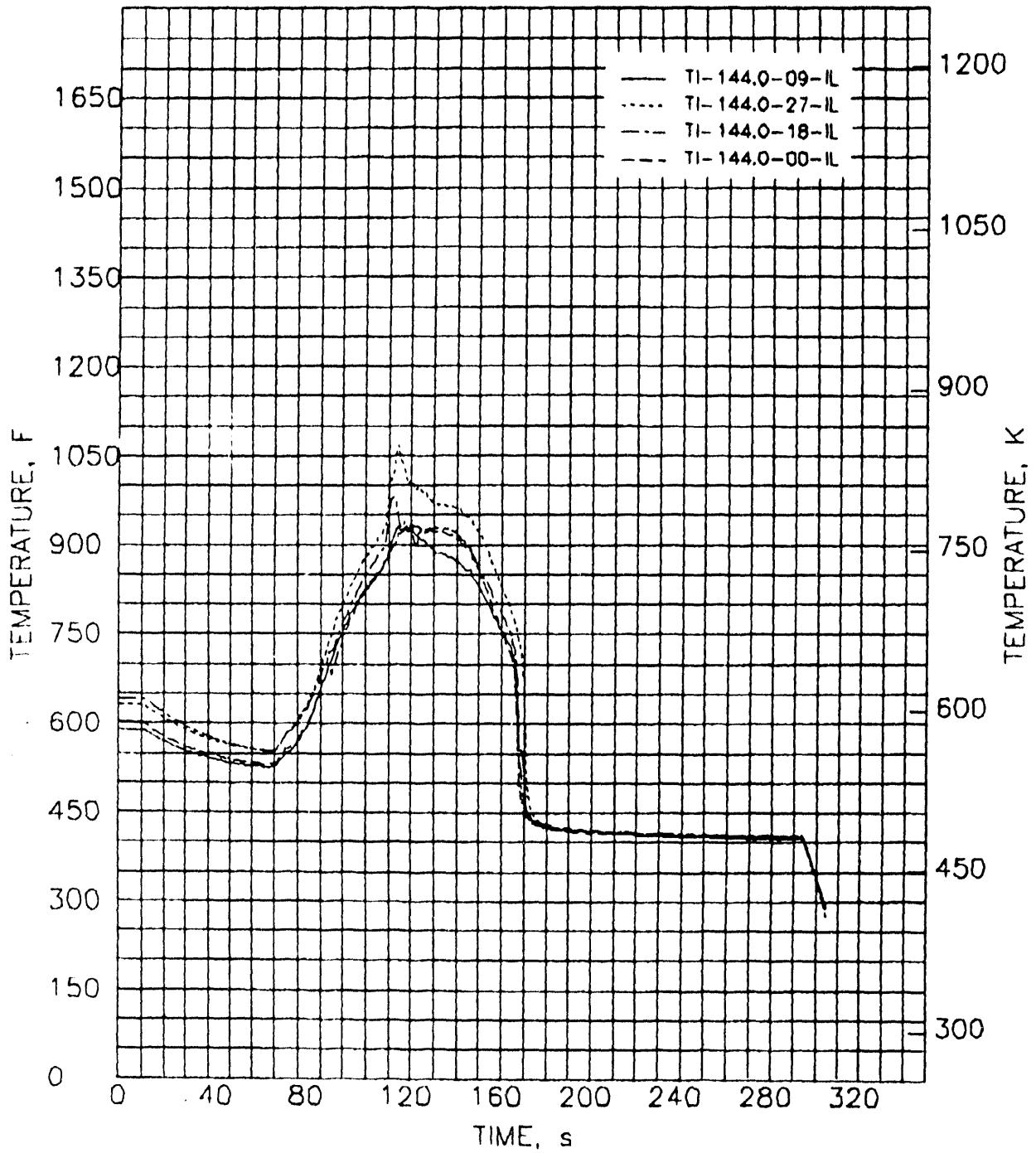


FIGURE D.4. Shroud Inner Liner Temperatures at Level 144

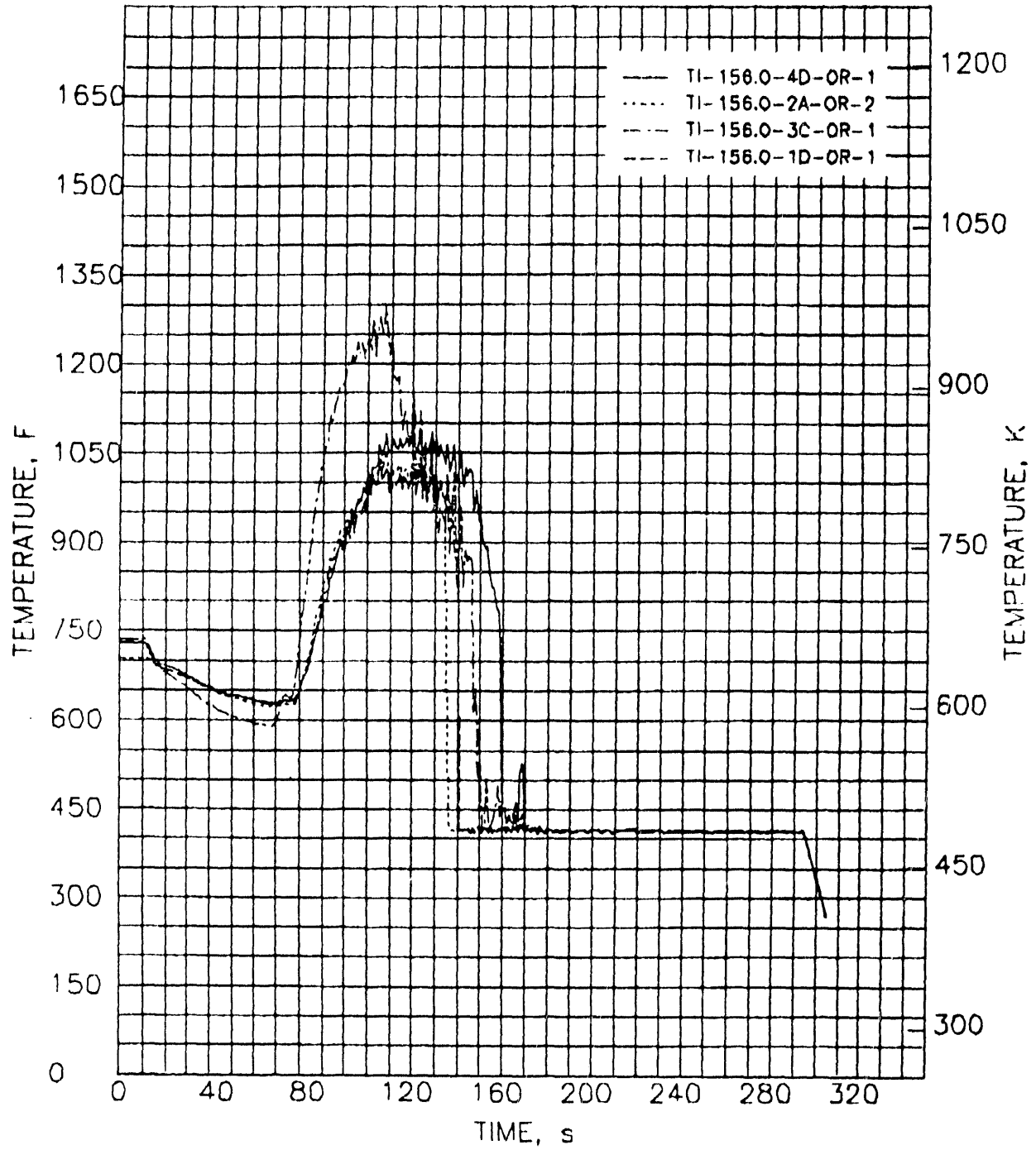


FIGURE D.5. Shroud Inner Liner Temperature at Level 156

APPENDIX E

TRANSIENT OUTSIDE SHROUD TEMPERATURES
DURING THE MT-6A TRANSIENT

APPENDIX E

TRANSIENT OUTSIDE SHROUD TEMPERATURES
DURING THE MT-6A TRANSIENT

Appendix E presents outside shroud temperatures during the MT-6A transient. The low shroud temperatures verify that the insulated shroud performs well.

The remainder of this appendix consists of the following figures:

E.1	Shroud Outside Temperatures at Level 79	E.2
E.2	Shroud Outside Temperatures at Level 102	E.3
E.3	Shroud Outside Temperatures at Level 123	E.4
E.4	Shroud Outside Temperatures at Level 144	E.5
E.5	Shroud Outside Temperatures at Level 169	E.6

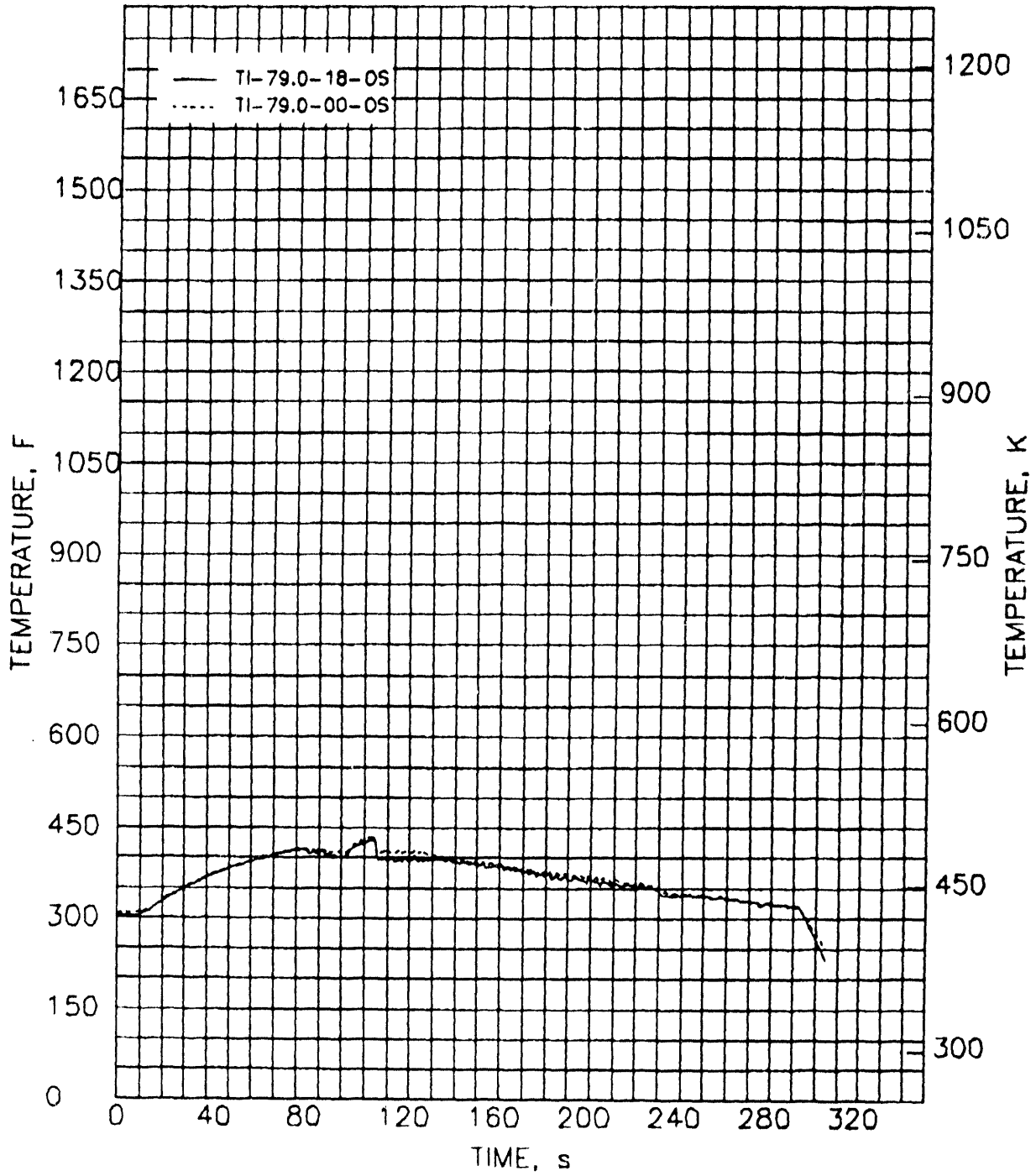


FIGURE E.1. Shroud Outside Temperatures at Level 79

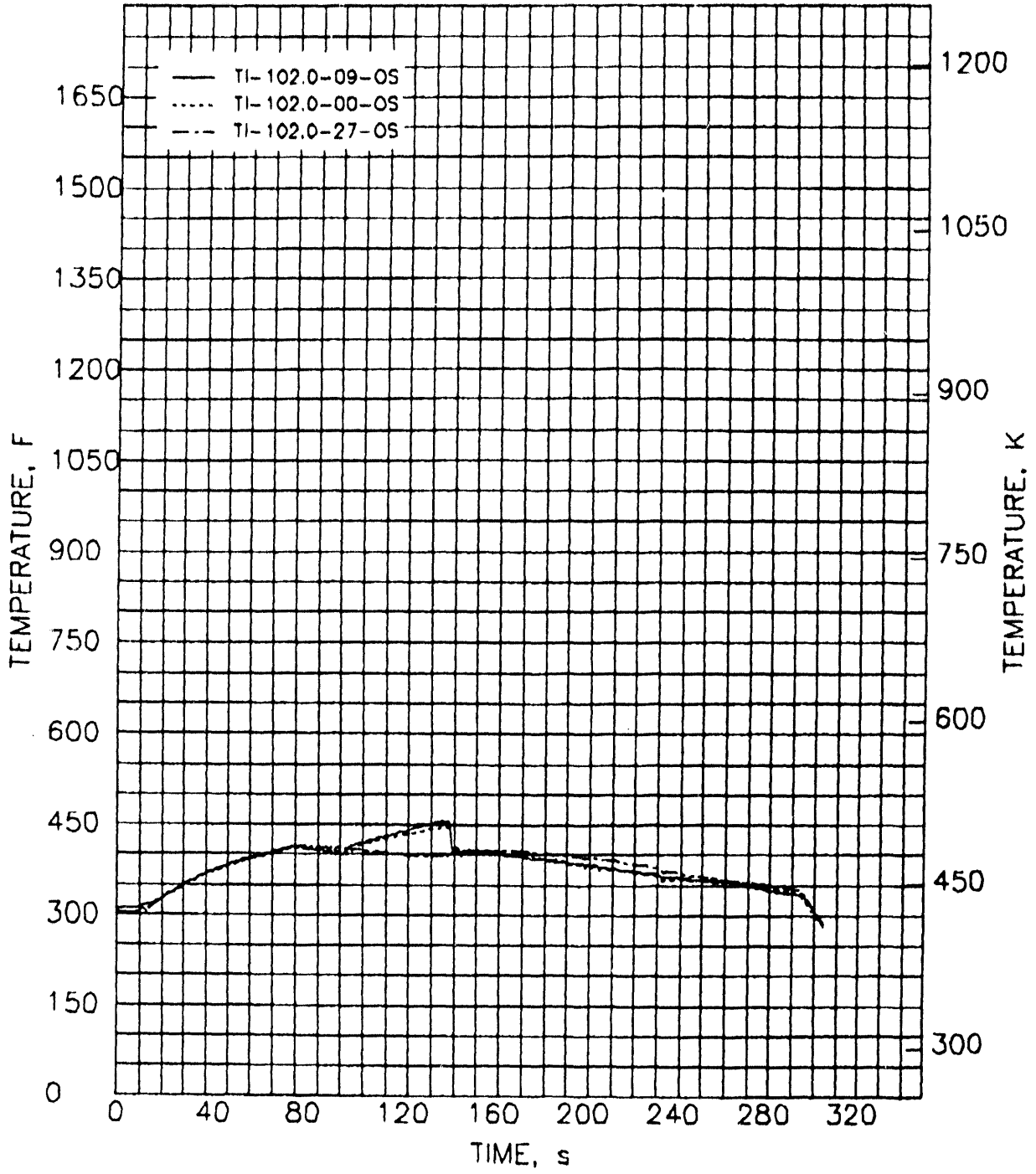


FIGURE E.2. Shroud Outside Temperatures at Level 102

DISTRIBUTION

No. of
Copies

OFFSITE

- 2 DOE/Office of Scientific and Technical
Information

- 2 U.S. Nuclear Regulatory Commission
Office of Nuclear Regulatory Research
Washington, D.C. 20555
ATTN: T. J. Walker, NLN344
R. W. Wright, NLN344

ONSITE

- DOE Richland Operations Office
D. C. Langstaff

- 9 Pacific Northwest Laboratory
F. E. Panisko, P8-34
G. L. Tingey, P8-34
Publishing Coordination
Technical Report Files (5)
NRC Project Office

**DATE
FILMED**

11 / 24 / 93

END

